Chapter 6

Cryosphere and Hydrology

Lead Author
John E. Walsh

Contributing Authors
Oleg Anisimov, Jon Ove M. Hagen, Thor Jakobsson, Johannes Oerlemans, Terry D. Prowse, Vladimir Romanovsky, Nina Savelieva, Mark Serreze, Alex Shiklomanov, Igor Shiklomanov, Steven Solomon

Consulting Authors
Anthony Arendt, David Atkinson, Michael N. Demuth, Julian Dowdeswell, Mark Dyurgerov, Andrey Glazovsky, Roy M. Koerner, Mark Meier, Niels Reeh, Oddur Sigurðsson, Konrad Steffen, Martin Truffer

Contents

Summary

Recent observational data present a generally consistent picture of cryospheric change shaped by patterns of recent warming and variations in the atmospheric circulation. Sea-ice coverage has decreased by 5 to 10% during the past few decades. The decrease is greater in the summer; new period-of-record minima for this season were observed several times in the 1990s and early 2000s. The coverage of multi-year ice has also decreased, as has the thickness of sea ice in the central Arctic. Snow-covered area has diminished by several percent since the early 1970s over both North America and Eurasia. River discharge over much of the Arctic has increased during the past several decades, and on many rivers the spring discharge pulse is occurring earlier. The increase in discharge is consistent with an irregular increase in precipitation over northern land areas. Permafrost temperatures over most of the subarctic land areas have increased by several tenths of a degree to as much as 2 to 3 ºC during the past few decades. Glaciers throughout much of the Northern Hemisphere have lost mass over the past several decades, as have coastal regions of the Greenland Ice Sheet. The glacier retreat has been especially large in Alaska since the mid-1990s. During the past decade, glacier melting resulted in an estimated sea-level increase of 0.15 to 0.30 mm/yr. Earlier breakup and later freeze-up have combined to lengthen the ice-free season of rivers and lakes by up to three weeks since the early 1900s throughout much of the Arctic. The lengthening of the ice-free season has been greatest in the western and central portions of the northern continents. While the various cryospheric and atmospheric changes are consistent in an aggregate sense and are quite large in some cases, it is likely that low-frequency variations in the atmosphere and ocean have played at least some role in forcing the cryospheric and hydrological trends of the past few decades.

Model projections of climate change indicate a continuation of recent trends throughout the 21st century, although the rates of the projected changes vary widely among the models. For example, arctic river discharge is likely to increase by an additional 5 to 25% by the late 21st century. Trends toward earlier breakup and later freeze-up of arctic rivers and lakes are likely if the projected warming occurs. Models project that the wastage of arctic glaciers and the Greenland Ice Sheet will contribute several centimeters to global sea-level rise by 2100. The effects of thermal expansion and isostatic rebound are superimposed on the glacial contributions to sea-level change, all of which combine to produce a spatially variable pattern of projected sea-level rise of several tens of centimeters in some areas (the Beaufort Sea and much of the Siberian coast) and sea-level decrease in other areas (e.g., Hudson Bay and Novaya Zemlya). Increased inflow of cold, fresh water to the Arctic Ocean has the potential for significant impacts on the thermohaline circulation and global climate.

Models project that summer sea ice will decrease by more than 50% over the 21st century, which would extend the navigation season in the Northern Sea Route by between two and four months. Snow cover is projected to continue to decrease, with the greatest decreases projected for spring and autumn. Over the 21st century, permafrost degradation is likely to occur over 10 to 20% of the present permafrost area, and the southern limit of permafrost is likely to move northward by several hundred kilometers. Arctic coastal erosion and coastal permafrost degradation are likely to accelerate this century in response to a combination of arctic warming, sea-level rise, and sea-ice retreat.

6.1. Introduction

The term "cryosphere" is defined (NRCC, 1988) as: "That part of the earth's crust and atmosphere subject to temperatures below 0 ºC for at least part of each year". For purposes of monitoring, diagnosis, projection, and impact assessment, it is convenient to distinguish the following components of the cryosphere: sea ice, seasonal snow cover, glaciers and ice sheets, permafrost, and river and lake ice. Sections 6.3–6.7 address each of these variables separately. In addition, section 6.2 addresses precipitation and evapotranspiration, which together represent the net input of moisture from the atmosphere to the cryosphere. Section 6.8 addresses the surface flows that are the primary hydrological linkages between the terrestrial cryosphere and other parts of the arctic system. These surface flows will play a critical role in determining the impact of cryospheric change on the terrestrial and marine ecosystems of the Arctic, as well as on arctic and perhaps global climate. Finally, section 6.9 addresses sea-level variations that are likely to result from changes in the cryosphere and arctic hydrology.

The different components of the cryosphere respond to change over widely varying timescales, and some of these are not in equilibrium with today's climate. The following sections examine recent and ongoing changes in each cryospheric component, as well as changes projected for the 21st century. Summaries of the present distributions of each variable precede the discussions of change. Each section also includes brief summaries of the impacts of the projected changes, although these summaries rely heavily on references to later chapters that cover many of the impacts in more detail. Each section concludes with a brief description of the key research needs that must be met to reduce uncertainties in the diagnoses and projections discussed. Relevant information from indigenous peoples on cryospheric and hydrological variability is given in Chapter 3.

6.2. Precipitation and evapotranspiration

6.2.1. Background

The cryosphere and hydrological system will respond not only to changes in the thermal state of the Arctic, but also to available moisture. For example, higher temperatures will alter the phase of precipitation, the length of the melt season, the distribution of permafrost, and

the depth of the active layer, with consequent impacts on river discharge, subsurface storage, and glacier mass balance. However, these systems also depend on the balance between precipitation (P) and evapotranspiration/sublimation (collectively denoted as E).

The distribution of P and E in the Arctic has been a subject of accelerating interest in recent years. Two factors account for this surge of interest. The first is the realization that variations in hydrological processes in the Arctic have major implications not only for arctic terrestrial and marine ecosystems, but also for the cryosphere and the global ocean. The second arises from the large uncertainties in the distribution of P and E throughout the Arctic. Uncertainties concerning even the present-day distributions of P and E are sufficiently large that evaluations of recent variations and trends are problematic. The uncertainties reflect:

- the sparse network of *in situ* measurements of P (several hundred stations, with very poor coverage over northern Canada and the Arctic Ocean), and the virtual absence of such measurements of E (those that do exist are mostly from field programs of short duration);
- the difficulty of obtaining accurate measurements of solid P in cold windy environments, even at manned weather stations;
- the compounding effects of elevation on P and E in topographically complex regions of the Arctic, where the distribution of observing stations is biased toward low elevations and coastal regions; and
- slow progress in exploiting remote sensing techniques for measuring high-latitude P and E owing to the heterogeneous emissivity of snow- and ice-covered surfaces, difficulties with cloud/snow discrimination, and the near-absence of coverage by ground-based radar.

Progress in mapping the spatial and seasonal distributions of arctic P has resulted from the use of information on gauge bias adjustment procedures, for example, from the World Meteorological Organization (WMO) Solid Precipitation Measurement Intercomparison (Goodison et al., 1998). Colony et al. (1998), Yang (1999), and Bogdanova et al. (2002) recently completed summaries of P over the Arctic Ocean, where only measurements from coastal and drifting ice stations are available. The Bogdanova et al. (2002) study, which accounts for all the major systematic errors in P measurement, found the mean annual bias-corrected P for the central Arctic Ocean to be 16.9 cm – 32% higher than the uncorrected value. The spatial pattern shows an increase from minimum values of <10 cm/yr over Greenland and 15 to 20 cm/yr over much of the Arctic Ocean, to >50 cm/yr over parts of the North Atlantic subpolar seas.

Estimates of evaporation over the Arctic Ocean are scarce. The one-year Surface Heat Budget of the Arctic Ocean (SHEBA) project collected some of the best measurements during 1997 and 1998 in the Beaufort Sea. These observations showed that evaporation was nearly zero between October and April, and peaked in July at about 7 mm/month (Persson et al., 2002).

Serreze et al. (2003) compiled estimates of P and E for the major terrestrial watersheds of the Arctic using data from 1960 to 1989. Table 6.1 presents basin-averaged values of mean annual P, precipitation minus evapotranspiration (P-E), runoff (R), and E (computed in two ways). In this study, P was derived from objectively analyzed fields of gauge-adjusted station measurements; P-E from the atmospheric moisture flux convergences in the National Centers for Environmental Prediction/National Center for Atmospheric Research (NCEP/NCAR) reanalysis; and R from gauges near the mouths of the major rivers. E was computed in two ways: E1 is the difference between the independently derived P and P-E, and E2 is the difference between basin-averaged P and R.

The two estimates of E differ by as much as 20%, providing a measure of the uncertainty in the basin-scale means of the hydrological quantities. At least some, and probably most, of the uncertainty arises from biases in measurements of P. All basins show summer maxima in P and E, and summer minima in P-E (Fig. 6.1).

Precipitation minus evapotranspiration is essentially zero during July and August in the Mackenzie Basin, and negative during June and July in the Ob Basin, illustrating the importance of E in the hydrological budget of arctic terrestrial regions. In addition, about 25% of July P in the large Eurasian basins is associated with the recycling of moisture from E (Serreze et al., 2003). The relatively low ratios of R to P (R/P, Table 6.1) in the Ob Basin are indicative of the general absence of permafrost (19% coverage in this basin, see section 6.8.2), while the relatively high ratios (and smaller E values) in the Lena and Mackenzie Basins are consistent with larger proportions of permafrost, which reduces infiltration and enhances R.

Table 6.1. Mean annual water budget components in four major drainage basins based on data from 1960 to 1989 (Serreze et al., 2003).

	P (mm)	P-E (mm)	E1 (mm)	E2 (mm)	R (mm)	R/P
Ob	534	151	383	396	138	0.26
Yenisey	495	189	306	256	239	0.48
Lena	403	179	224	182	221	0.55
Mackenzie	411	142	269	241	171	0.41

P: mean annual precipitation; P-E: precipitation minus evapotranspiration; E1: difference between the independently-derived P and P-E; E2: difference between basin-averaged P and R; R: runoff.

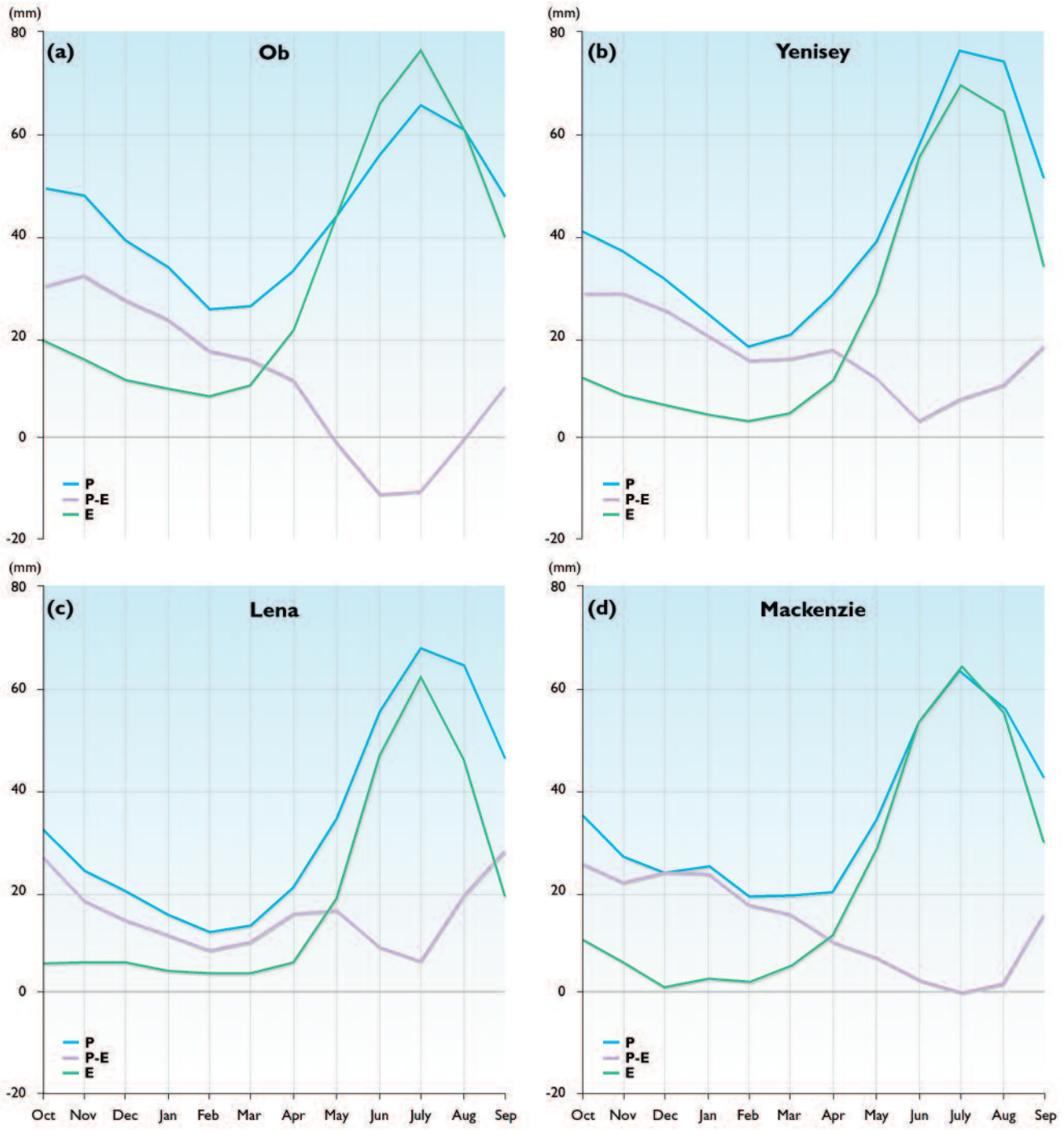

Fig. 6.1. Mean monthly precipitation (P), precipitation minus evapotranspiration (P-E), and evapotranspiration (E) for the four major arctic watersheds, using data from 1960 to 1989. E is the calculated difference between P and P-E (E1 in text). Seasonal cycle corresponds to water year (Serreze et al., 2003).

Additional estimates of the freshwater budget components of arctic and worldwide rivers, using data for earlier years, are provided by Oki et al. (1995). Rouse et al. (2003) provide a more detailed analysis of the Mackenzie Basin water cycle. The present-day hydrological regimes of the various arctic subregions are discussed further in sections 6.4 and 6.8.

6.2.2. Recent and ongoing changes

Given the uncertainties in the climatologies of arctic P and E, it is not surprising that information on recent variations and trends in these variables is limited. Time series obtained from reanalyses are subject to inhomogeneities resulting from changes in the input data over multi-decadal timescales, while trends computed using station data are complicated by measurement errors. Changes in the rain/snow ratio during periods of warming or cooling at high-latitude sites further complicate the use of *in situ* measurements for trend determination (Forland and Hanssen-Bauer, 2000).

The Intergovernmental Panel on Climate Change (IPCC, 1996, 2001) has consistently reported 20th-century P increases in northern high latitudes (55°–85° N; see Fig. 3.11 of IPCC, 1996). The increase is similar to that

in Karl's (1998) "Arctic region", which includes the area poleward of 65° N but excludes the waters surrounding southern Greenland. In both cases, the greatest increase appears to have occurred during the first half of the 20th century. However, the time series are based on data from the synoptic station network, which is unevenly distributed and has undergone much change. Nevertheless, the increase in the early 20th century is reproduced by some model simulations of 20th-century climate (Kattsov and Walsh, 2000; Paeth et al., 2002).

Groisman and Easterling (1994) present data showing an increase in P over northern Canada (poleward of 55° N) since 1950. For the period since 1960, the gauge-adjusted and basin-averaged data of Serreze et al. (2003) show no discernible trends in mean annual P over the Ob, Yenisey, Lena, and Mackenzie Basins. However, summer P over the Yenisey Basin decreased by 5 to 10% over the four decades since 1960. The variations in P in these basins are associated with variations in the atmospheric circulation.

Although they are subject to the caveats that accompany trends of derived quantities in a reanalysis, trends of annual E (determined primarily by summer E) in the NCEP/NCAR reanalysis are negative in the Ob Basin and positive in the Yenisey and Mackenzie Basins. Serreze et al. (2003) suggest that recent increases in winter discharge from the Yenisey Basin may have been associated with permafrost thawing within the basin in recent decades.

Further discussion of recent trends in variables associated with P may be found in sections 6.4.2 and 6.8.2.

6.2.3. Projected changes

The five ACIA-designated climate models (section 1.4.2), forced with the B2 emissions scenario (section 4.4.1), were used to project 21st-century change in P, E, and P-E. The models are the CGCM2 (Canadian Centre for Climate Modelling and Analysis), CSM_1.4 (National Center for Atmospheric Research), ECHAM4 OPYC3 (Max-Planck Institute for Meteorology), GFDL-R30_c (Geophysical Fluid Dynamics Laboratory), and HadCM3 (Hadley Centre for Climate Prediction and Research). Model projections are presented as averages for the Arctic Ocean and for the five largest arctic river basins: the Ob, Yenisey, Pechora, Lena, and Mackenzie. The models differ widely in their simulations of baseline (1981–2000) values of P, E, and P-E (Table 6.2). For each of the three variables (P, E, and P-E), the projected changes by 2071–2090 are generally smaller than the range in baseline values simulated by the different models.

Table 6.2. Ranges in baseline (1981–2000) values of mean annual precipitation and evapotranspiration simulated by the five ACIA-designated models for the Arctic Ocean and major arctic river basins.

	P (mm)	E (mm)
Arctic Ocean	220[a] – 504[b]	39[b] – 92[c]
Ob	708[c] – 1058[d]	302[a] – 426[d]
Yenisey	604[c] – 898[b]	224[a] – 276[b]
Lena	552[c] – 881[b]	200[c] – 312[d]
Pechora	493[c] – 1080[b]	144[c] – 246[d]
Mackenzie	670[c] – 958[d]	330[c] – 557[a]

P: Precipitation; E: Evapotranspiration.
[a]ECHAM4/OPYC3; [b]CGCM2; [c]CSM_1.4; [d]HadCM3.

In general, the models project modest increases in P by the end of the 21st century. Figure 6.2 illustrates the changes projected for the 2071–2090 time slice as percentages of the baseline (1981–2000) values simulated by the models. The values of P, E, and P-E projected for the earlier time slices are generally between the models' baseline values and those for the 2071–2090 time slice, although sampling variations result in some instances of non-monotonicity, especially when the changes are small. As indicated in Fig. 6.2, there is a wider across-model range in projected changes in E than in projected changes in P. There is even considerable disagreement among the models concerning the sign of the changes in E: in every region, at least one model projects a decrease, although most of the projected changes are positive. However, the baseline values for E from which the changes occur are much smaller than the corresponding baseline values for P (Table 6.2), so the projected unit changes in E are generally smaller than the projected unit changes in P.

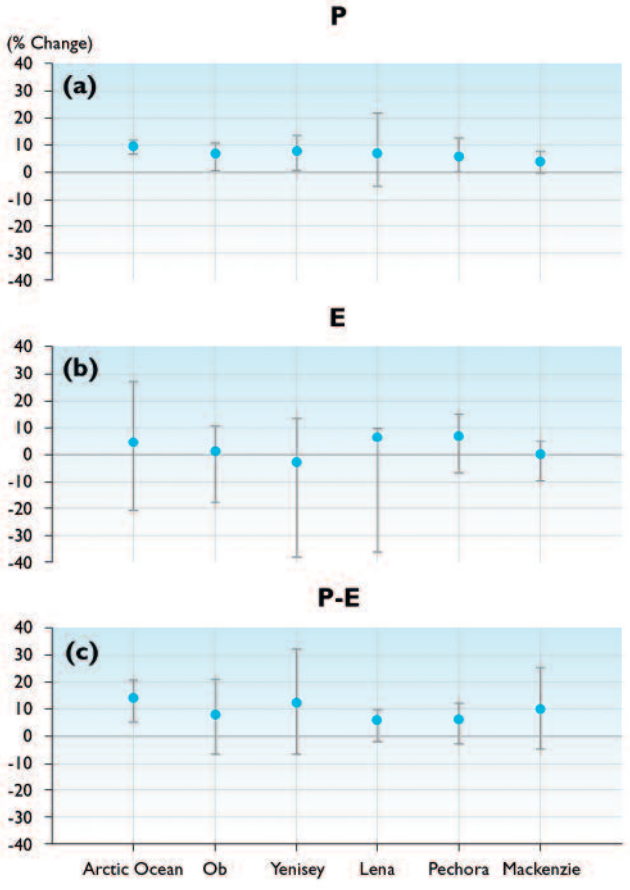

Fig. 6.2. Percentage change in (a) precipitation, (b) evapotranspiration, and (c) precipitation minus evapotranspiration between 1981–2000 and 2071–2090 projected by the five ACIA-designated models for the Arctic Ocean and five major arctic river basins. Solid circles are five-model means; vertical line segments denote the ranges of the five model projections.

Of the variables considered here, the one with the greatest relevance to other parts of the arctic system is P-E, which represents the net moisture input to the surface from the atmosphere. With one exception (the CSM_1.4, which projects the least warming of the five models), the projected changes in P-E are positive (Fig. 6.2). The greatest increase, 14% (averaged across all models), is projected to occur over the Arctic Ocean, where even the CSM_1.4 projects an increase in P-E. Over the terrestrial watersheds, the projected increases range from 6 to 12% (averaged across all models). These changes are considerably smaller than the departures from the means occurring during individual years and even during multi-year periods in the model simulations. Since the projected changes in P and P-E are generally positive, it is likely that the most consequential changes in these variables will be increases in the frequency and/or duration of wet periods. However, the annual averaging of the variables shown in Fig. 6.2 obscures a potentially important seasonality. The projected changes in P-E are generally smaller, and occasionally negative, over the major river basins during the warm season. This relative decrease in projected P-E during summer is the result of two factors: an increase in E due to projected temperature increases; and a longer season with a snow-free surface and above-freezing temperatures in the upper soil layers, resulting in greater projected E. Consequently, the model projections point to the distinct possibility that increased river flow rates during winter and spring will be accompanied by decreased flow rates during the warm season. The latter is consistent with the results of the Mackenzie Basin Impact Study (Cohen, 1997).

6.2.4. Impacts of projected changes

On other parts of the physical system

The projected increases in P, and more importantly in P-E, imply an increase in water availability for soil infiltration and runoff. The increases in P-E projected to occur by 2071–2090 over the major terrestrial watersheds imply that the mean annual discharge to the Arctic Ocean will increase by 6 to 12%. Since the mean annual P-E over the Arctic Ocean is projected to increase by 14% over this period, a substantial increase in the freshwater supplied to the Arctic Ocean is projected to occur by the later decades of the present century. If there is an increase in the supply of fresh water to the Arctic Ocean, it will increase the stratification of the Arctic Ocean, facilitate the formation of sea ice, and enhance freshwater export from the Arctic Ocean to the North Atlantic (sections 6.5.4 and 6.8.4). In addition, increased aquatic transport and associated heat fluxes across the coastal zone are likely to accelerate the degradation of coastal permafrost in some areas.

The projected increases in P and P-E imply generally wetter soils when soils are not frozen, increased surface flows above frozen soils, wetter active layers in the summer, and greater ice content in the upper soil layer during winter. To the extent that the projected increase in P occurs as an increase in snowfall during the cold season (section 6.4), the Arctic Ocean and its terrestrial watersheds will experience increases in snow depth and snow water equivalent, although the seasonal duration may be shorter if warming accompanies the increase in P. Moreover, the projected increase in mean annual P-E obscures important seasonality. Recent trends of increasing E in the Yenisey and Mackenzie Basins (section 6.2.2) raise the possibility that P-E will actually decrease during the summer when E exceeds P, resulting in a drying of soils during the warm season.

On ecosystems

The projected increase in P-E over the terrestrial watersheds will increase moisture availability in the upper soil layers, favoring plant growth in regions that are presently moisture-limited. However, as previously noted, projected increases in E during the summer are likely to lead to warm-season soil drying and reduced summer river levels. Thawing of permafrost, which could increase the subsurface contribution to streamflow and possibly mitigate the effect of increased E during summer, is another complicating factor.

The projected increase in river discharge is likely to increase nutrient and sediment fluxes to the Arctic Ocean, with corresponding impacts on coastal marine ecosystems (section 9.3.2). If P increases during winter and ice breakup accelerates, an increase in flood events is likely. Higher flow rates in rivers and streams caused by such events are likely to have large impacts on riparian regions and flood plains in the Arctic. Wetland ecosystems are likely to expand in a climate regime of increased P-E, with corresponding changes in the fluxes of trace gases (e.g., carbon dioxide and methane) across the surface–atmosphere interface.

Projected increases in P and P-E will result in generally greater availability of surface moisture for arctic residents. In permafrost-free areas, water tables are likely to be closer to the surface, and moisture availability for agriculture will increase. During the spring period when enhanced P and P-E are likely to increase river levels, the risk of flooding will increase. Lower water levels during the summer would affect river navigation, increase the threat from forest fires, and affect hydropower generation.

6.2.5. Critical research needs

It is apparent from Table 6.2 and Fig. 6.2 that models differ widely in their simulations of P and P-E in baseline climate simulations and in projections of future climate. The result is a very large range in uncertainty for future rates of moisture supply to the arctic surface. There is an urgent need to narrow the range in uncertainty by determining the reasons for the large across-model variances in P and E, and by bringing the mod-

els' baseline simulations of P and E into closer agreement with observational data. That the observational data are also uncertain indicates a need for collaboration between the observational and modeling communities, including the remote sensing community, in reconciling models and data.

The most problematic variable of those considered is E. Despite its direct relevance to the surface moisture budget and to terrestrial ecosystems, very few observational data are available for assessing model simulations of E. The 21st-century simulations summarized here show that the models do not agree even on the sign of the changes in E in the Arctic. Improved model parameterizations of E will need to address factors such as the effects of vegetation change and simulation of transpiration rates using more realistic vegetation parameters, such as leaf area index instead of a single crop factor. Datasets for validating and calibrating model-simulated E (including better use of satellite data) are one of the most urgent needs for developing scenarios of arctic hydrology.

6.3. Sea ice

6.3.1. Background

Sea ice has long been regarded as a key potential indicator and agent of climate change. In recent years, sea ice has received much attention in the news media and the scientific literature owing to the apparent reduction in coverage and thickness of sea ice in the Arctic. Since the potential impacts of these changes on climate, ecosystems, and infrastructure are large, sea ice is a highly important variable in an assessment of arctic change. Section 6.9.1 discusses sea ice within the context of coastal stability and sea-level rise.

Owing to the routine availability of satellite passive microwave imagery from the Scanning Multichannel Microwave Radiometer and the Special Sensor Microwave/Imager (SSM/I) sensors, sea-ice coverage has been well monitored since the 1970s. Figure 6.3 shows mean sea-ice concentrations for the months of the climatological maximum (March) and minimum (September) for the period 1990 to 1999 derived from SSM/I data. The accuracy of passive microwave-derived sea-ice concentrations varies from approximately 6% during winter to more than 10% during summer. The sea-ice variable most compatible with pre-satellite information (based largely on ship reports) is sea-ice extent, defined as the area of ocean with an ice concentration of at least 15%. Arctic sea-ice extent, including all subpolar seas except the Baltic, ranges from about 7 million km^2 at its September minimum to about 15 million km^2 at its March maximum. The areal coverage of sea ice (excluding open water poleward of the ice edge) ranges from 5 to 6 million km^2 in late summer to about 14 million km^2 in the late winter (Parkinson et al., 1999). Interannual variability in the position of the sea-ice edge is typically one to five degrees of latitude for a particular geographic region and month. The departures from normal at a particular time vary regionally in magnitude and in sign.

While ice extent and areal coverage have historically been used to monitor sea ice, ice thickness is an equally important consideration within the context of the sea-

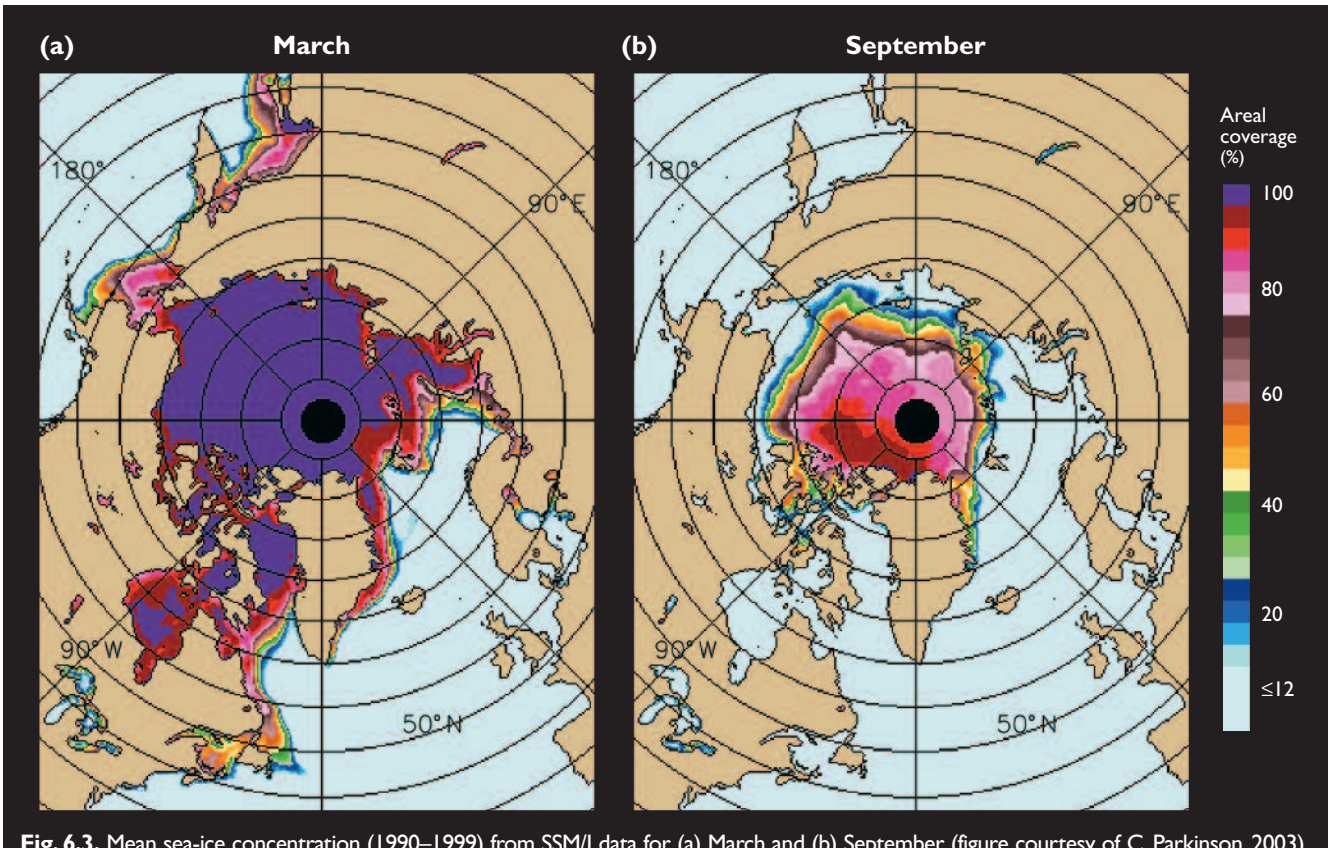

Fig. 6.3. Mean sea-ice concentration (1990–1999) from SSM/I data for (a) March and (b) September (figure courtesy of C. Parkinson, 2003).

ice mass budget. Unfortunately, sea-ice thickness measurements are less routine, consisting largely of upward-looking sonar measurements from occasional and irregular submarine cruises and, in recent years, from moored sonar on or near the continental shelves. In addition, direct measurements of fast-ice (sea ice attached to the shore) thickness have been made for several decades in some coastal regions, and occasional direct measurements have been made in the central Arctic at manned ice camps. The general pattern of sea-ice thickness has been determined, but it is subject to variations and uncertainties that have not been well quantified. Sea-ice thickness generally increases from the Siberian side of the Arctic to the Canadian Archipelago, largely in response to the mean pattern of sea-ice drift and convergence (although air temperatures are also generally lower on the Canadian side of the Arctic Ocean). In areas of perennial sea ice, the seasonal cycle of melt and ablation has an amplitude of about 0.5 to 1.0 m.

The albedo of sea ice is of critical importance to the surface energy budget and to the ice-albedo feedback, both of which can accelerate sea-ice variations over timescales ranging from the seasonal to the decade-to-century scale of interest in the context of climate change. The albedo of sea ice and snow-covered sea ice has been measured throughout the annual cycle at a local scale (e.g., at ice stations such as SHEBA). However, the albedo of sea ice over scales of 10 to 100 km^2 is strongly dependent on the surface state (snow-covered versus bare ice, melt-pond distribution, and the proportion of open water, i.e., leads and polynyas). Robinson et al. (1992) summarized several years of interannual variations in surface albedo in the central Arctic Ocean. Similar compilations depicting decadal or longer-scale variations, or variations outside the Arctic Ocean, do not exist despite the potential value of such datasets for assessing the ice-albedo–temperature feedback.

6.3.2. Recent and ongoing changes

There has been an apparent reduction in sea ice over the past several decades, although this varies by region, by season, and by the sea-ice variable measured. Figure 6.4 shows the time series of Northern Hemisphere sea-ice extent, in terms of the seasonal cycle and the interannual variations (departures from climatological mean daily ice extent), for the period 1972 to 2002. Passive microwave imagery was available almost continuously during this period. Arctic sea-ice extent decreased by $0.30\pm0.03 \times 10^6$ km^2/10 yr between 1972 and 2002, but by $0.36\pm0.05 \times 10^6$ km^2/10 yr between 1979 and 2002, indicating a 20% acceleration in the rate of decrease (Cavalieri et al., 2003). Over the full 31-year period, the trend in summer (September) is $-0.38\pm 0.08 \times 10^6$ km^2/10 yr, whereas in winter (March) the trend is $-0.27\pm0.05 \times 10^6$ km^2/10 yr. For the 24-year period (1979–2002), the corresponding summer and winter trends are $-0.48\pm0.13 \times 10^6$ km^2/10 yr and $-0.29\pm0.06 \times 10^6$ km^2/10 yr, respectively (Cavalieri et al., 2003). These trends contrast with those of

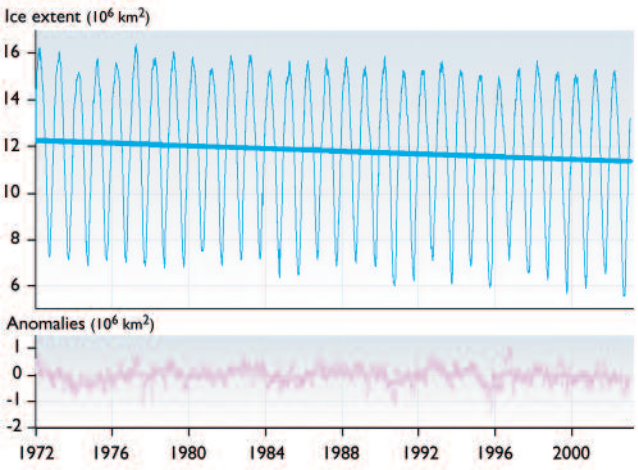

Fig. 6.4. Daily arctic sea-ice extent (upper) and anomalies (lower) between 1972 and 2002. A linear trend line is superimposed on the daily extents and a 365-day running mean has been applied to the daily anomalies (Cavalieri et al., 2003).

Southern Hemisphere sea ice, where the trends are either close to zero or slightly positive, depending on the period of analysis.

The recent trend of decreasing sea ice has also been identified in the coverage of multi-year sea ice in the central Arctic Ocean. An analysis of passive microwave-derived coverage of multi-year sea ice in the Arctic showed a 14% decrease in winter multi-year sea ice between 1978 and 1998 (Johannessen et al., 1999). Comiso (2002) analyzed trends in end-of-summer minimum ice cover for 1979 to 2000. Figure 6.5 contrasts the sea-ice concentrations at the time of ice minima during the first and second halves of the study period. The decrease is especially large north of the Russian and Alaskan coasts. The rate of decrease in perennial sea ice (9% per decade) computed by Comiso (2002) is consistent with the trend in multi-year sea-ice coverage found by Johannessen et al. (1999), and is slightly greater than the rate of decrease in total ice-covered area in recent decades (Cavalieri et al., 2003).

The decrease in sea-ice extent over the past few decades is consistent with reports from indigenous peoples in various coastal communities of the Arctic. In particular, the themes of a shortened ice season and a deteriorating sea-ice cover have emerged from studies that drew upon the experiences of residents of Sachs Harbor, Canada and Barrow, Alaska, as well as communities on St. Lawrence Island in the Bering Sea (Krupnik and Jolly, 2002).

Vinnikov et al. (1999) extended the record back to the 1950s using data from ships, coastal reports, and aircraft surveys, and found that the trends are comparable to those of the satellite period and are statistically significant. This study also compared the observed trends of the past several decades with estimates of natural (low-frequency) variability generated by a Geophysical Fluid Dynamics Laboratory (GFDL) climate model and showed that the decrease in arctic sea-ice extent is highly unlikely to have occurred as a result of natural vari-

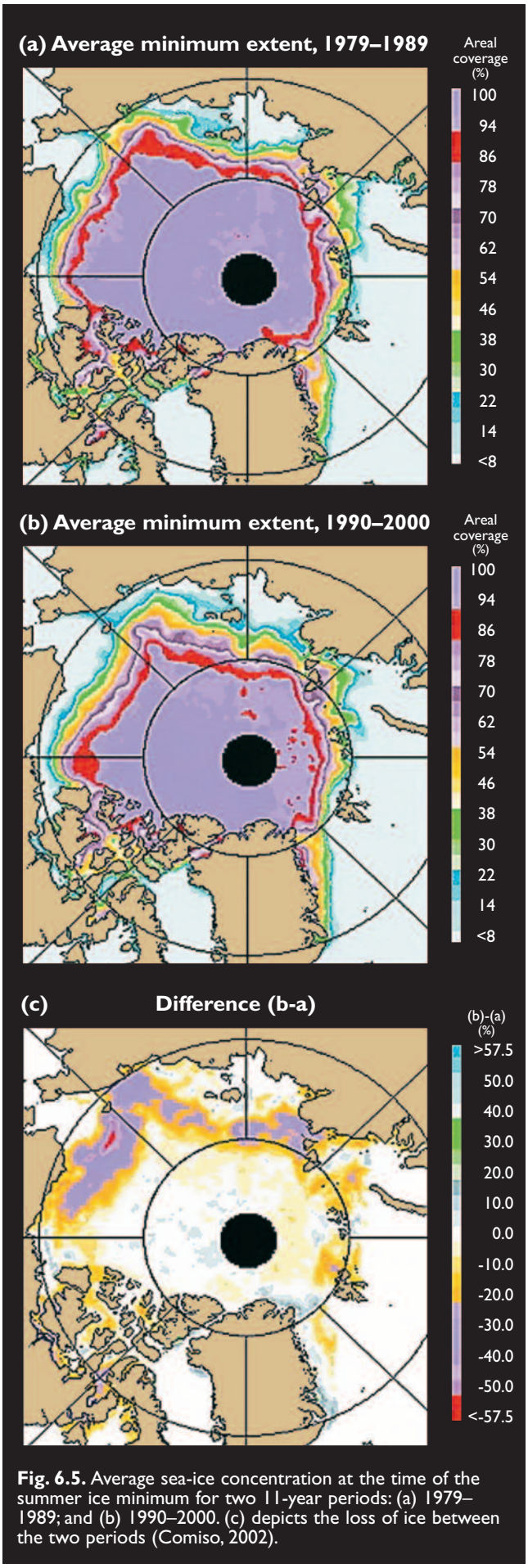

Fig. 6.5. Average sea-ice concentration at the time of the summer ice minimum for two 11-year periods: (a) 1979–1989; and (b) 1990–2000. (c) depicts the loss of ice between the two periods (Comiso, 2002).

ability alone. However, this conclusion is based on the assumption that the natural variability of sea ice can be reliably inferred from climate model simulations.

For longer timescales, the lack of sea-ice data limits estimates of hemispheric-scale trends. However, sufficient data are available for portions of the North Atlantic subarctic, based largely on historical ship reports and coastal observations, to permit regional trend assessments over periods exceeding 100 years. Perhaps the best-known record is the Icelandic sea-ice index, compiled by Thoroddsen (1917) and Koch (1945), with subsequent extensions (e.g., Ogilvie and Jonsson, 2001). The index combines information on the annual duration of sea ice along the Icelandic coast and the length of coastline affected by sea ice. Figure 6.6 shows several periods of severe sea-ice conditions, especially during the late 1800s and early 1900s, followed by a long interval (from about 1920 to the early 1960s) in which sea ice was virtually absent from Icelandic waters. However, an abrupt change to severe ice conditions in the late 1960s serves as a reminder that decadal variability is a characteristic of sea ice. Since the early 1970s, sea-ice conditions in the vicinity of Iceland have been relatively mild.

In an analysis that drew upon ship reports from the ocean waters east of Iceland, Vinje (2001) found that the extent of ice in the Nordic Seas during April had decreased by about 33% since the 1860s (Fig. 6.7). However, this dataset and longer versions spanning the past several centuries indicate large variations in trends over multi-decadal periods. Some earlier multi-decadal periods show trends comparable to those of the past several decades.

A widely cited study by Rothrock et al. (1999), based on a comparison of upward-looking sonar data from submarine cruises during 1958–1976 and 1993–1997, found a decrease of about 40% (1.3 m) in the sea-ice draft (proportional to thickness) in the central Arctic Ocean from the earlier to the later period. Wadhams and Davis (2000) provide further submarine-measured evidence of sea-ice thinning in the Arctic Ocean.

While the findings concerning ice draft and multi-year sea-ice coverage are compatible, the trends in ice draft have been evaluated using data from a relatively small subset of the past 45 years. Anisimov et al. (2003)

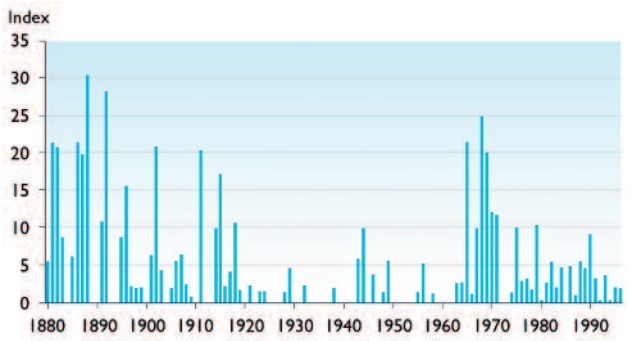

Fig. 6.6. Annual values of the Icelandic sea-ice index (T. Jakobsson, 2003).

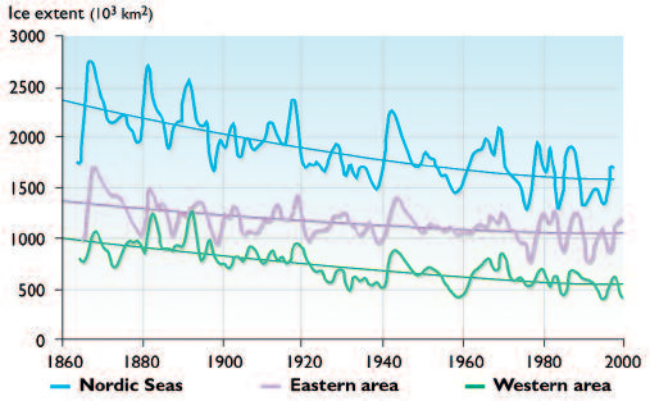

Fig. 6.7. Historical record of April sea-ice extent (two-year running means) in the Nordic Seas and in their eastern and western subregions (Vinje, 2001).

showed that a one-year shift in the sample of years examined by Rothrock et al. (1999) results in a much weaker trend in sea-ice draft. There are also indications that at least some of the decrease in ice thickness is a consequence of variations in the wind-driven advection of sea ice and that increases in ice thickness in unsampled regions (e.g., offshore of the Canadian Archipelago) may partially offset the decreases in the central Arctic Ocean detected in the 1990s (Holloway and Sou, 2002). Specifically, the sea-ice drafts in the western Arctic Ocean (Beaufort sector) appear to have decreased by about 1.5 m between the mid-1980s and early 1990s when the Beaufort Gyre weakened considerably in association with a change in the Arctic Oscillation (AO), altering the ice drift and dynamics in the region near the North Pole (Tucker et al., 2001). Proshutinsky and Johnson (1997) show that the pattern of arctic sea-ice drift has historically varied between two regimes, characterized by relatively strong and weak phases of the Beaufort anticyclone.

The association between the AO (or the North Atlantic Oscillation – NAO) and arctic sea ice is increasingly used to explain variations in arctic sea ice over the past several decades (e.g., Kwok, 2000; Parkinson, 2000; Rigor et al., 2002). Research has related the wind forcing associated with this atmospheric mode to sea-ice export from the Arctic Ocean through Fram Strait to the North Atlantic Ocean (Kwok and Rothrock, 1999), and to ice conditions along the northwestern coastline of the Canadian Archipelago (Agnew et al., 2003). However, studies of longer periods suggest that such associations with Fram Strait sea-ice export may not be temporally robust because of relatively subtle shifts in the centers of action of the NAO (Hilmer and Jung, 2000). Cavalieri (2002) reveals a consistent relationship over decadal timescales between Fram Strait sea-ice export and the phase of atmospheric sea-level pressure wave 1 at high latitudes. The phase of this wave appears to be a more sensitive indicator of Barents Sea low-pressure systems that drive sea ice through Fram Strait than the NAO index. In general, the role of sea-ice motion in diagnoses of historical change and projections of future change is largely unexplored.

6.3.3. Projected changes

This section summarizes the changes in sea ice projected for the 21st century by the five ACIA-designated models. In the case of the CGCM2 model, an ensemble of three different 21st-century simulations was available. The models all project decreases in sea-ice extent during the 21st century, although the time series contain sufficient variability that increases are found over occasional intervals of one to ten years, especially when coverage in specific regions of the Arctic is examined.

Two factors hamper quantitative comparisons of the projected changes in sea ice. First, the sea-ice variables archived by the various modeling centers vary from model to model, ranging from the presence of ice (binary 1/0) to concentration, thickness, and grid-cell mass. Since all of these variables permit evaluations of sea-ice extent (defined as the area poleward of the ice edge), ice extent is used for comparisons between the various models. Second, the sea ice simulated by these models for the baseline climate (1981–2000) is generally not in agreement with observed coverage (e.g., Fig. 6.3), especially when coverage in specific regions is considered. These biases in the baseline climate will confound interpretations of the model-derived coverage for a future time (e.g., the ACIA time slices centered on 2020, 2050, and 2080), since changes from a biased initial state are unlikely to result in a projected state that is free of biases. In an attempt to optimize the informational content of the projections of sea ice, the future sea-ice states projected by each model have been crudely adjusted by adding to each projection the baseline climate bias of sea ice for the particular model, month, and longitude. The need for this type of ad hoc adjustment will be eliminated as coupled atmosphere–ocean–ice model simulations become more realistic. The following synthesis of projections includes examples of both the raw (unadjusted) projections and the adjusted projections.

Figure 6.8 shows the 21st-century time series of total Northern Hemisphere sea-ice extent for March and September projected by the five models. The upper panels show the raw (unadjusted) time series and the lower panels show the adjusted time series. While the trends and variations are the same in both panels for a particular model, the starting points in 2000 are generally not, owing to the biases in the baseline climate simulations. Many of the differences between the models' unadjusted projections are due to the differences in the simulated baseline (1981–2000) sea-ice extent. For example, the unadjusted March sea-ice extents simulated for 1981–2000 range from approximately 13 to 20 million km^2, while the corresponding observational value, averaged over the entire month of March for the period 1990–1999, is about 14.5 million km^2. The models' raw projections show an even greater range in September, varying from about 2 to 11 million km^2, compared to the observational value of approximately 8 million km^2. The CSM_1.4 model consistently projects the greatest

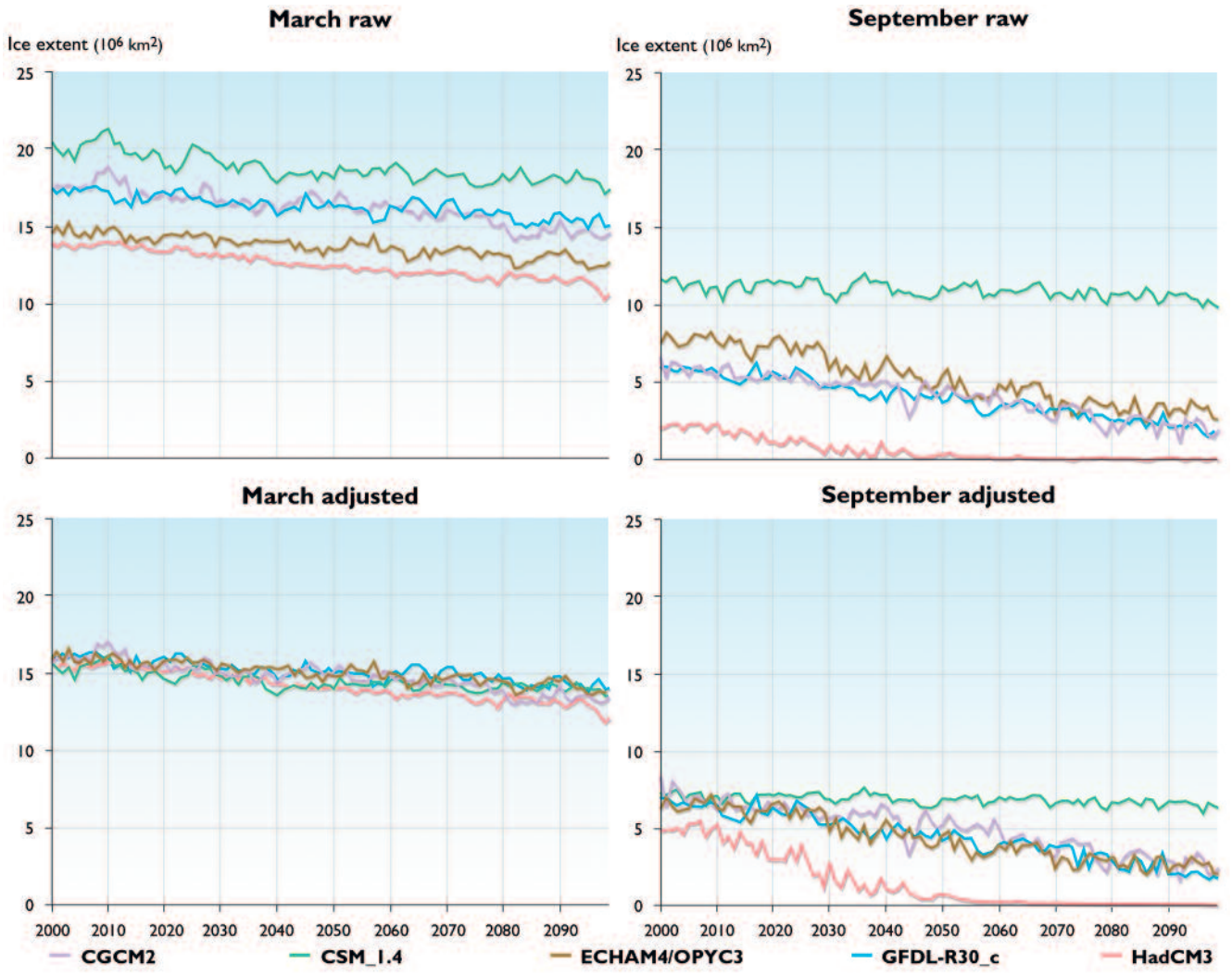

Fig. 6.8. 21st-century total Northern Hemisphere sea-ice extent projected by the five ACIA-designated models for March (left panels) and September (right panels). Upper panels show raw (unadjusted) model output; lower panels show projections adjusted for biases in simulated baseline (1981–2000) sea ice.

sea-ice extent, while the CGCM2 model consistently projects the least ice extent.

The raw projections from the CGCM2 model indicate an ice-free Arctic during September by the mid-21st century, but this model simulated less than half of the observed September sea-ice extent at the start of the 21st century. There is very little difference between the three ensemble simulations from the CGCM2 model, indicating that the initial conditions are less important than the choice of the model. None of the other models projects ice-free summers in the Arctic by 2100, although the sea-ice extent projected by the HadCM3 and ECHAM4/OPYC3 models decreases to about one-third of initial (2000) and observed September values by 2100.

For March, the projected decreases in sea-ice extent by 2100 vary from about 2 to 4 million km^2. Unlike September, none of the model projections for 2100 is close to ice-free in March, although the sea-ice extent projected by the CGCM2 model is only about 10 million km^2, which is about two-thirds of the initial (2000) March extent. A large proportion of the differences between the projected March sea-ice extents in 2100 is attributable to the differences in the initial (2000) ice extent simulated by the models.

Table 6.3 summarizes the 21st-century changes in mean annual sea-ice extent projected by the models. The greatest reductions in sea-ice cover, both as actual areas and as percentage reductions, are projected by the model with the least initial (2000) sea ice, while the smallest losses are projected by the model with the most initial (2000) sea ice. Insofar as sea-ice extent and mean ice thickness are positively correlated, this relationship is not surprising, i.e., the models projecting the greatest ice extent also project the thickest ice, which is more difficult to lose in a climate change scenario. However, the association found here between the initial sea-ice extent and the rate of ice retreat does not seem to be present in the Coupled Model Intercomparison Project suite of coupled global models (Bitz, pers. comm., 2003). Flato (2004) illustrated this lack of association.

When projections are examined on the basis of the the four ACIA regions (section 18.3), some spatial variations in the model-projected sea-ice retreat are apparent. However, the regional differences are generally small, and

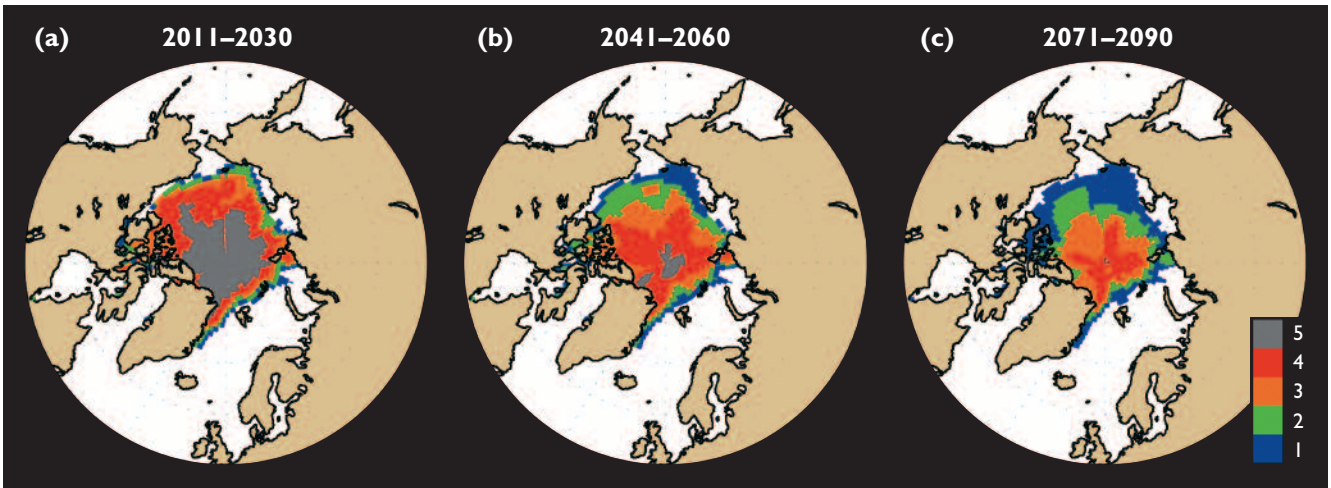

Fig. 6.9. Five-model composite maps of sea-ice coverage for September (a) 2011–2030, (b) 2041–2060, and (c) 2071–2090, expressed in terms of the number of models (out of five) that project the presence of sea ice during September for at least 50% of the years in the time slice.

are considerably less than the differences between the models. Winter sea-ice retreat, as measured by the changes in projected March ice extent, is greatest in Region 3 (150° E–120° W) for three of the model simulations (GFDL-R30_c, HadCM3, CSM_1.4). In the CGCM2 simulation, the March retreat is greatest in Region 1 (30° W–60° E). For the summer, the models show more regional variation in their projections of the greatest retreat. The GFDL-R30_c model projects the greatest summer sea-ice loss in Region 3, which is projected to become ice-free in September by the end of the 21st century. The HadCM3 and CGCM2 models project the most rapid retreat in Region 1, which is projected to become ice-free by 2100 using the unadjusted results from both simulations. The CSM_1.4 model projects little sea-ice loss in any region during the summer.

"Best estimates" of the sea-ice distributions in the ACIA time slices (2011–2030, 2041–2060, and 2071–2090) can be obtained by compositing the adjusted fields of sea ice from the five models. Figures 6.9 and 6.10 show these fields for September and March, respectively, expressed in terms of the number of models (out of five) that project the presence of sea ice during the specified month for at least 50% of the years in the time slice. Comparisons with Fig. 6.3 provide measures of the changes from 1990–1999 observed values. The distributions in Figs. 6.9 and 6.10 illustrate the tendency for the projected reductions in sea ice to be greater, especially as a percentage of the initial (2000) values, in September than in March. The September values for all of the time slices are less than the maximum of five (models projecting the presence of sea ice) over much of the Arctic Ocean (Fig. 6.9), which at present is largely ice-covered in September.

The projected reduction in sea-ice extent in winter (March, Fig. 6.10) is less than in summer, especially when expressed as a percentage of the present coverage. Most of the Arctic Ocean is projected to remain ice-covered in March, although the March sea-ice edge is projected to retreat substantially in the subpolar seas. However, the models that simulate sea-ice thickness or mass per grid cell project that the ice becomes thinner in the central Arctic Ocean throughout the 21st century.

6.3.4. Impacts of projected changes

On other parts of the physical system

The projected changes in sea ice extent and thickness are sufficiently large that their impact on the surface energy and moisture budgets will be substantial, affecting climate at least locally and regionally. For the five ACIA-designated models, the amount by which sea-ice extent is projected to decrease is correlated with the amount by

Table 6.3. Changes in mean annual Northern Hemisphere sea-ice extent between 2000 and 2100 projected by the five ACIA-designated models.

	Unadjusted projections			Adjusted projections		
	Ice extent (10^6 km^2)		Change (%)	Ice extent (10^6 km^2)		Change (%)
	2000	2100		2000	2100	
CGCM2	9.7	5.6	-42	12.3	6.6	-46
CSM_1.4	16.5	14.2	-14	12.3	10.8	-12
ECHAM4/OPYC3	11.9	8.9	-25	12.3	9.3	-24
GFDL-R30_c	11.9	8.5	-29	12.3	8.6	-30
HadCM3	12.8	9.4	-27	12.3	9.1	-26

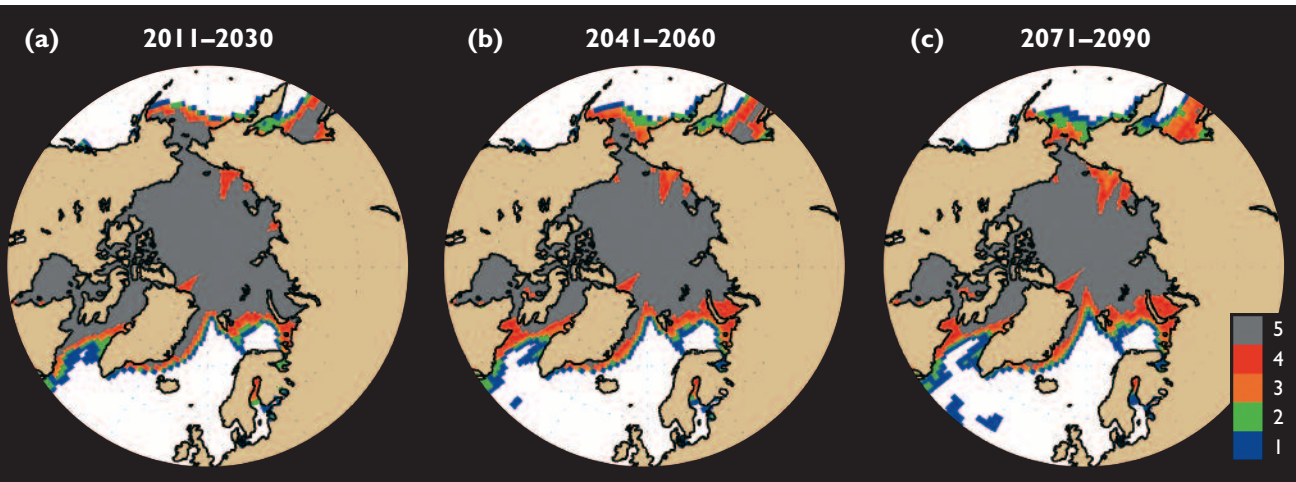

Fig. 6.10. Five-model composite maps of sea-ice coverage for March (a) 2011–2030, (b) 2041–2060, and (c) 2071–2090, expressed in terms of the number of models (out of five) that project the presence of sea ice during March for at least 50% of the years in the time slice.

which the Arctic is projected to warm (section 4.4.2) throughout the 21st century. This ranges from the relatively weak warming and small sea-ice retreat projected by the CSM_1.4 model to the strongest warming and greatest retreat projected by the CGCM2 model. For many months, especially in autumn and early winter, the projected loss of sea ice is unambiguously associated with the degree of warming projected by a particular model. Interestingly, the projected loss of sea ice is also consistently related to the models' projected global surface air warming.

A loss of sea ice is likely to enhance atmospheric humidity and cloudiness, and the general increase in precipitation noted in section 6.2 is at least partially attributable to the projected reduction in sea ice in the 21st-century scenarios, especially over and near the areas of sea-ice retreat. In areas of sea-ice retreat, ocean temperature and salinity near the surface will change, as will the upper-ocean stratification. Biogenic aerosol fluxes are also likely to increase.

There is potential for feedback between meteorological conditions and oceanographic conditions in that greater expanses of open water (at above-freezing temperatures) could strengthen low-pressure systems as they move across the arctic seas. More intense low-pressure systems will increase sea level and storm-surge height owing to the hydrostatic effect. Changes in sea-ice concentrations will also affect wave generation through the magnitude of the wind stress acting directly on the ocean.

On ecosystems

Light penetration in the upper ocean will increase in areas of sea-ice retreat, affecting phytoplankton blooms and the marine food web. Changes in ocean temperature accompanying a retreat in sea ice are likely to affect the distribution of fish stocks (Chapter 13). Marine mammals (e.g., walrus and polar bears) that rely on sea ice as a platform will be forced to find new habitats, and whale migration routes are likely to change as sea ice retreats.

On people

If the projected changes in sea ice occur, commercial navigation opportunities (section 16.3.7), and opportunities for offshore mineral extraction (section 16.3.10) will increase. Fish and mammal harvests are likely to be affected, and tourism activities are likely to increase. The absence of sea ice in previously ice-covered areas will have impacts on some types of military operations. Vulnerability to storms is likely to increase in low-lying coastal areas as the ice-free season lengthens, with corresponding impacts on residents and infrastructure (section 16.2.4.2). The stability of coastal sea ice for travel and other purposes will be reduced, with negative impacts on traditional subsistence activities.

6.3.5. Critical research needs

The discussion in section 6.3.3 focused on the large-scale sea-ice properties that can be simulated by models. The importance of small/subgrid-scale processes on large-scale behavior should also be emphasized. Among the main challenges involved in modeling ocean mixing in ice-covered seas is a representation of the effects of small-scale inhomogeneities in sea-ice cover (primarily lead fraction and distribution). This affects the surface exchange fluxes of momentum, heat, freshwater, and greenhouse gases (GHGs), and mixing processes under the ice. Processes specific to the surface boundary layer include the radically different surface fluxes in ice-covered versus ice-free fractions of a climate model grid cell; the strongly asymmetrical behavior of ice basal melting versus freezing; the interaction of tides and currents with ice-bottom morphology; and the modification of momentum transfer mechanisms as surface wave effects are replaced by stress transfer through the sea-ice cover. These are all subgrid-scale effects. Their successful representation in a climate model requires a combination of detailed observations, mathematical and physical process modeling, stochastic analysis, and numerical modeling at a range of resolutions and physical complexity. The

understanding and modeling of these processes are critical to more consistent and accurate simulations of sea-ice cover and climate. The inadequate treatment of small-scale processes may have contributed to the systematic errors in the model simulations discussed in section 6.3.3. These errors are limited to some regions and seasons for a few of the models, but are more pervasive in others. The errors increase the uncertainty in the projected rates of change in sea-ice variables. Thus, reducing or eliminating these errors is a high priority for assessments of future change in the arctic marine environment.

Model resolution is presently inadequate to capture changes in sea ice in coastal areas and in geographically complex areas such as the Canadian Archipelago. For example, finer resolution is required to address the types of sea-ice change that will affect navigability in the Northwest Passage. Section 16.3.7 addresses changes affecting the Russian Northern Sea Route (the Northeast Passage).

Data on surface albedo, particularly its seasonal, interannual, and interdecadal variations, are needed for a more rigorous assessment of the albedo–temperature feedback, including its magnitude in the present climate and the validity of its treatment in climate models. Field programs have made local measurements of surface albedo, radiative fluxes, and associated cloud parameters, but such data have not been fully exploited for model simulations of climate change. Also, the albedo–temperature feedback almost certainly involves changes in cloudiness, yet the nature and magnitude of these cloud-related effects are unknown.

Systematically compiled data on sea-ice thickness are needed to provide a spatial and temporal context for the recent decrease in sea ice observed in the central Arctic Ocean. The possibility that compensating increases in sea-ice thickness have occurred in other (unmeasured) areas of the Arctic Ocean raises fundamental questions about the nature and significance of the decreases detected in the vicinity of the submarine measurements. Satellite techniques for measuring sea-ice thickness throughout the Arctic would be particularly valuable. Moreover, the apparent redistribution of sea ice in recent decades indicates the importance of including ice motion in model-derived scenarios of change.

Finally, the role of sea-ice variations in the thermohaline circulation of the North Atlantic and the global ocean (section 2.5.1) must be clarified. While the potential exists for sea-ice variations to have significant global impacts (Mauritzen and Hakkinen, 1997), variations in the temperature and salinity of ocean water advected poleward from lower latitudes may explain much of the variability in deep convection in the subpolar seas. A better understanding of the relationship between sea ice and ocean circulation is perhaps the highest priority for assessments of arctic–global interactions, given the potential for sea ice to have a substantial effect on the thermohaline circulation, which in turn has the potential to change the climate of northern Europe and much of the Arctic Ocean.

6.4. Snow cover

6.4.1. Background

Terrestrial snow cover is the most rapidly varying cryospheric variable on the surface of the earth. An individual frontal cyclone can change the area of snow-covered land (or sea ice) by 0.1 to 1.0 million km^2 in a matter of days. Snow cover also displays large spatial variability in response to wind, and to topographic and vegetative variations. Yet it is the spatially integrated accumulation of snow over one to two seasons that has important hydrological implications for arctic terrestrial regions and the polar oceans, and hence for terrestrial and marine ecosystems. Snow also represents the fundamentally important accumulation component of ice sheets and glaciers (section 6.5). Finally, snow cover influences the ground thermal regime and therefore the permafrost changes (section 6.6) that have additional hydrological implications (section 6.8).

Before the availability of satellite imagery in the 1960s, snow cover was determined from occasional aerial photographs and from point measurements, often made at weather stations spaced irregularly over the land surface. In cold and windy environments such as the Arctic, point measurements are inaccurate because snow gauges are inefficient and drifting snow contaminates the measurements (Goodison and Yang, 1996). In addition, even accurate point measurements may not be representative of large-area or regional snow-cover conditions. The inaccuracy of the point measurements makes them inadequate for mapping the detailed spatial structure of snow coverage and depth, especially in regions of significant topography. Because snow cover is easily identified in visible and near-infrared wavelength bands, owing to its high reflectance, satellites have proven valuable in monitoring variations in snow cover at various scales over the past three to four decades. Unfortunately, most sensors cannot measure snow depth or water equivalent (Dankers and De Jong, 2004).

The present distribution of snow cover in the Northern Hemisphere, excluding permanently glaciated areas such as Greenland, varies from <1 million km^2 in late August to 40 to 50 million km^2 in February (Ramsay, 1998; Robinson, 1993). The large range in the February values indicates the interannual variability. Figure 6.11 shows the frequency of snow cover on the land areas of the Northern Hemisphere from 1966 to 2000 during winter (December), early and late spring transition months (February and May), and an autumn transition month (October). It is apparent that snow is a quasi-permanent feature of the arctic terrestrial landscape during winter. The variability inherent in subarctic land areas during the spring (Fig. 6.11b), when insolation is relatively strong, implies that the timing of the snowmelt, which reduces the surface albedo by 20 to

60%, can strongly affect surface absorption of solar radiation. Models have demonstrated the importance of snow cover for the surface energy budget, soil temperature, and the permafrost active layer (Ling and Zhang, 2003; Sokratov and Barry, 2002). Snow cover is also highly variable in October (Fig. 6.11c), when insolation and hence the potential for snow to affect the surface absorption of solar radiation is weaker. Snow is rarely present over the subarctic land areas in July and August.

The hydrologically important characteristic of snow cover is its water equivalent, since this moisture is eventually released to the atmosphere by sublimation or evaporation, or to the polar oceans by runoff. Some of the snow water is siphoned off for human use prior to its eventual release to the atmosphere or ocean. Estimated fields of snow water equivalent (or snow depth) can be derived from satellite passive microwave measurements (Armstrong and Brodzik, 2001; Chang et al., 1987; Goodison and Walker, 1995). Although the spatial coverage of these measurements is complete and their broad spatial patterns are correct, there are large uncertainties and errors for areas in which vegetative masking (vegetation obscuring the underlying snow, making the ground appear darker) is significant (e.g., the boreal forests of the subarctic). Even allowing for the uncertainties, the derived snow water equivalents represent large water supplies that are released to other parts of the climate system during spring melt.

Station-derived climatologies of snow depth represent alternatives to the satellite-derived estimates and their associated uncertainties. Such climatologies have been compiled for Canada (e.g., Brown R. and Braaten, 1998) and for Russia (e.g., Ye H. et al., 1998). However, these compilations are subject to elevation- and location-related biases in the station networks. Section 6.4.2 summarizes broad-scale variations in these trends.

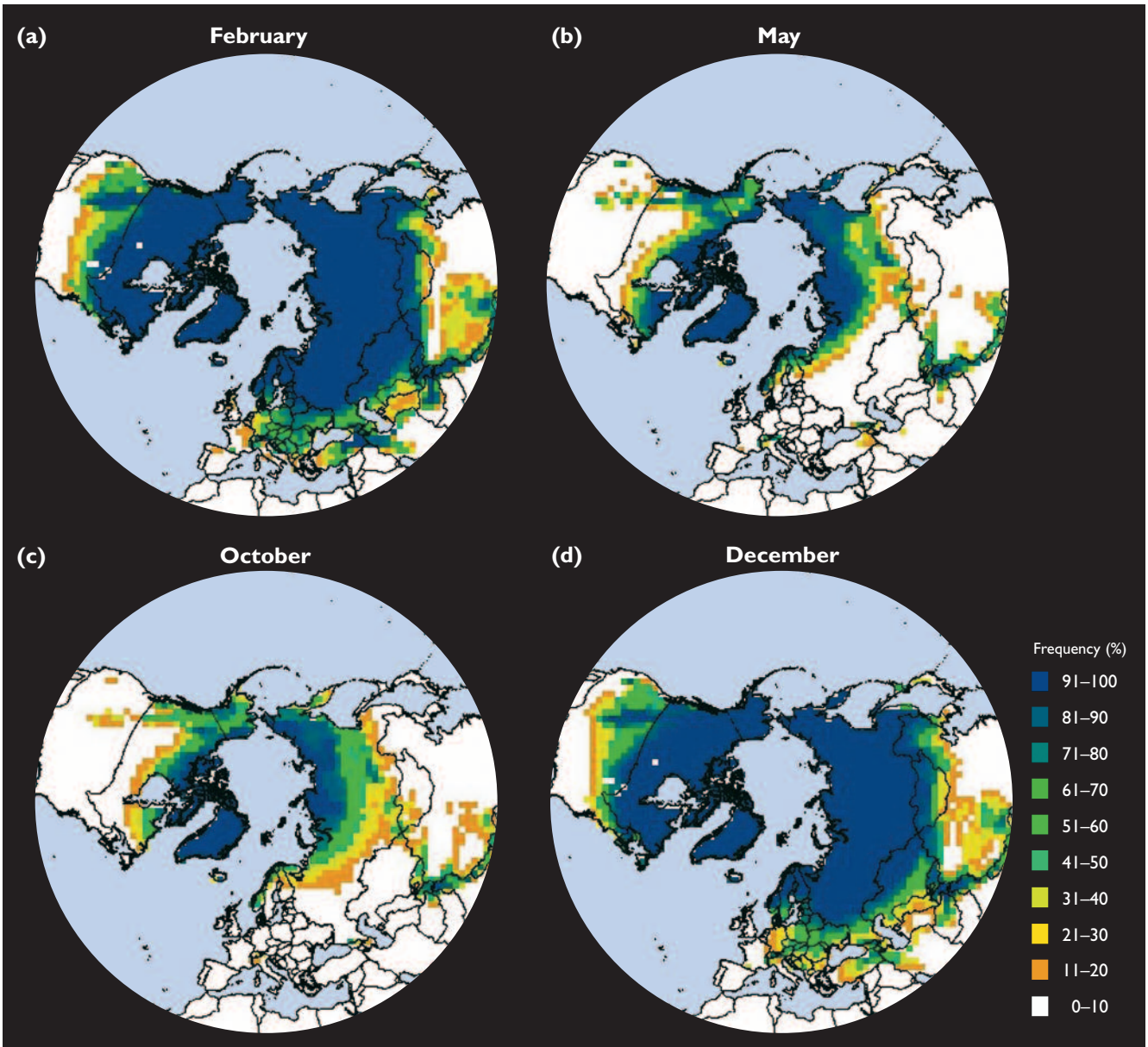

Fig. 6.11. Frequency of snow cover on the land areas of the Northern Hemisphere during early and late spring transition months (February and May), an autumn transition month (October), and winter (December). Frequency is determined by the percentage of weeks in the specified month over the 35-year period 1966 to 2002 that a location had snow cover. In all panels, the 50% contour (in the green zone) represents the approximate climatological mean position of the snow boundary (figure courtesy of D. Robinson, 2003).

Radionov et al. (1997) compiled statistics of snow depth and duration over the central Arctic Ocean using measurements obtained at the Russian drifting ice stations, primarily between the 1950s and 1990.

Over glaciated regions, where snow stakes and altimetry are major sources of information, the problem of spatial integration of snow measurements is quite different from that over regions of seasonal snow cover. Section 6.5 discusses mass-balance measurements for glaciers and ice caps on a regional basis.

Albedo is highly relevant to the role of snow in the surface thermal regime. The albedo of snow-covered land areas is highly variable, depending on snow depth, snow age, and the masking characteristics of vegetation. There are few systematic compilations of surface albedo over snow cover, so the climatology and variability of surface albedo are not well documented at the circumpolar scale. Winther (1993) and others have studied albedo variations on a regional basis.

Snow is a key variable in the rates of soil warming and permafrost thawing. Because snow effectively insulates the upper soil layers during winter, increases in snow depth generally result in higher soil temperatures during the cold season, while an absence of snow results in more rapid and greater cooling of the soil. If snowfall changes substantially as climate changes, warming and thawing or cooling and freezing may significantly affect the upper soil layers. Permafrost models (section 6.6) require information on snow cover in addition to air temperature if they are to provide valid simulations of variations in the temperature and water phase in the upper soil layers. In general, climate models treat the subsurface effects of snow rather crudely, particularly with regard to the freeze-thaw cycle of soils over seasonal to centennial timescales.

6.4.2. Recent and ongoing changes

Over a few months, snow cover in the Northern Hemisphere (excluding sea ice, Greenland, and glaciers) varies between the 0 to 5 million km^2 typical of summer and the more than 40 million km^2 typical of winter. The rapidity of the expansion and retreat (melt) is comparable in the autumn and spring, and indicates the short timescales for variations in snow cover relative to other cryospheric variables. Interannual variations are also rapid. Figure 6.12, for example, shows the 12-month running means of snow extent between 1972 and 2003, the period of homogeneous visible satellite data. While these fluctuations complicate the detection and interpretation of trends, least-squares fits to the time series in Fig. 6.12 indicate that the areal coverage of snow has decreased over the past few decades. The decrease for the Northern Hemisphere is nearly 10% over the period 1972 to 2003. Both North America and Eurasia show decreases, although the decrease is greatest for Eurasia. However, the decrease is highly seasonal, varying from no significant change in autumn and winter to decreases

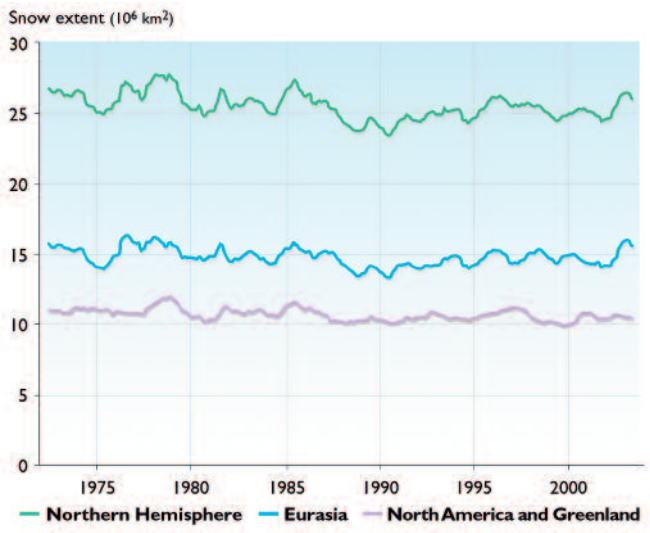

Fig. 6.12. Twelve-month running mean of snow extent in the Northern Hemisphere from 1972 to 2003, showing the entire hemisphere, North America and Greenland, and Eurasia (data from D. Robinson, 2003).

greater than 10% in spring and summer (Fig. 6.13). The large areal decrease in spring is correlated with the large spring warming over the northern land areas (section 2.6.2). The summer trend, to which the arctic land areas are probably making key contributions, has received little attention in the literature.

For the period before satellite data were available, variations and trends in snow cover have been assessed largely on a regional basis. North American snow cover shows a general decrease in spring (March–April) extent since the 1950s (Fig. 6.13a), although there are indications that spring snow extent increased during the earlier part of the 20th century. The spring decrease is also apparent in the Eurasian data (Fig. 6.13b). The total extent of Northern Hemisphere snow during spring and summer was lower in the 1990s than at any time in the past 100 years (IPCC, 2001). However, the longer records shown in Fig. 6.13 do not indicate a systematic decrease in snow cover during autumn or early winter for either landmass.

Recent variations in snow depth are more difficult to assess because of measurement and remote-sensing difficulties in vegetated areas. For the pre-satellite era, the sparseness of the synoptic station network precluded systematic mapping of snow depth in many high-latitude areas. Nevertheless, there have been compilations and analyses of snow-depth data for particular regions. Snow depth appears to have decreased over much of Canada since 1946, especially during spring (Brown R. and Braaten, 1998). Winter snow depths have decreased over European Russia since 1900 (Meshcherskaya et al., 1995), but have generally increased elsewhere over Russia during the past few decades (Fallot et al., 1997), in agreement with the increase in precipitation noted in section 6.2.2. Ye H. (2001) reports a small (several day) increase in the snow-season length, due primarily to later snowmelt, over north-central and northwest Asia

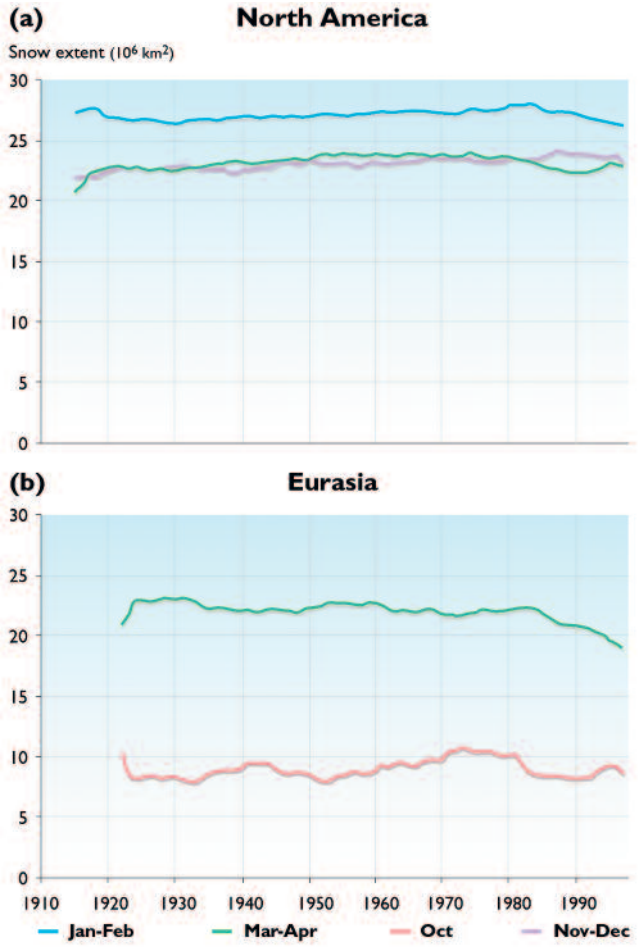

Fig. 6.13. Eleven-year running mean of snow cover extent from 1915 to 1997 for (a) North America and (b) Eurasia (data from R. Brown, 2000).

for the period 1937 to 1994. However, this study excludes the years since 1994, during which northern Asia has been relatively warm in winter and spring.

Over the central Arctic Ocean, measurements at Russian North Pole ice stations from the mid-1950s to 1990 suggest a decrease in snow depth, although considerable variability is superimposed on this decrease (Radionov et al., 1997). Measurements of total precipitation at the same sites show little indication of any systematic trend (Radionov et al., 1997).

Thus, there are consistent indications of spring warming of arctic terrestrial regions (section 2.6.2.1) and earlier disappearance of snow cover. Associated changes are the earlier breakup of ice-covered lakes and rivers (section 6.7) and a seasonal advance (from early spring to late winter) in the timing of the primary pulse of river discharge in the Arctic (section 6.8).

6.4.3. Projected changes

Simulations of 21st-century climate from the five ACIA-designated climate models (section 4.4) were examined for projected changes in snow cover. These changes are complicated by the conflicting effects of higher temperatures, which will result in a poleward retreat of the snow margin, but which are also likely to contribute to an acceleration of the hydrological cycle and – in those regions that remain consistently below freezing – an increase in snowfall and possibly snow depth (water equivalent).

Table 6.4 summarizes the changes in snow cover projected by the five ACIA-designated models, including snow cover simulated for the baseline climate (1981–2000) and the changes averaged over each of the three ACIA time slices: 2011–2030, 2041–2060, and 2071–2090. It is apparent that the projected changes in mean annual snow cover are not large, even by 2071–2090 when the changes range from -9 to -18%.

However, there is a notable seasonality to the changes in snow cover. Table 6.5 summarizes the changes projected to occur between the baseline (1981–2000) and 2071–2090 by season. While the percentage changes are greatest in summer (when areal coverage is very small in the present climate), the actual decrease in snow-covered area is greatest in spring (April and May).

A more detailed evaluation (Table 6.6) shows that the months with the largest projected reductions in snow extent are April and November, followed by May, March, and December. The changes most relevant to arctic hydrology are those that occur in spring, when a reduction in snow cover implies an earlier pulse of river discharge to the Arctic Ocean and coastal seas. That the greatest projected changes occur during the spring, late autumn, and early winter indicates a shortened snow season in the model simulations for the late 21st century. Figure 6.14 illustrates the distribution of snow cover during the 2071–2090 time slice for March, May,

Table 6.4. Northern Hemisphere mean annual snow cover simulated by the five ACIA-designated models for baseline climate (1981–2000) and percentage change from the baseline projected for each of the ACIA time slices.

	Snow cover (10^6 km^2)	Percentage change from baseline (1981–2000)		
	1981–2000	2011–2030	2041–2060	2071–2090
CGCM2	27.8	-7	-13	-17
CSM_1.4	23.8	-3	-5	-9
ECHAM4/OPYC3	18.6	-6	-13	-18
GFDL-R30_c	31.9	-4	-7	-10
HadCM3	23.0	-4	-8	-10
Observed	23.2			

Table 6.5. Seasonal change in snow extent (10^6 km^2) between 1981–2000 and 2071–2090 projected by the five ACIA-designated models.

	Winter (Dec–Feb)	Spring (Mar–May)	Summer (Jun–Aug)	Autumn (Sep–Nov)
CGCM2	-5.8	-6.8	-3.2	-3.2
CSM_1.4	-2.8	-3.2	-0.4	-2.2
ECHAM4/OPYC3	-5.5	-6.2	-0.6	-3.4
GFDL-R30_c	-2.3	-5.1	-0.6	-4.6
HadCM3	-2.8	-3.1	-0.5	-3.0
Five-model mean	-3.8	-4.9	-1.1	-3.3

October, and December. A comparison with the present-day frequency distributions for May, October, and December (Fig. 6.11) shows that the snow retreat is modest but visually noticeable, especially in May.

6.4.4. Impacts of projected changes

On other parts of physical system

The primary effects of a reduction in snow cover will be on the surface energy budget (hence soil temperature and permafrost) and on the surface moisture budget (runoff, evaporation). However, the effects of changes in snow cover will vary seasonally. During winter, snow insulates the ground, so a reduction in snow cover or depth will lead to cooling of the underlying ground. During spring, a decrease in snow cover will lower the surface albedo, leading to enhanced absorption of solar radiation and warming of the ground. For sea ice, decreased snow cover will accelerate ice melt in the spring while increased snow cover will retard ice melt.

Changes in snow cover also have the potential to influence significantly the distribution of vegetation (Bruland and Cooper, 2001), which can then influence the atmosphere through changes in vegetative masking, surface albedo, and the surface energy budget. Snow cover also affects the exchange of GHGs between the land surface and the atmosphere, as documented in the Land Arctic Physical Processes experiment (Anon, 1999).

On ecosystems

The growth season of high-latitude vegetation, and hence primary production and carbon dioxide (CO_2) uptake, depends strongly on the timing of snow disappearance, which in turn depends on antecedent snow accumulation. Snow insulates underlying vegetation and other biota (e.g., mammals, insects). The runoff pulse produces large biogeochemical fluxes from terrestrial to marine ecosystems, and changes in the spring snowmelt will affect both the timing and intensity of this pulse. An important characteristic of snow cover is its structure, especially the presence of ice layers that can result from thaw–freeze cycles or from freezing rain events. The presence of ice layers can severely hamper winter grazing by wildlife (section 12.2.4). Unfortunately, neither the observational database nor the model output can provide useful information on the presence of ice layers in snow, although it is reasonable to assume that a warming climate will increase the frequency of winter freeze–thaw cycles and freezing rain events in arctic terrestrial regions.

On people

Changes in the amount of snow will have impacts on transportation (e.g., feasibility, safety, costs); recreation activities and the businesses dependent on them (e.g., ski resorts, snow machines); snow loading on structures and removal costs; avalanche hazards in areas with steep topography; and water supplies for various population sectors. Because the costs of clearing snow from roads are significant in many mid- and high-latitude communities, economic consequences of changes in the amount of snow are very likely. In addition, changes in the length of the snow-free season would affect agricultural, industrial, and commercial activities as well as transportation in many high-latitude communities. Changes in the amount of snow and the length of the snow season will also directly affect the subsistence activities of indigenous communities.

6.4.5. Critical research needs

Global climate model simulations of snow extent have shown some improvement over the past decade (Frei et al., 2003). However, a climatology of the spatial distribution of snow water equivalent in each month is a critical need for model validation and hydrological simulations. This is especially urgent for high latitudes, where there are few *in situ* measurements of snow water equivalent to complement the estimates derived from passive microwave measurements. Information on snow albedo over northern terrestrial regions, especially for vegetated areas and for the late winter and spring seasons when the timing of snowmelt is hydrologically critical, is an additional requirement. Global daily snow-albedo products derived from the Moderate-

Table 6.6. Five-model monthly means of the projected change in snow extent (10^6 km^2) between 1981–2000 and 2071–2090.

	Jan	Feb	Mar	Apr	May	Jun	Jul	Aug	Sep	Oct	Nov	Dec
Change in extent	-3.7	-3.8	-4.2	-5.4	-5.0	-2.1	-0.9	-0.3	-1.2	-3.6	-5.1	-4.0

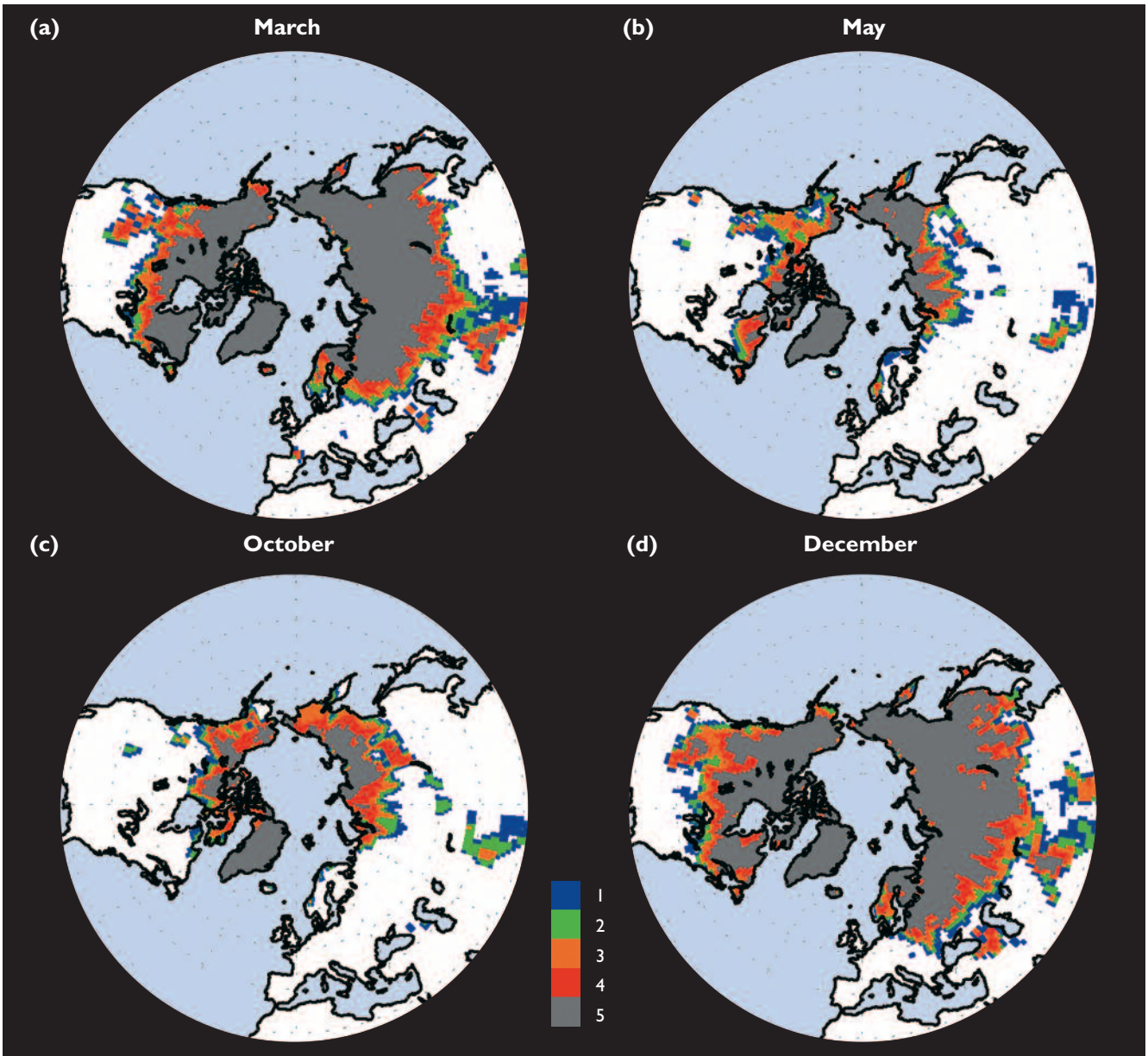

Fig. 6.14. Distribution of snow cover during the 2071–2090 time slice for March, May, October, and December, using as the measure of coverage the number of models (out of five) that project the presence of snow during the specified month for at least half of the years in the time slice.

Resolution Imaging Spectroradiometer are now available (Hall et al., 2002); such products should be used for quantitative assessments of large-scale albedo variations and for climate model validation.

The ability of models to simulate the snowmelt process also needs further investigation within the context of arctic hydrology. This should result in evaluations of feedbacks between the timing of snowmelt and broader changes in terrestrial ecosystems.

A potentially important but often overlooked process is the sublimation of snow, especially when enhanced by blowing snow. Sublimation can be a key part of the hydrological cycle locally and regionally (Pomeroy and Li, 2000), yet climate models do not include the enhancement of sublimation by blowing snow, and some models do not include even the direct sublimation of snow from the surface.

6.5. Glaciers and ice sheets

6.5.1. Background

Dowdeswell and Hagen (2004) estimated that the total volume of land ice in the Arctic is about 3.1 million km^3, which corresponds to a sea-level equivalent of about 8 m. In terms of volume and area, the largest feature is the Greenland Ice Sheet, which covers about four times the combined area of the glaciers and ice caps of Alaska, the Canadian Arctic, Iceland, Svalbard, Franz Josef Land, Novaya Zemlya, Severnaya Zemlya, and northern Scandinavia (Table 6.7). However, unlike most small glaciers and ice caps, more than half the surface of the Greenland Ice Sheet is at altitudes that remain well below freezing throughout the year. Hence, relative to the Greenland Ice Sheet, the smaller ice caps and glaciers are susceptible to greater percentage

changes of mass and area in response to changes in temperature and precipitation.

The arctic glaciers and ice caps are irregularly distributed in space (Fig. 6.15), and are located in very different climatic regimes. The glaciers in southern Alaska and Iceland are subject to a maritime climate with a relatively small annual temperature range and high precipitation rates (a few meters per year). Conversely, the glaciers in the Canadian High Arctic are in a very continental climate. The summer is short, the annual temperature range is very large, and precipitation is about 0.25 m/yr. The conditions on Svalbard and the Russian Arctic islands fall between these two climatic regimes.

The Greenland Ice Sheet covers a wide latitude belt. The climate is dry and cold in the north, although summer temperatures can be high, with mean July temperatures of up to 5 to 6 °C (Ohmura, 1997). The North Atlantic storm track directly influences the southeastern part of the ice sheet. Maritime air masses are pushed onto the ice sheet and release large amounts of moisture. The accumulation rates are greatest in this part of the Greenland Ice Sheet.

The morphology of arctic glaciers shows great variety (e.g., Williams R. and Ferrigno, 2002). Some ice caps are dome-shaped, with lobes and outlet glaciers in which the ice drains away from the accumulation area to the melting regions or calving bays. Examples occur in the Canadian Arctic, Iceland, and the Russian Arctic islands. In other regions, large glaciers originate from ice fields that cover the area between mountain ranges (e.g., in southern Alaska). Many regions (e.g., Svalbard) also have a large number of individual valley glaciers.

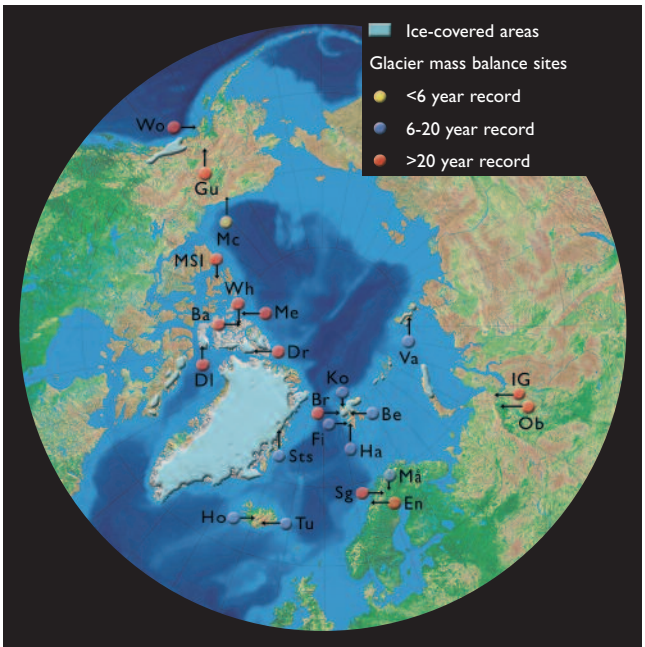

Fig. 6.15. Ice-covered areas and the location of glaciers and ice caps for which mass balance data are available. Wo: Wolverine Glacier, Gu: Gulkana Glacier, Mc: McCall Glacier, MSI: Melville South Ice Cap, Ba: Baby Glacier, Me: Meighen Ice Cap, Dl: Devon Ice Cap, Dr: Drambui Glacier, Ho: Hofsjökull, Tu: Tungnarjökull, Br: Austre Brøggerbreen, Ko: Kongsvegen, En: Engabreen, Sg: Storglaciären, IG: Igan, Ob: Obruchev, Va: Vavilov, Ha: Hansbreen, Wh: White, Be: Bear Bay, Fi: Finsterwalderbreen, Ma: Storglaciären, Sts: Storstrommen (modified from Dowdeswell et al., 1997).

There are many surging glaciers in the Arctic. In a surging event, glacier fronts can move forward many kilometers (sometimes more than 10 km) in a matter of years. After a surge, a build-up phase starts and the glacier accumulates mass for the next surge. Depending on the size of the glacier, the duration of the build-up phase ranges from a few decades to a few centuries. Surging glaciers occur in Alaska, Canada, Svalbard, and Iceland, and have also been observed in other areas of the Arctic. A surge event may change the flow and geometry of the glacier. While an individual surge is not directly related to climate change, increased melting may have an effect on the periodicity of surging.

Glaciers, ice caps, and ice sheets respond to climate changes over very different timescales depending on their size, shape, and temperature condition. The smaller glaciers are likely to respond quickly, with shape, flow, and front position changing over a few years or a few decades, while the Greenland Ice Sheet responds to climate changes over timescales of up to millennia. Parts of the Greenland Ice Sheet may still be responding to climate variations that occurred thousands of years ago.

Many glaciers in dry regions have low accumulation rates. Consequently, it takes a long time before the climate signal penetrates into these glaciers, and over a 100-year timescale, the effects are unlikely to be very large. However, in areas where meltwater penetration increases, the effect of latent heat release is likely to cause a faster response in the thermal regime.

Because arctic glaciers have such a wide variety of morphological and climatic regimes, the most difficult task in this assessment is to extrapolate results for a few glaciers and ice caps to all ice masses in the Arctic. Mass-balance measurements have been conducted on some glaciers for shorter or longer periods (Fig. 6.15), but only a small fraction of the glaciated area is moni-

Table 6.7. Ice coverage in arctic regions with extensive glaciation (Dowdeswell and Hagen, 2004).

	Glacier area (10^3 km^2)
Greenland Ice Sheet	1640.0
Canadian Arctic (>74° N)	108.0
Canadian Arctic (<74° N)	43.4
Alaska	75.0
Iceland	10.9
Svalbard	36.6
Franz Josef Land	13.7
Novaya Zemlya	23.6
Severnaya Zemlya	18.3
Norway/Sweden	3.1

tored. Attempts have been made to extrapolate measurements, parameters, and models from a small number of glaciers to obtain regional estimates (e.g., Dyurgerov and Meier, 1997), although extrapolation introduces considerable uncertainty into conclusions about ongoing and future changes in the area and volume of land ice and associated changes in sea level (section 6.5.3).

Glaciers gain mass from snowfall and lose mass mainly through iceberg calving, surface melting and runoff, and melting under floating ice shelves. The specific net balance is the net annual change in mass per square meter, often expressed in kg/m^2 or meter water equivalent (mwe). The mass balance is positive in the accumulation zone and negative in the ablation zone. The equilibrium line separates the accumulation and ablation zones.

Meltwater formed at the surface may percolate into the snowpack and refreeze to form ice lenses and glands. Eventually the meltwater freezes onto the ice surface below the snowpack to form superimposed ice. Part of this ice subsequently melts in the summer, but the remainder survives. Refreezing and the formation of superimposed ice can have a significant influence on the energy budget of the melt process (Ambach, 1979) and can decrease the altitude of the equilibrium line. The quantitative effects of refreezing on the mean specific balance of a glacier are not well understood, and are rarely treated well in mass-balance models. With respect to relatively rapid climate change, an important question is whether the increasing amounts of meltwater will add to runoff or be retained in cold firn (compact, granular snow that is over one year old) fields.

Iceberg calving is another process for which a universal model does not exist. For many glaciers in the Arctic, the amount of ice lost by meltwater runoff is larger than the amount lost by calving, but calving is significant for many glaciers (typically 15 to 40% of the total mass loss for glaciers on the islands in the Eurasian Arctic sector) (Dowdeswell and Hagen, 2004). For the Greenland Ice Sheet, the IPCC (2001) estimated that the losses from meltwater runoff and calving are of the same order of magnitude. Researchers have attempted to determine a linear relationship between the calving rate and water depth or ice thickness at the glacier front. This seems to work for many individual glaciers, but the coefficients show large spatial variation.

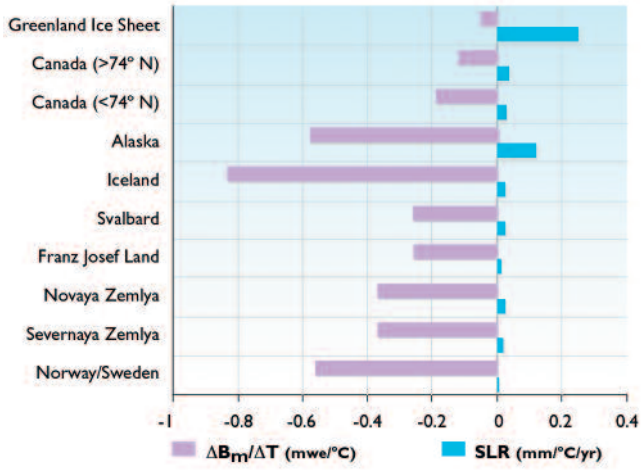

Fig. 6.16. Mass-balance sensitivity to temperature change (lavender) and potential sea-level rise (blue) for the arctic regions with extensive glaciation listed in Table 6.7. $\Delta B_m/\Delta T$ is the change in mass balance (meter water equivalent) per °C of temperature change; SLR is sea-level rise (J. Oerlemans, 2003).

The mass-balance sensitivities vary widely among glaciers. Differences in the sensitivity to annual anomalies of temperature and precipitation reach one order of magnitude. In the high Arctic, where winter temperatures are consistently below freezing, only the summer temperature affects the mass balance. In a maritime climate such as for Iceland, sensitivity to temperature change is much greater, and temperature anomalies in other seasons are also important. For all glaciers in maritime climates, where most of the summer precipitation falls as rain, the sensitivity to precipitation anomalies shows a marked seasonality.

The sensitivity of a glacier to atmospheric forcing can be estimated using a mass-balance model and the field measurements that are required for calibrating the model. The potential contribution to sea-level rise from an entire region is obtained by multiplying the annual climate sensitivities (expressed in millimeters) by the total glacier area in the region. However, the mass-balance sensitivity for a region must be extrapolated from the calculations for specific glaciers. Figure 6.16 summarizes mass-balance sensitivities to temperature for the Arctic regions in Table 6.7 and shows the corresponding consequences for global sea level.

Recent events have demonstrated the potential for calving glaciers to undergo very rapid change. Calving glaciers that have retreated over large distances during the last hundred years, or even the last few decades, exist throughout the Arctic and subarctic. Well-documented examples include Jakobshavn Isbrae, West Greenland (Weidick et al., 1992; Williams R.S., 1986), Breidamerkurjökull, Iceland (Björnsson et al., 2001), Columbia Glacier, Alaska (Pfeffer et al., 2000), and Kronebreen and Hansbreen in Svalbard (Jania and Kaczmarska, 1997, Lefauconnier et al., 1994).

Although understanding of the processes that control calving is limited (e.g., Van der Veen, 1996, 1997), a clear relation to climatic forcing is not evident. Many internal mechanisms play a role, including sedimentary and erosive processes below and in front of a glacier tongue. During retreat, some calving glaciers tend to "jump" from pinning point to pinning point; other glaciers retreat steadily over a rather simple bed. While climatic factors will affect the extent of calving glaciers over the long term, the response of many glaciers is of an irregular and episodic nature, and is therefore unpredictable.

6.5.2. Recent and ongoing changes

The general pattern of glacier and ice-cap variations in the Arctic (apart from the Greenland Ice Sheet) is a retreat of glacier fronts, indicating a volume decrease since about 1920 that follows a period of general temperature increase throughout the Arctic. However, there are large regional variations in the magnitude of this retreat, and it is not known whether thickening in the accumulation areas may be compensating for some or all of the frontal retreat. Long-term mass-balance investigations have been conducted for only a few glaciers (Fig. 6.15), which occupy less than 0.1% of the total glaciated area in the Arctic. For the measured glaciers, no clear trends are discernible in the mass-balance parameters, winter accumulation, or summer melting prior to 1990 (Dowdeswell et al., 1997; Jania and Hagen, 1996). Several of the glaciers had a negative mass balance, but with no acceleration in the melt rate. However, changes in these trends since 1990 have been observed. Arendt et al. (2002) observed increased and accelerating melting of Alaskan glaciers, and the same trend has been reported for the Devon Ice Cap in northern Canada (Koerner, pers. comm., 2003).
In other parts of the Arctic (e.g., Svalbard), no accelerated melting has been observed (Hagen and Liestøl, 1990; Lefauconnier et al., 1999). In subarctic areas (i.e., Scandinavia), increased precipitation and positive mass balance were observed from 1988 to 1998, although the mass balances have generally been negative since 1998 (Dowdeswell and Hagen, 2004; Dyurgerov and Meier, 1997; Jania and Hagen, 1996).

Figure 6.17 presents a spatially integrated picture of arctic ice caps and mountain glaciers, obtained by grouping glaciers into geographic regions and assuming that glaciers in the same region have similar mass balances (Church J. et al., 2001; Dyurgerov and Meier, 1997). The figure shows the accumulated ice volume change since 1960 in three areas: the North American Arctic (Alaska and Canada); the Russian Arctic (arctic islands, northeast Siberia, and polar Urals); and the European Arctic (Scandinavia, Svalbard, Iceland, and Jan Mayen). The arctic-wide volume change, which is negative and dominated by changes in the North American Arctic, is also shown. The net accumulation in the European Arctic (primarily Scandinavia) is due to the increased precipitation accompanying the northward shift of the Atlantic storm track in recent decades, when the NAO has been in a predominantly positive phase.

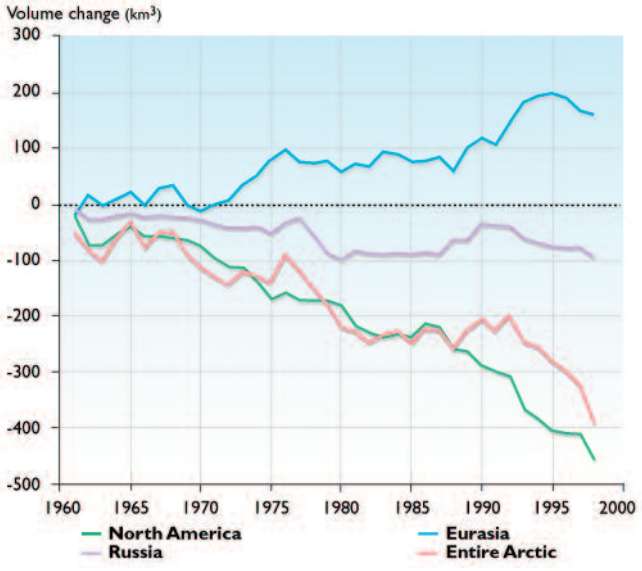

Fig. 6.17. Accumulated annual volume change in ice caps and glaciers in the North American Arctic, the Russian Arctic, the Eurasian Arctic, and the entire Arctic (M. Dyurgerov, 2003).

6.5.2.1. Alaska

The total area of Alaskan glaciers is approximately 75 000 km^2. The largest glaciers in Alaska occur along the southern and western shores of the Pacific Mountain System. Despite the vast number and size of Alaskan glaciers, mass-balance data are available for only a very few.

Arendt et al. (2002) estimated the volume changes in 67 Alaskan glaciers between the mid-1950s and the mid-1990s using airborne laser altimetry measurements, and found that the glaciers had thinned at an average rate of 0.52 m/yr. Extrapolating this thinning rate to all glaciers in Alaska results in an estimated volume change of -52±15 km^3/yr, which is equivalent to a sea-level rise of 0.14±0.04 mm/yr. Additional measurements from 28 of these glaciers between the mid-1990s and 2000–2001 indicate that the rate of thinning has increased to -1.8 m/yr. When this rate of thinning is extrapolated to all Alaskan glaciers, the equivalent sea-level rise is 0.27±10 mm/yr, which is nearly double the estimated contribution from the Greenland Ice Sheet during the same period (Rignot and Thomas, 2002). This rapid wastage of Alaskan glaciers represents about half the estimated loss of mass by glaciers worldwide (Meier and Dyurgerov, 2002), and the largest glacial contribution to sea-level rise yet deduced from measurements (Arendt et al., 2002).

6.5.2.2. Canadian Arctic

The mass-balance records in the eastern Canadian Arctic are among the longest in existence, with many covering more than 40 years. The larger ice masses had slightly negative mass balances between the early 1960s and the mid-1980s (Koerner, 1996), although the balances became increasingly negative both with diminishing size of the ice caps and/or with a more westerly location. No persistent trends were observed in any of the data prior to the mid-1980s. However, the mass balances have become increasingly negative since the mid-1980s (Koerner and Lundgaard, 1995). Summer mass-balance trends determine the annual balance trends; the winter balances have shown no significant trend over the entire 40-year period. This indicates that, as in other parts of the Arctic, summer temperature drives variations in the annual mass balance. At present, there are no systematic observations of mass balance in the western Canadian Arctic.

Ice core records show that, while the present mass balance is negative, it was more negative in the early part of the present interglacial, when substantial glacier retreat occurred (Koerner, 2002). Balances that were more positive occurred over the past 3000 years, terminating with the onset of the modern warming period about 150 years ago.

In the subarctic areas of the Canadian Cordillera, Demuth et al. (2002) found a period of declining glacier-derived discharge during the last half of the 20th century, despite a general warming trend. This decline appears to be due to the substantial contraction of outlet glaciers since the Neoglacial maximum stage (ca. 1850).

6.5.2.3. Greenland Ice Sheet

The Greenland Ice Sheet (1 640 000 km^2) is the largest ice mass in the Arctic. Two factors contribute to the difficulty of measuring the total mass balance of the Greenland Ice Sheet: short-term (interannual to decadal) fluctuations in accumulation and melt rate cause variations in surface elevation that mask the long-term trend; and climate changes that occurred hundreds or even thousands of years ago still influence ice flow, as do changes that are more recent.

The geological and historical records show that the marginal zone of the Greenland Ice Sheet has thinned and retreated over the past hundred years (Weidick, 1968). Whether this mass loss was compensated, partly or fully, by thickening in the interior is unknown. Although several expeditions have crossed the ice sheet since the late 19th century, the earliest measurements of sufficient precision to permit calculation of surface-elevation change are those made by the British North Greenland Expedition (BNGE), which crossed the ice sheet during 1953 and 1954. Comparing these data to modern surface elevations measured by satellite radar altimetry and airborne laser altimetry shows that between 1954 and 1995, ice thickness along the BNGE traverse changed little on the northeast slope, whereas ice on the northwest slope thinned at a rate of up to 30 cm/yr (Paterson and Reeh, 2001). Height measurements repeated in 1959, 1968, and 1992 along a profile across the ice sheet in central Greenland showed thickening on the western slope between 1959 and 1968, but subsequent thinning between 1968 and 1992 (Möller, 1996), probably reflecting decadal-scale fluctuations in accumulation rates.

The IPCC (2001) provides estimated of the individual terms of the mass budget of the Greenland Ice Sheet, consisting of: accumulation (520±26 km^3/yr); runoff (329±32 km^3/yr); and iceberg calving (235±33 km^3/yr). There are large uncertainties in these estimates, but they show that calving and surface melting are of the same order of magnitude.

Rignot and Thomas (2002) mapped estimated thickening rates in Greenland by synthesizing airborne laser altimeter and satellite-borne radar altimeter surveys, mass-budget calculations, and direct measurements of changes in surface elevation. The higher-elevation areas appear to be in balance to within 1 cm/yr, although temporal variations in snow accumulation rates create local thickening or thinning rates of up to 30 cm/yr. In contrast, the coastal regions appear to have thinned rapidly between the 1993–1994 and 1998–1999 laser altimeter surveys (Krabill et al., 1999). A conservative estimate of the rate of net ice loss (~50 km^3/yr) corresponds to a sea-level rise of 0.13 mm/yr. Since variations in summer temperatures do not explain the rapid thinning of many outlet glaciers, the coastal thinning is apparently a result of glacier dynamics rather than a response to atmospheric warming (Rignot and Thomas, 2002). Alternatively,

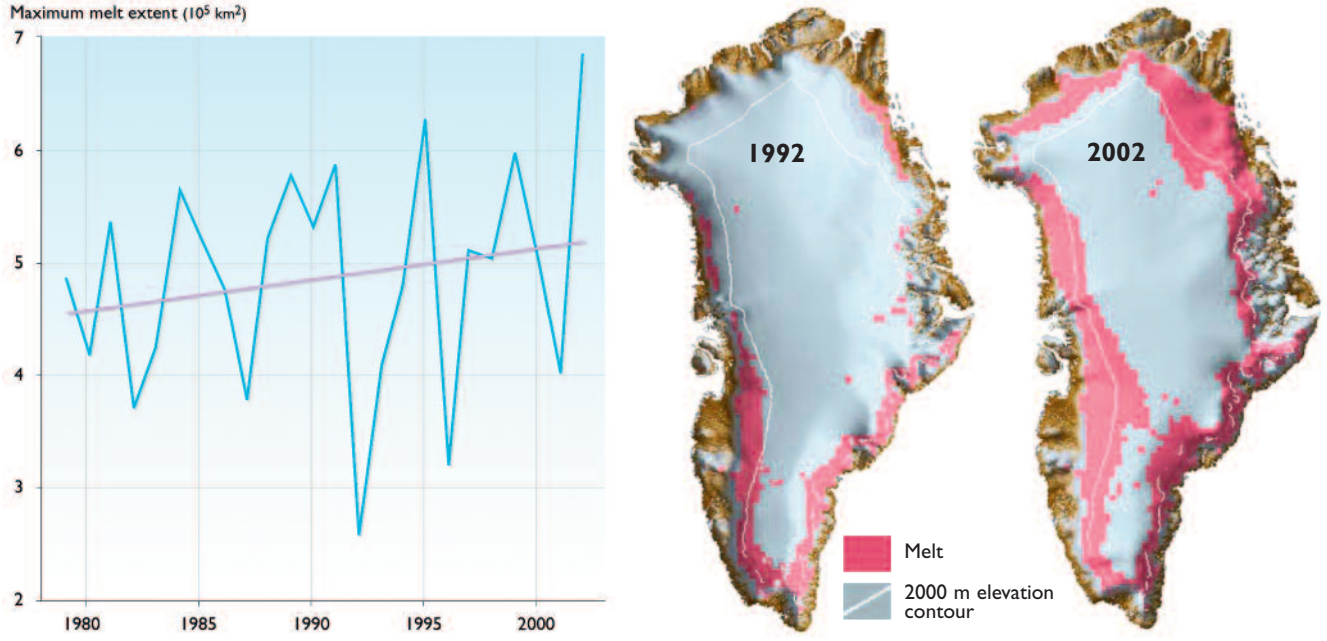

Fig. 6.18. Time series of maximum summer melt extent over Greenland from 1979 to 2002 (left) and the melt extent in 1992 and 2002 (right) (figure provided by K. Steffen, 2003).

Zwally et al. (2002) suggested that increased basal lubrication, due to additional surface meltwater reaching the glacier beds via crevasses and moulins, may play a role in outlet glacier thinning.

The extent of surface melt over Greenland increased between 1979 and 2002, although large interannual variations are superimposed on this increase. Figure 6.18 shows the time series of the maximum summer melt extent, together with maps of the melt areas in 1992 (year of minimum melt) and 2002 (year of maximum melt).

6.5.2.4. Iceland

Most Icelandic glaciers are subject to a maritime climate, with annual precipitation of up to 7 m at the highest elevations. Annual glacier-front variations are monitored at about 50 sites, and complete records from 1930 to the present exist for some of the glaciers (Sigurðsson, 1998), which show a clear response to variations in climate during this period (Jóhannesson and Sigurðsson, 1998). Mass-balance measurements have been made annually at several ice caps for 10 to 15 years (Björnsson et al., 2002; Sigurðsson, 2002). The glaciers in Iceland, particularly those on the south and southeast coasts, have a very great annual turnover of freshwater. During a year of strongly negative mass balance the glaciers can add more than 10 km^3 (equivalent to 0.03 mm global sea-level rise) to the normal precipitation runoff from the glaciated areas. Between 1991 and 2001, Vatnajökull Ice Cap lost 0.6% of its mass (Björnsson et al., 2002), equivalent to 24 km^3 of runoff or a global sea-level rise of 0.06 mm.

Icelandic glaciers advanced almost continuously during the Little Ice Age (c.1400–1900), and reached a maximum extent about 1890 (Sigurðsson, 2005). During the first quarter of the 20th century, glacier fronts retreated slightly. The rate of retreat increased significantly in the 1930s, but decreased after 1940. About 1970, most non-surging glaciers in Iceland started advancing. This period of advance was more or less continuous until the late 1990s. By 2000, all Icelandic glaciers were retreating, owing to consistently negative mass balances after 1995 (Sigurðsson, 2002).

6.5.2.5. Svalbard

The ice masses of Svalbard cover an area of approximately 36 600 km^2. Annual mass-balance measurements have been made on several Svalbard glaciers for up to 30 years (Hagen and Liestøl, 1990; Lefauconnier et al., 1999). No significant changes in mass balance have been observed during the past 30 years. The measured mean net mass balance has been negative, with no discernible change in trend. The winter accumulation is stable, and annual variations are small. The mean summer ablation is also stable with no significant trend. However, there are large interannual variations, and summer ablation drives the variations in the annual net mass balance. The low-altitude glaciers are shrinking steadily but with a slightly smaller negative net balance than those observed three decades ago. Glaciers with high-altitude accumulation areas have mass balances close to zero.

6.5.2.6. Scandinavia

Glaciers in the western maritime region of southern Scandinavia grew slowly between 1960 and 1988. Mass balances became even more positive (or less negative) between 1988 and 1998. The increase in net mass balance was due to greater winter snowfall, in contrast to Svalbard where summer ablation drives the variability in net balance. Positive mass balances due to greater winter snowfall were also observed in northern Scandinavia, at least at latitudes below 68° N.

However, low accumulation rates and high ablation rates resulted in negative mass balances for all Scandinavian glaciers between 1999 and 2003. Reichert et al. (2001) used model-based calculations to show that natural variability (e.g., the NAO) can explain many of the shorter-term variations in the mass balance of Scandinavian glaciers.

6.5.2.7. Novaya Zemlya

The glacier area of Novaya Zemlya is about 23 600 km^2 (Glazovsky, 1996; Koryakin, 1997). No direct mass-balance measurements have been made on Novaya Zemlya, but several studies of glacier extent indicate a general retreat and thus negative mass balance. Koryakin (1997) reported reductions in glacier area on Novaya Zemlya during each of four periods spanning 1913 to 1988. Zeeberg and Forman (2001) reported that tidewater calving glaciers on north Novaya Zemlya receded rapidly (>300 m/yr) during the first half of the 20th century. However, 75 to 100% of the net 20th-century retreat occurred by 1952; between 1964 and 1993, half the studied glaciers were stable, while the remainder retreated <2.5 km.

Mass losses from calving appear to be greater than mass losses from recession. The annual iceberg flux from the 200 km of calving fronts on Novaya Zemlya has been estimated to be about 2 km^3/yr (Glazovsky, pers. comm., 2003).

6.5.2.8. Franz Josef Land

The primary measurements available for the Franz Josef Land archipelago (glacier area 13 700 km^2) are of glacier extent rather than mass balance. Franz Josef Land glaciers receded between 1953 and 1993, resulting in an estimated change in glacier area of -210 km^2, and a corresponding volume change of -42 km^3 (Glazovsky, 1996). The largest changes appear to have occurred in southern parts of the ice caps on the different islands of the archipelago.

6.5.2.9. Severnaya Zemlya

Very few measurements of mass balance have been made in the Russian Arctic islands (Glazovsky, 1996). The only

comprehensive data are those from the Vavilov Ice Cap (1820 km^2) on October Revolution Island (79° N) in Severnaya Zemlya, where the mass balance did not differ significantly from zero over a ten-year period beginning in 1975. Observations of changing ice-front positions suggest that the glaciers of the Vavilov Ice Cap have generally been retreating during the 20th century, providing a qualitative indication that the mean mass balance has been negative over this period, but less negative than in the other Russian Arctic islands.

6.5.3. Projected changes

In view of the limited knowledge of arctic glaciers and the uncertainties discussed in section 6.5.2, a mass-balance sensitivity approach (Dyurgerov and Meier, 1997; Óerlemans and Reichert, 2000) was used to project future change in glaciers and ice sheets. The monthly anomalies in surface temperature and precipitation generated by the five ACIA-designated models (section 4.4) were used to calculate projected changes in glacier mass balance. Projected regional changes were extrapolated from the sensitivities of glaciers for which mass-balance data exist. These projections assume that the glaciers are in balance with the baseline climates (temperature and precipitation) simulated by the models, although this assumption is unlikely to be correct (see section 6.5.5).

This approach to projecting changes in mass balance does not include glacier or ice-sheet dynamics, calving, or an explicit treatment of internal accumulation (refreezing of meltwater that percolates into the glacier); other types of mass-balance models would provide different results. Nevertheless, the use of a single mass-balance model implies that the range in projected mass-balance changes described in this section can be attributed solely to differences in the projections of temperature and precipitation generated by the five ACIA-designated models.

The output from each mass-balance model run (using input from the different ACIA-designated models) was first averaged over the regions listed in Table 6.7 (the Greenland Ice Sheet was split into four parts). The results are summarized in Fig. 6.19, which shows the projected contribution of arctic land ice to sea-level rise between 2000 and 2100. The results from the different models diverge significantly over time, ranging from close to zero to almost six centimeters by 2100. The result using output from the CSM_1.4 model is an outlier. This model projects a large increase in precipitation for the Arctic, which compensates for the enhanced ablation associated with the modest temperature rise projected by the model. The effects of temperature on glacier and ice cap mass balances projected by the different models are generally similar. The differences in the projected changes in sea level are therefore primarily due to differences in the modeled precipitation rates.

If the CSM_1.4 outlier is not included, the mean of the projected changes in sea level is an increase of approximately 4 cm between 2000 and 2100. This change is somewhat smaller than the 70-year (2000–2070) increase of 5.7 cm estimated by Van de Wal and Wild (2001). However, the model used by Van de Wal and Wild was forced with doubled CO_2 concentrations throughout the 70-year simulation, rather than the gradual increase of GHGs in the B2 emissions scenario used to force the ACIA-designated models (section 4.4.1). In addition, the 70-year simulation used prescribed sea surface temperatures, while the coupled ACIA-designated models generate sea surface temperatures as part of the simulation process.

At a regional scale, the differences between the model projections are even greater. The projections do not even agree on the sign of the contribution of arctic land ice to sea-level change resulting from precipitation changes in some regions (e.g., Svalbard), indicating that model projections of changes in glacier mass balance at a regional scale are highly uncertain.

Of the five ACIA-designated models, the ECHAM4/OPYC3 model projects the greatest temperature effects on the mass balance of glaciers and ice caps. Earlier versions of this model were used by Ohmura et al. (1996) to assess possible changes in the Greenland Ice Sheet driven by climate change, and by Van de Wal and Wild (2001) as noted previously. Figure 6.20 compares the projected contributions to sea-level change (due to temperature effects alone) from various regions using output from the ECHAM4/OPYC3 model. The Greenland Ice Sheet is projected to make the largest contribution, which is a direct consequence of its size. Although the glaciers in Alaska cover a much smaller area, they are also projected to make a large contribution, in agreement with recent analyses (Arendt et al., 2002; Meier and Dyurgerov, 2002). For Alaskan glaciers, the relative-

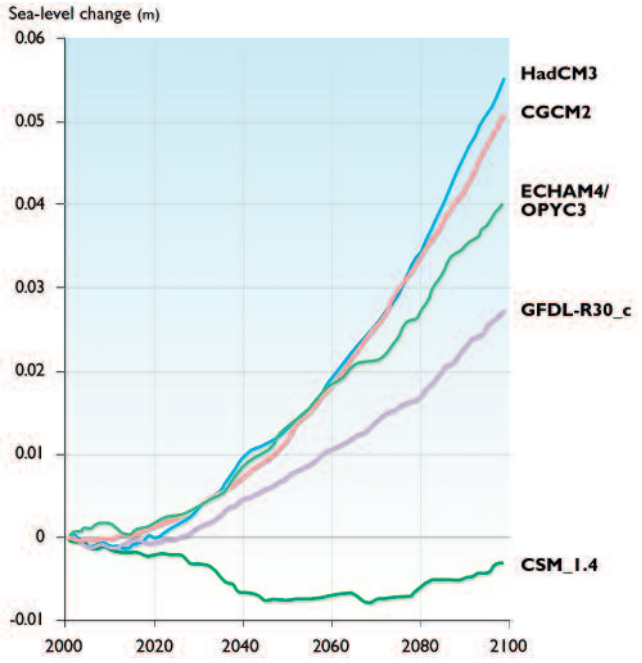

Fig. 6.19. Projected contribution of arctic land ice to sea-level change between 2000 and 2100, calculated using output from the five ACIA-designated models (J. Oerlemans, 2003).

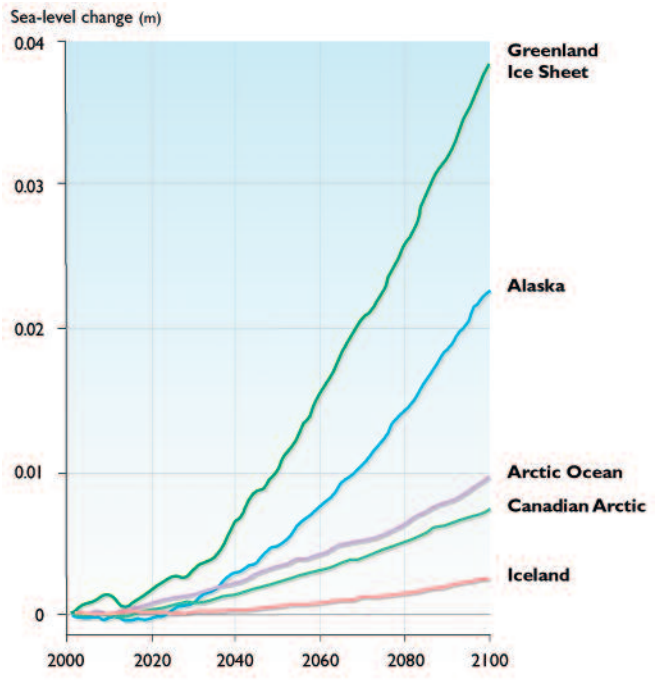

Fig. 6.20. Projected contribution of arctic land ice to sea-level change between 2000 and 2100 for various regions, calculated from ECHAM4/OPYC3 model output using temperature effects only (J. Oerlemans, 2003).

ly large sensitivity to temperature change drives the regional changes. Glaciers and ice caps in the Eurasian Arctic Ocean (Svalbard, Franz Josef Land, Severnaya Zemlya, and Novaya Zemlya) are projected to contribute about the same amount as those in the Canadian Arctic. Section 6.9 reviews all of the variables that may contribute to future sea-level change.

6.5.4. Impacts of projected changes

On other parts of the physical system

The greatest impact of changes in the mass of arctic land ice over decade-to-century timescales is likely to be a change in the freshwater input to the high-latitude oceans, which will change ocean stratification in sensitive areas such as the Greenland and Labrador Seas. Sea-ice production and export are also likely to be affected if more freshwater goes into the oceans and stabilizes the water column (section 9.2.3.1). In some areas, increased freshwater flux is likely to increase the formation of sea ice. Over longer timescales, changes in glacial ice (especially the Greenland Ice Sheet) may affect the geoid and the rotation rate of the earth.

On ecosystems

To the extent that changes in freshwater influx affect upper-ocean stratification (and possibly sea ice), impacts on marine ecosystems are likely. Riparian ecosystems are also likely to be affected by changes in river flow and aufeis (ice formed when water from a stream emerges and freezes on top of existing ice) production. Any significant change in sea level will have impacts on ecosystems in low-lying coastal areas.

On people

The greatest direct impacts on humans from changes in arctic land ice are likely to result from changes in global sea level, which will affect coastal communities in many parts of the Arctic. Other possible impacts include changes in hydropower production and water supply from glacier-fed lakes and reservoirs. Changes in iceberg production will increase or decrease hazards to shipping and navigation.

6.5.5. Critical research needs

The compilation of an up-to-date global glacier inventory is a critical research need. For some regions, existing inventories are sparse; inventories also need to be updated where glacier areas have changed. A global satellite-derived dataset of exposed ice areas is a minimum requirement. Ideally, a complete glacier database describing individual glacier locations, areas, and geometries should be compiled, so that mass-balance measurements on individual benchmark glaciers can be extrapolated to unmeasured glaciers with greater certainty.

For future projections, it would be useful to develop additional mass-balance models so that spatial variations can be better depicted and so that the records can be extended back in time at locations for which atmospheric data are available. For this purpose, additional mass-balance observations should be obtained in regions where existing data are particularly sparse, in order to provide credibility and a sense of the uncertainties in model projections of future trends. It is also important to continue the ongoing monitoring of glacier mass balance with *in situ* measurements on selected glaciers in order to improve understanding of the response of glaciers to climate change, improve model projections of future change, and calibrate remote-sensing data.

Improved climate model projections of temperature and precipitation over ice-covered regions are a top priority for improving projections of changes in glaciers, ice sheets, and sea level. As the results in section 6.5.3 imply, the ranges in the projected changes in temperature and precipitation among the ACIA-designated models are far greater than the mean changes projected for glaciated areas. The application of the mass-balance sensitivity approach described in section 6.5.3 also requires analyses of the likely discrepancies between mass balances calculated from the models' baseline simulations of temperature and precipitation and the present-day glacier mass balances.

With regard to sea level, a critical need is to determine whether the recent negative mass balance and increasing summer melt area of the Greenland Ice Sheet (equivalent to at least 0.13 mm/yr sea-level rise) are part of a long-term trend (Rignot and Thomas, 2002). Continued monitoring of the ice sheet, using, for example, radar and laser altimeters such as those planned for the Cryosphere Satellite (CryoSat) and the Ice, Cloud and

Land Elevation Satellite (ICESat), is likely to improve understanding of the current mass balance of the Greenland Ice Sheet.

In order to improve projections of *future* mass-balance changes, the following studies should be given high priority:

- improving understanding of albedo changes and feedback mechanisms;
- studies of outlet glacier dynamics with emphasis on their potential for triggering persistent, rapid changes in ice-sheet volume;
- improving ice-dynamic models for determining the long-term response of the ice sheet to past climate change;
- improving parameterization and verification of internal-accumulation models; and
- improving understanding of the relationships between climate change, meltwater penetration to the bed, and changes in iceberg production.

Future changes in mass balance are strongly dependent on future changes in climate. Consequently, the ability to project changes in the mass balance of the Greenland Ice Sheet is linked closely to the ability of atmosphere–ocean general circulation models (AOGCMs) to project changes in regional climate over Greenland. For example, recent AOGCM model runs project a greater increase in the accumulation rate over Greenland associated with a temperature increase than did previous studies (Van de Wal et al., 2001). If the latest projections prove to be accurate, increases in accumulation would largely compensate for the increased runoff resulting from projected temperature increases.

6.6. Permafrost

6.6.1. Terrestrial permafrost

6.6.1.1. Background

Permafrost is soil, rock, sediment, or other earth material with a temperature that has remained below 0 °C for two or more consecutive years. Permafrost underlies most of the surfaces in the terrestrial Arctic. Permafrost extends as far south as Mongolia (Sharkhuu, 2003), and is present in alpine areas at even lower latitudes. Figure 6.21 shows the distribution of permafrost in the Northern Hemisphere, classified into continuous, discontinuous, and sporadic zones. In the continuous zones, permafrost occupies the entire area (except below large rivers and lakes). In the discontinuous and sporadic zones, the percentage of the surface underlain by permafrost ranges from 10 to 90%. Discontinuous permafrost underlies a larger percentage of the landscape than does sporadic permafrost, although there is not a standard definition of the boundary between the two zones (Fig. 6.21 uses 30% coverage as the boundary). In the Northern Hemisphere, permafrost zones occupy approximately 26 million km^2 or about 23% of the exposed land area, but permafrost actually underlies 13 to 18% of the exposed land area (Anisimov and Nelson, 1997; Zhang T. et al., 2000). Distinctions are made between permafrost that is very cold (temperatures of -10 °C and lower) and thick (500–1400 m), and permafrost that is warm (within 1 or 2 °C of the melting point) and thin (several meters or less). Ground ice (0–20 m depth) in permafrost exhibits large spatial variability, with generally much more ice in lowland permafrost than in mountain permafrost (Brown J. et al., 1998).

The role of permafrost in the climate system is threefold (Anisimov and Fitzharris, 2001). First, because it provides a temperature archive, permafrost is a "geoindicator" of environmental change. At depths below 15 to 20 m, there is generally little or no annual cycle of temperature, so seasonality does not influence warming or cooling. Second, permafrost serves as a vehicle for transferring atmospheric temperature changes to the hydrological and biological components of the earth system. For example, the presence of permafrost significantly alters surface and subsurface water fluxes, as well as vegetative functions. Third, changes in permafrost can feed back to climate change through the release of trace gases such as CO_2 and methane (CH_4), linking climate change in the Arctic to global climate change (Anisimov et al., 1997; Fukuda, 1994).

The active layer is the seasonally thawed layer overlying permafrost. Most biogeochemical and hydrological

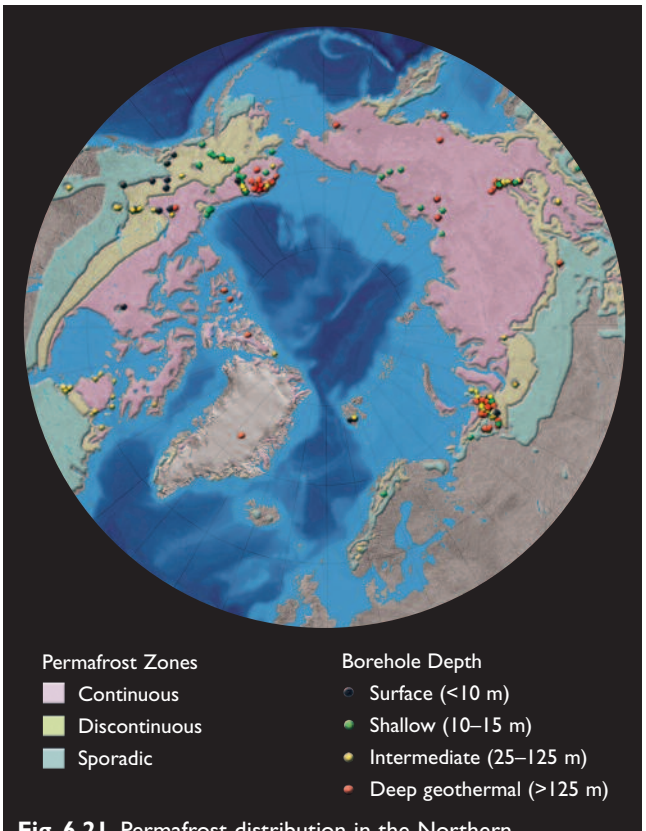

Fig. 6.21. Permafrost distribution in the Northern Hemisphere. Colored circles are locations of candidate boreholes for permafrost temperature monitoring by the GTN-P (based on Romanovsky et al., 2002).

processes in permafrost are confined to the active layer, which varies from several tens of centimeters to one to two meters in depth. The rate and depth of active-layer thaw are dependent on heat transfer through layers of snow, vegetation, and organic soil. Snow and vegetation (with the underlying organic layer) have low thermal conductivity and attenuate annual variations in air temperature. During summer, the thermal conductivity of the organic layer and vegetation is typically much smaller than in winter. This leads to lower heat fluxes in summer and ultimately keeps permafrost temperatures lower than they would be in the absence of vegetation and the organic layer. The latent heat associated with evapotranspiration and with melting and freezing of water further complicates the thermodynamics of the active layer. Over longer timescales, the thawing of deep permafrost layers can lag considerably (decades or centuries) behind a warming of the surface because of the large latent heat of fusion of ice (Riseborough, 1990). Moreover, thermal conductivity is typically 20 to 35% lower in thawed mineral soils than in frozen mineral soils. Consequently, the mean annual temperature below the level of seasonal thawing can be 0.5 to 1.5 °C lower than on the ground surface.

Thawing of permafrost can lead to subsidence of the ground surface as masses of ground ice melt, and to the formation of uneven topography known as thermokarst. The development of thermokarst in some areas of warm and discontinuous permafrost in Alaska has transformed some upland forests into wetlands (Osterkamp et al., 2000). Recent thaw subsidence has also been reported in areas of Siberia (Fedorov, 1996) and Canada (Smith et al., 2001). Climate-induced thermokarst and thaw subsidence may have detrimental impacts on infrastructure built upon permafrost (Anisimov and Belolutskaia, 2002; Nelson, 2003; Nelson et al., 2001), as section 16.3 discusses in more detail. Permafrost degradation can also pose a serious threat to arctic biota through either oversaturation or drying (Callaghan and Jonasson, 1995). The abundance of ground ice is a key factor in subsidence, such that areas with little ice (e.g., the Canadian Shield or Greenland bedrock masses) will suffer fewer subsidence effects when permafrost degrades.

Seasonal soil freezing and thawing are the driving forces for many surficial processes that occur in areas with permafrost or seasonally frozen soils. Cryoturbation, a collective term for local vertical and lateral movements of the soil due to frost action, is one of these potentially important cryogenic processes (see Washburn (1956) for a review). Cryoturbation typically occurs in the permafrost zone, but also occurs in soils that freeze only seasonally. Cryoturbation can cause the downward displacement of organic material from the near-surface organic horizons to the top of the permafrost table, resulting in sequestration of organic carbon in the upper permafrost layer (Williams P. and Smith, 1989). During the past several thousand years, a significant amount of organic carbon has accumulated in permafrost due to this process.

6.6.1.2. Recent and ongoing changes

Because surface temperatures are increasing over most permafrost areas (section 2.6.2), permafrost is receiving increased attention within the context of past and present climate variability. Measurements of ground temperature in Canada, Alaska, and Russia have produced a generally consistent picture of permafrost warming over the past several decades. Lachenbruch and Marshall (1986) were among the first to document systematic warming by using measurements from permafrost boreholes in northern Alaska to show that the surface temperature increased by 2 to 4 °C between the beginning of the 20th century and the mid-1980s. Measurements conducted by Clow and Urban (see Nelson, 2003) in the same Alaska borehole network indicated further warming of about 3 °C since the late 1980s. Figure 6.22 confirms this warming with results from a site-specific permafrost model driven by observed air temperatures and snow depths for the period 1930 to 2003, calibrated using measurements of permafrost temperatures between 1995 and 2000. While warming has predominated since 1950, considerable interannual variability is also apparent.

Data from northwestern Canada, indicating that temperatures in the upper 30 m of permafrost have increased by up to 2 °C over the past 20 years (Burn, see Couture et al., 2003; Nelson, 2003), provide further evidence of warming. Although cooling of permafrost in the Ungava Peninsula of eastern Canada in recent decades has been widely cited as an exception to the dominant warming trend, Brown J. et al. (2000) and Allard et al. (see Nelson, 2003) indicated that shallow permafrost temperatures in the region have increased by up to nearly 2 °C since the mid-1990s. Smith et al. (2003) reported warming in the upper 30 m of permafrost in the Canadian High Arctic since the mid-1990s. Smaller temperature increases, averaging 1 °C or less, have been reported in northwestern Siberia (Chudinova et al., 2003; Pavlov and Moskalenko, 2002). Measurements from a network of recently drilled boreholes in mountainous areas of Europe indicate warming of a degree or less (Harris and Haeberli, 2003), while Isaksen et al.

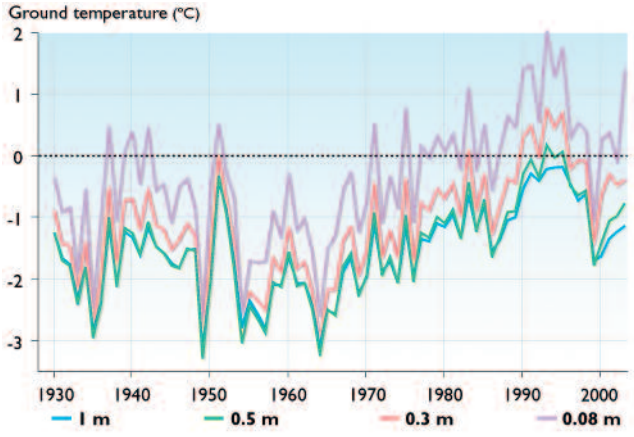

Fig. 6.22. Simulated mean annual ground temperature at Fairbanks (Bonanza Creek), Alaska, from 1930 to 2003 (V. Romanovsky, 2004).

(2001) have reported warming of Scandinavian permafrost. Table 6.8 summarizes recent trends in permafrost temperatures in terms of region, time period, and the approximate temperature change over the period of record. In general, the changes in permafrost temperature are consistent with other environmental changes in the circumpolar Arctic (Anisimov et al., 2003; Serreze et al., 2000).

Most of the boreholes mentioned in this section are included in an emerging system for comprehensive monitoring of permafrost temperatures (Fig. 6.21), the Global Terrestrial Network for Permafrost (GTN-P), established with the assistance of the International Permafrost Association. Burgess et al. (2000) provide an overview of the GTN-P.

6.6.1.3. Projected changes

At present, land-surface parameterizations used in global climate models such as those designated by the ACIA (section 4.2.7) do not adequately resolve the soil, and the models do not archive the soil output needed to assess changes in permafrost distribution and active-layer characteristics. The more viable approach to date has been the use of AOGCM output as input to soil modules run in an off-line mode, often in combination with baseline climatic data obtained from meteorological observations (Anisimov and Poliakov, 2003). This section summarizes results from several studies that used this approach with output from the ACIA-designated models to show spatially distributed fields of projected changes in permafrost for three different times in the 21st century.

Circumpolar projections

At the circumpolar scale, climate change can be expected to reduce the area occupied by frozen ground and to cause shifts between the zones of continuous, discontinuous, and sporadic permafrost, comparable to the changes that occurred during warm epochs in the past (Anisimov et al., 2002). Such changes can be projected using a relatively simple frost-index-based model of permafrost driven by scenarios of climate change. Anisimov and Nelson (1997) used this method to calculate areas occupied by near-surface permafrost in the Northern Hemisphere under present-day climatic conditions and climatic conditions projected for the 2041–2060 time slice. Scenarios of climate change used in these calculations were based on the results from several transient and equilibrium experiments with general circulation models. These results have been updated (Anisimov, unpubl. data, 2003) using output from the five ACIA-designated models (section 4.4). Table 6.9 presents projections of the area occupied by different permafrost zones in 2030, 2050, and 2080. Results for

Table 6.8. Recent trends in permafrost temperature (Romanovsky et al., 2002, updated).

Region	Depth (m)	Period of record	Permafrost temperature change[a] (°C)	Reference
United States				
Trans-Alaska pipeline route	20	1983–2000	+0.6 to +1.5	Osterkamp, 2003; Osterkamp and Romanovsky, 1999
Barrow Permafrost Observatory	15	1950–2001	+1	Romanovsky et al., 2002
Russia				
East Siberia	1.6–3.2	1960–1992	+0.03/yr	Romanovsky, pers. comm., 2003
Northwest Siberia	10	1980–1990	+0.3 to +0.7	Pavlov, 1994
European north of Russia, continuous permafrost zone	6	1973–1992	+1.6 to +2.8	Pavlov, 1994
European north of Russia, discontinuous permafrost zone	6	1970–1995	up to +1.2	Oberman and Mazhitova, 2001
Canada				
Alert, Nunavut	15–30	1995–2000	+0.15/yr	Smith et al., 2003
Northern Mackenzie Basin, Northwest Territories	28	1990–2000	+0.1/yr	Couture et al., 2003
Central Mackenzie Basin, Northwest Territories	15	1985–2000	+0.03/yr	Couture et al., 2003
Northern Québec	10	late 1980s–mid-1990s	-0.1/yr	Allard et al., 1995
Norway				
Juvvasshøe, southern Norway	~5	past 60–80 years	+0.5 to +1.0	Isaksen et al., 2001
Svalbard				
Janssonhaugen	~5	past 60–80 years	+1 to +2	Isaksen et al., 2001

[a]Temperature change over period of record, unless otherwise noted.

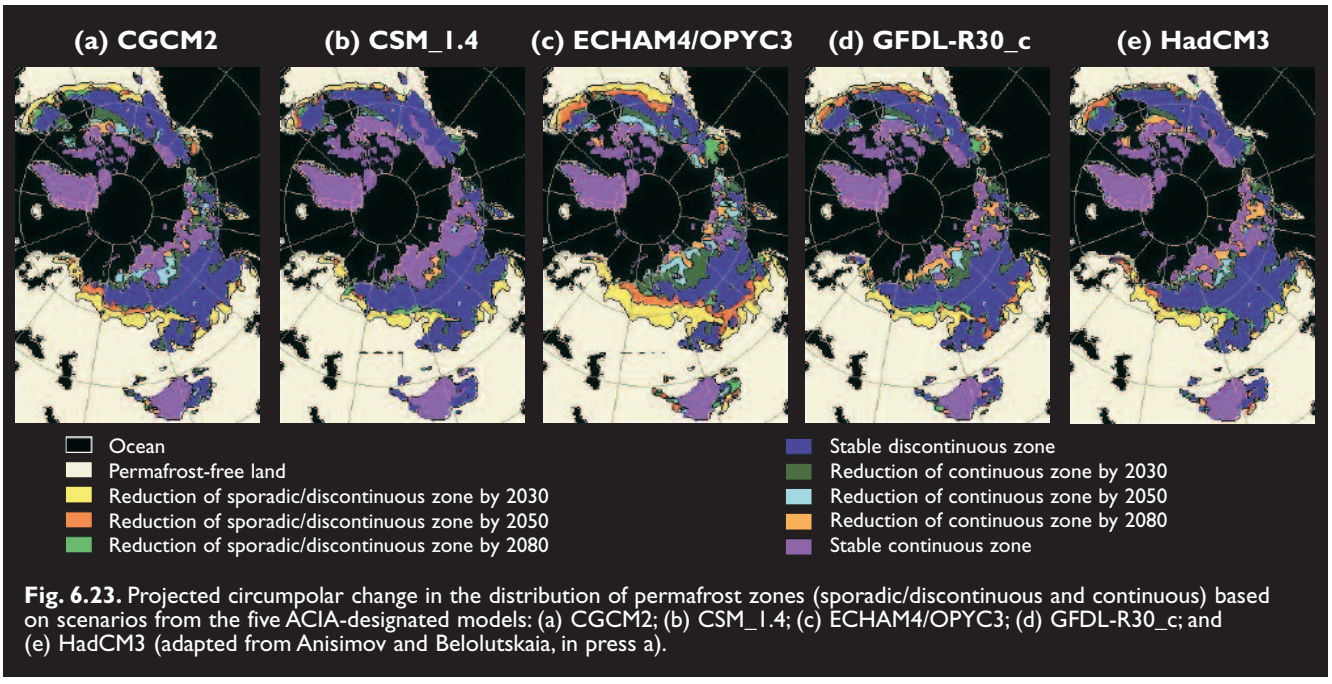

Fig. 6.23. Projected circumpolar change in the distribution of permafrost zones (sporadic/discontinuous and continuous) based on scenarios from the five ACIA-designated models: (a) CGCM2; (b) CSM_1.4; (c) ECHAM4/OPYC3; (d) GFDL-R30_c; and (e) HadCM3 (adapted from Anisimov and Belolutskaia, in press a).

2030 rather than 2020 are shown because the latter show little change from present-day distributions.

The projected reductions in the area occupied by near-surface permafrost (the uppermost few meters of frozen ground; conditions in the deeper layers are not addressed in these projections) vary substantially depending on the scenario used, indicating that the uncertainties in the forcing data are large. Among the five model scenarios, the two outliers are the ECHAM4/OPYC3-based scenario, which projects the greatest contraction of the area occupied by near-surface permafrost, and the CSM_1.4 scenario that projects only modest changes. Projections from the three other scenarios (CGCM2, GFDL-R30_c, and HadCM3) are relatively close to each other. According to the "median" GFDL-R30_c-based scenario, the total area occupied by near-surface permafrost is projected to decrease by 11, 18, and 23% by 2030, 2050, and 2080, respectively. The projected contractions of the continuous near-surface permafrost zone for the same years are 18, 29, and 41%, respectively. Figure 6.23 shows the projected changes in the distribution of permafrost zones (continuous and sporadic/discontinuous) calculated using output for 2030, 2050, and 2080 from the five ACIA-designated models.

A progressive increase in the depth of seasonal thawing could be a relatively short-term reaction to climate

Table 6.9. Projected area occupied by permafrost zones in 2030, 2050, and 2080 calculated using output from the five ACIA-designated models.

		Total permafrost		Continuous permafrost	
		Area (10^6 km^2)	% of present-day value	Area (10^6 km^2)	% of present-day value
CGCM2	2030	23.72	87	9.83	79
	2050	21.94	81	8.19	66
	2080	20.66	76	6.93	56
ECHAM4/OPYC3	2030	22.30	82	9.37	75
	2050	19.31	71	7.25	58
	2080	17.64	65	5.88	47
GFDL-R30_c	2030	24.11	89	10.19	82
	2050	22.38	82	8.85	71
	2080	20.85	77	7.28	59
HadCM3	2030	24.45	90	10.47	84
	2050	23.07	85	9.44	76
	2080	21.36	78	7.71	62
CSM_1.4	2030	24.24	89	10.69	86
	2050	23.64	87	10.06	81
	2080	21.99	81	9.14	74

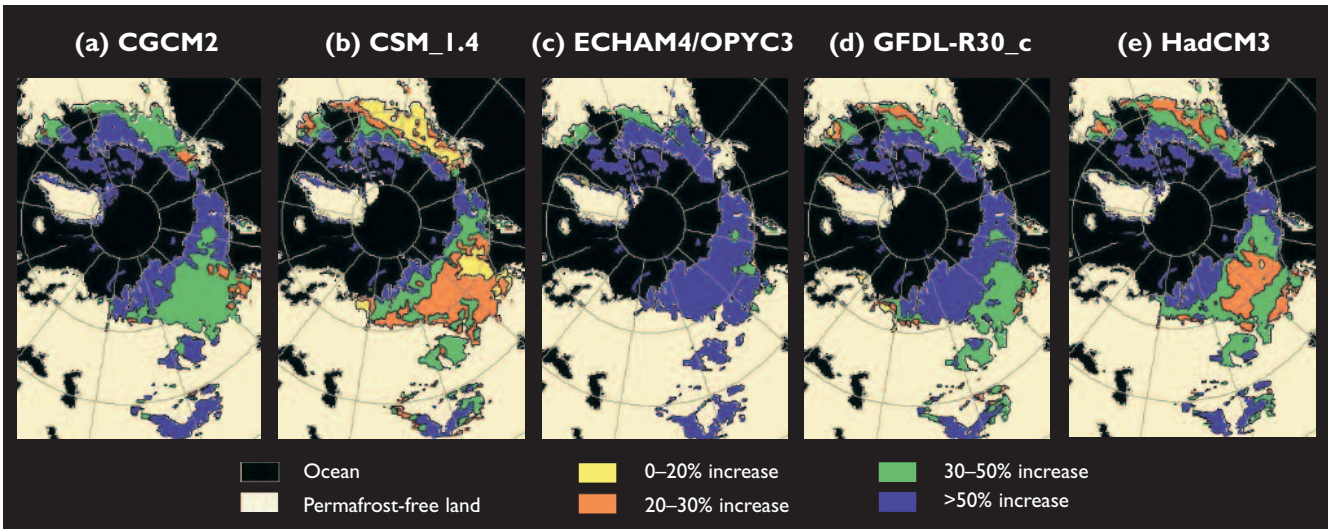

Fig. 6.24. Projected change in active-layer depth between 1981–2000 and 2050, calculated using output from the five ACIA-designated models: (a) CGCM2; (b) CSM_1.4; (c) ECHAM4/OPYC3; (d) GFDL-R30_c; and (e) HadCM3 (Anisimov et al., 1997, updated).

change in permafrost regions, since it does not involve any lags associated with the thermal inertia of the climate/permafrost system. One of the most successful and frequently used approaches to active-layer mapping is based on semi-empirical methods developed primarily for the practical needs of cold-regions engineering, but adjusted for use at the hemispheric scale. The fundamentals of these methods were formulated by Russian geocryologists (Garagulya, 1990; Kudryavtsev, 1974) and have been used by other investigators (e.g., Anisimov et al., 1997; Romanovsky and Osterkamp, 1995; Sazonova and Romanovsky, 2003). Monthly temperature and precipitation simulated by the ACIA-designated models for baseline (1981–2000) and year 2050 climate conditions were used as input to the Kudryavtsev (1974) model to calculate projected changes in seasonal thaw depth during the first half of the 21st century (Fig. 6.24). The projected increases in active-layer depth range from 0 to 20% to more than 50%.

The calculations require several assumptions about soil, organic layer, vegetation, and snow-cover properties (see Anisimov et al., 1997). Digital representation of soil properties for each cell was obtained from the Global Ecosystems Database (Staub and Rosenzweig, 1987). Over much of the permafrost area, the calculations were made for silt covered with a 10 cm organic layer. The calculations assume that vegetation does not change as temperatures increase, although a study by Anisimov and Belolutskaia (in press b) indicates that climate-induced vegetation changes are likely to both largely offset the effects of warming in the northernmost permafrost regions and enhance the degradation of sporadic and discontinuous permafrost. The projected changes represent the behavior of permafrost with highly generalized properties averaged over 0.5° by 0.5° grid cells. Owing to the effects of local environmental factors, including topography and vegetation variations, seasonal thaw depth is characterized by pronounced spatial and temporal variability that cannot be resolved at the scale of the model calculations. More details on the spatial variability of environmental features, including low-level vegetation, would improve the spatial accuracy of the projected changes in permafrost (e.g., Smith and Burgess, 1999).

The maps in Fig. 6.24 provide a broad picture of the projected hemispheric-scale changes in seasonal thaw depth under changing climate conditions. These projections are generally consistent with the results obtained from the more detailed regional studies for Alaska and Siberia. Although the results of the calculations are model-specific, there is a general consensus among the models that seasonal thaw depths are likely to increase by more than 50% in the northernmost permafrost loca-

Table 6.10. Projected regional increases in mean annual air temperature (ΔT_a), permafrost temperature (ΔT_s), and depth of seasonal thaw (ΔZ) between 1981–2000 and 2050, calculated using output from the five ACIA-designated models.

	ΔT_a (°C)	ΔT_s (°C)	ΔZ (%)
Arctic coast of Alaska and Canada	2.0–3.0	2.0–2.5	≥50
Central Canada	1.5–2.5	1.0–2.0	≤30
West coast of Canada	1.0–2.0	0.5–1.5	≤10
Northern Scandinavia	1.5–2.0	1.0–2.0	≤10
Siberia	2.0–3.0	2.0–2.5	≥50
Yakutia	1.5–2.5	1.5–2.0	≤30
Russian Arctic coast	2.0–3.0	2.0–2.5	≥50

tions (including much of Siberia, the Far East, the North Slope of Alaska, and northern Canada) and by 30 to 50% in most other permafrost regions. Table 6.10 shows, by region, the range of changes in mean annual air temperature, permafrost temperature, and depth of seasonal thaw projected to occur between 1981–2000 and 2050 by the ACIA-designated models.

Regional projections

This section describes regional projections that were generated by soil models run at high resolution for an area in which relatively detailed information on soil properties was available. The soil information included soil temperatures used for model calibration. While this section presents results for northern Alaska, model-based evaluations of the sensitivities of permafrost to warming in other areas, including Canada, are also available (Smith and Burgess, 1999; Wright et al., 2000).

Detailed projections of future changes in permafrost in northern Alaska were obtained from a soil model (Zhuang et al., 2001) calibrated using observational data from three sites on the North Slope of Alaska. The two major types of vegetation in northern Alaska are tundra and taiga (boreal forest). Permafrost is continuous north of the Brooks Range and discontinuous in much of Interior Alaska to the south. Permafrost is >600 m thick in northern areas but is only one to several meters thick near its southern limits. In the lowlands of the southern discontinuous zone, where the mean annual air temperature ranges from -7 to 0 °C, the temperature of the permafrost below the layer of seasonal temperature variation ranges from -5 to -1 °C. In the continuous permafrost zone north of the Brooks Range, permafrost temperatures typically range from -11 to -4 °C.

Surface air temperature and snow-cover projections from the five ACIA-designated climate models and the older HadCM2 model (Sazonova and Romanovsky, 2003), forced with the B2 emissions scenario (section 4.4.1), were used as input to the soil model to project the active-layer and mean annual ground-temperature dynamics in northern Alaska between 2000 and 2100. The across-model average projected increase in mean annual air temperature between 2000 and 2100 ranges from 8 to 10 °C in the north to 4 to 6 °C in the southern part of the region.

In the central and northern areas of Alaska, projected increases in mean annual ground temperatures between 2000–2010 and 2100 range from 1 to 2 °C using the CGCM2 climate scenario to 5 °C using the HadCM3 and ECHAM4/OPYC3 scenarios (Fig. 6.25). The HadCM3, HadCM2, and ECHAM4/OPYC3 scenarios generate significant projected increases in mean annual ground temperatures over the entire area.

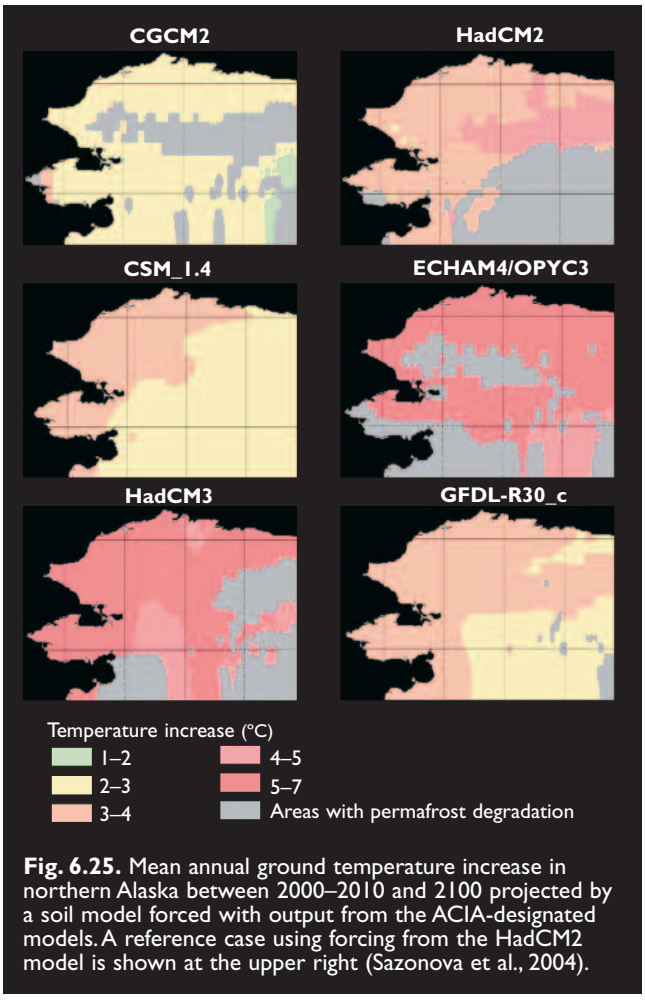

Fig. 6.25. Mean annual ground temperature increase in northern Alaska between 2000–2010 and 2100 projected by a soil model forced with output from the ACIA-designated models. A reference case using forcing from the HadCM2 model is shown at the upper right (Sazonova et al., 2004).

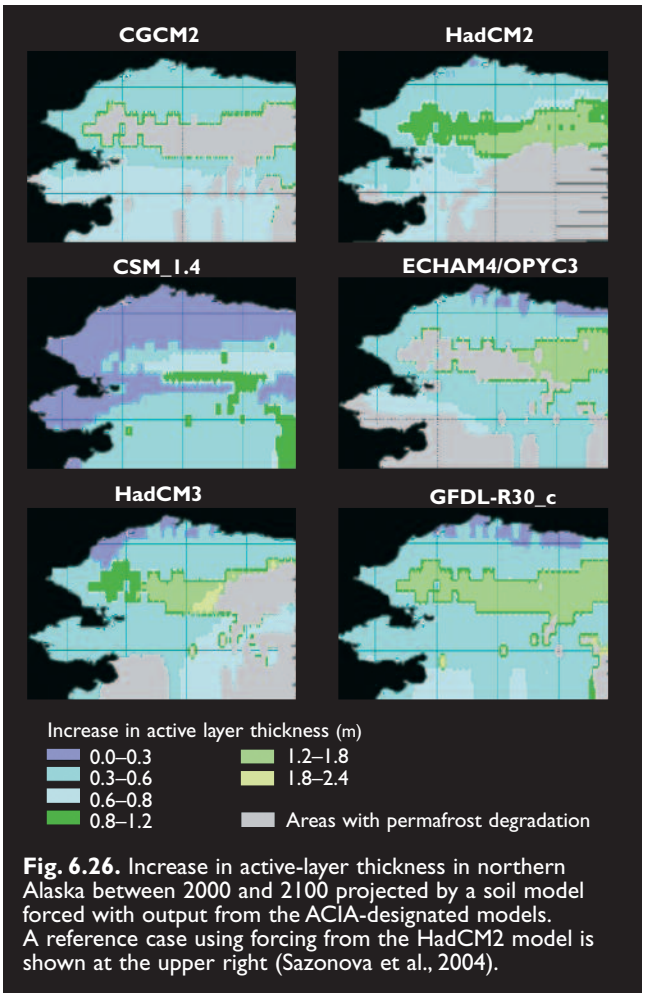

Fig. 6.26. Increase in active-layer thickness in northern Alaska between 2000 and 2100 projected by a soil model forced with output from the ACIA-designated models. A reference case using forcing from the HadCM2 model is shown at the upper right (Sazonova et al., 2004).

An analysis of the maximum active-layer thickness was also performed. All the scenarios project that, by 2100, the active-layer thickness is likely to increase by up to 1 m in areas occupied by coarse-grained material and rocks with high thermal conductivity, and by up to 0.5 m throughout the rest of the region (Fig. 6.26). The HadCM2, HadCM3, and ECHAM4/OPYC3 scenarios generate the greatest projected increases in active-layer thickness.

By 2100, all the scenarios except for the CSM_1.4 project that a zone with permafrost degradation (failure of some portion of the former active layer to refreeze during winter) will exist in northern Alaska (Fig. 6.26). The HadCM2 and GFDL-R30_c scenarios project that this zone will occupy the southeastern part of the modeled area. The HadCM2 scenario projects a relatively constant increase in this zone throughout the years, with almost one-third of the modeled area degraded by 2100. The ECHAM4/OPYC3 scenario projects the second largest zone of degradation by 2100, but the development of this zone throughout the century is not uniform. The CGCM2 scenario projects that this zone will be located in the southeastern and central parts of the modeled area and in the Brooks Range. The HadCM3 and ECHAM4/OPYC3 scenarios project that the zone will occupy the southeastern and southwestern parts of the modeled area and some parts of the Brooks Range (the eastern part in HadCM3, the western part in ECHAM4/OPYC3). The GFDL-R30_c scenario projects that the zone of permafrost degradation will occupy less than 5 to 7% of the modeled area. The CSM_1.4 scenario is an outlier in that it projects no permafrost degradation between 2000 and 2100.

Similar dependencies on climate model forcing scenarios have been found by Malevsky-Malevich et al. (2003), who used output from the same climate models to drive a different type of soil model. The results of these simulations showed that the projected active-layer response in Siberia would be greater in southern and western regions than in eastern and northern regions, indicating the potential importance of snow cover to projections of permafrost change (Stieglitz et al., 2003). The decrease in snow-cover duration is projected to be greater in southern and western Siberia than in northern and eastern Siberia, and greater in the spring season (section 6.4) when insolation is relatively high.

The scenarios of permafrost change clearly vary with the choice of climate model, and they contain many examples of decadal-scale variations that can complicate the detection of change. Nevertheless, the projected changes are substantial in nearly all cases, and terrestrial permafrost is likely to remain one of the more useful indicators of global change because large regions of the arctic terrestrial system now have mean annual temperatures close to 0 °C.

6.6.1.4. Impacts of projected changes

On other parts of the physical system

Projected climate change is very likely to increase the active-layer thickness and the thawing of permafrost at greater soil depths. The impacts of permafrost degradation include changes in drainage patterns and surface wetness resulting from subsidence and thermokarst formation, especially where soils are ice-rich. Thawing of ice-rich permafrost can trigger mass movements on slopes, and possibly increase sediment delivery to watercourses. Thawing of permafrost in peatlands and frozen organic matter sequestered by cryoturbation is likely to accelerate biochemical decomposition and increase the GHGs released into the atmosphere.

On ecosystems

Changes in surface drainage and wetness are likely to result in vegetative changes (e.g., shallow-rooted versus deeper-rooted vegetation, changes in plant density); the development of thermokarst has transformed some upland forests into extensive wetlands. Microbial, insect, and wildlife populations are likely to evolve over time as soil drainage and wetness change (section 7.4.1). Changes in drainage resulting from changes in the distribution of permafrost are also likely to affect terrestrial ecosystems, and will determine the response of peatlands and whether they become carbon sources or sinks (section 7.5.3).

On people

Permafrost degradation is likely to cause instabilities in the landscape, leading to surface settlement and slope collapse, which may pose severe risks to infrastructure (e.g., buildings, roads, pipelines). The possibilities for land use change with soil wetness. Offshore engineering (e.g., for resource extraction) is highly affected by coastal permafrost and its degradation (section 16.3.10). Containment structures (e.g., tailing ponds, sewage lagoons) often rely on the impermeable nature of frozen ground; thawing permafrost would reduce the integrity of these structures. Over the very long term, the disappearance of permafrost coupled with infrastructure replacement will eliminate many of the above concerns.

6.6.1.5. Critical research needs

In order to improve the credibility of model projections of future permafrost change throughout the Arctic, the soil/vegetation models must be validated in a more spatially comprehensive manner. In particular, there is a need for intercomparison of permafrost models using the same input parameters and standardized measures for quantifying changes in permafrost boundaries. Global models do not yet use such regionally calibrated permafrost models, nor do they treat the upper soil layers in sufficient detail to resolve the active layer. The need for additional detail is particularly great for areas with thin

permafrost (e.g., Scandinavia). Enhanced model resolution, and validation and calibration at the circumpolar scale, will be necessary before fully coupled simulations by global models will provide the information required for assessment activities such as the ACIA.

There is likely to be a significant linkage between changes in terrestrial permafrost and the hydrology of arctic drainage basins. Long-term field data are required to increase understanding of permafrost–climate interactions and the interaction between permafrost and hydrological processes, and for model improvement and validation. The active-layer measurements from the Circumpolar Active Layer Monitoring Program and the borehole measurements from the GTN-P will be especially valuable in this regard, if the numbers of sites are increased.

6.6.2. Coastal and subsea permafrost

6.6.2.1. Background

The terms subsea (or offshore) and coastal permafrost refer to geological materials that have remained below 0 °C for two or more years and that occur at or below sea level. At present, the thermal regime of subsea permafrost is controlled partially or completely by seawater temperature. Subsea permafrost has formed either in response to negative mean annual sea-bottom temperatures or as the result of inundation of terrestrial permafrost. Coastal permafrost includes the areas of permafrost that are near a coastline (offshore or onshore) and that are affected, directly or indirectly, by marine processes. Direct marine influences include seawater temperature, sea-ice action, storm surges, wave action, and tides. Indirect marine influences include the erosion of cliffs and bluffs. This review focuses on those parts of the permafrost environment found below the storm tide line, since the thermal and chemical environments that affect them are substantially different from those affecting terrestrial permafrost.

The development and properties of subsea permafrost are largely dependent on the detailed history of postglacial relative sea level. Coastal permafrost conditions are influenced by a range of oceanographic and meteorological processes, ranging from sea-ice thickness to storm-surge frequency. During the transition from terrestrial to submarine, permafrost is subjected to a set of intermediary environments that affect its distribution and state.

Based on the strict definition above, not all permafrost is frozen, since the freezing point of sediments may be depressed below 0 °C by the presence of salt or by capillary effects in fine-grained material. In the marine environment, non-frozen materials do not present serious problems for engineering activities, so modifiers are used to further define frozen permafrost as either ice-bonded, ice-bearing, or both (see Sellmann and Hopkins, 1984). Ice-bearing material refers to permafrost or seasonally frozen sediments that contain some ice. Ice-bonded sediments are mechanically cemented by ice. While the ice component of permafrost usually consists of pore or interstitial ice that fills the small spaces between individual grains of sand, silt, or gravel, it sometimes occurs in much larger forms referred to as "massive ice". Unfrozen fluids may be present in the pore spaces in both ice-bearing and ice-bonded materials. As with terrestrial permafrost, some subsea permafrost has an active (seasonally thawed) layer. Hubberten and Romanovskii (2003) discussed the characteristics of permafrost in one particular offshore environment, the Laptev Sea.

While the stability of terrestrial permafrost depends directly on atmospheric forcing (temperature and precipitation), the effect of atmospheric forcing on the stability of subsea permafrost is a second- or third-order impact mediated through oceanographic and sea-ice regimes. Most subsea permafrost formed during past glacial cycles, when continental shelves were exposed to low mean annual temperatures during sea-level lowstands, thus it is restricted to those parts of the Arctic that were not subjected to extensive glaciation during the Late Quaternary Period (Mackay, 1972). Permafrost that developed on exposed continental shelves during glacial epochs subsequently eroded when sea-level rise submerged the shelves during interglacial warm intervals and regraded the land surface to a quasi-equilibrium seabed profile. Positive mean annual sea-bottom temperatures degrade upland permafrost as it passes through the coastal zone, but with continued sea-level rise, the sea-bottom water temperature falls to negative values and permafrost degradation slows. Thus, in any locality, the distribution of relict subsea permafrost is a function of its original distribution on land, and the depth to ice-bonded or ice-bearing permafrost is a function of the time spent in the zone of positive sea-bottom temperatures along with other variables (e.g., volumetric ice content, salt content, etc.) (Mackay, 1972; Osterkamp and Harrison, 1977; Vigdorchik, 1980).

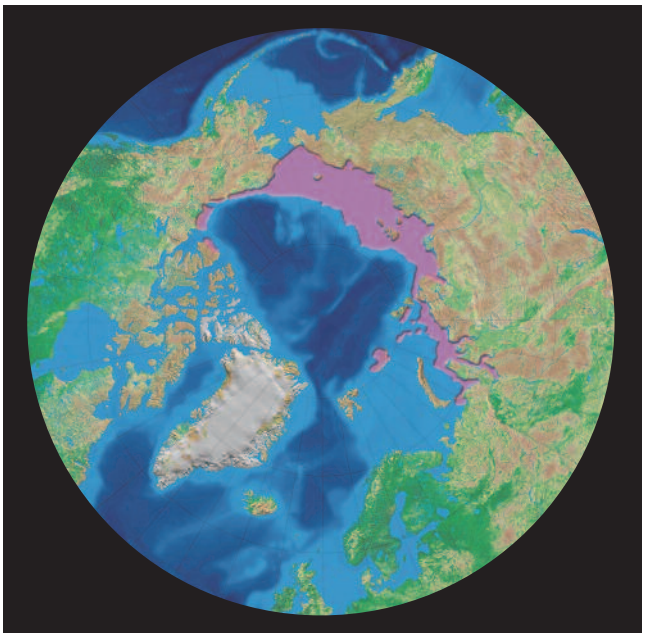

Fig. 6.27. Subsea permafrost distribution in the Arctic (based on Brown J. et al., 1998).

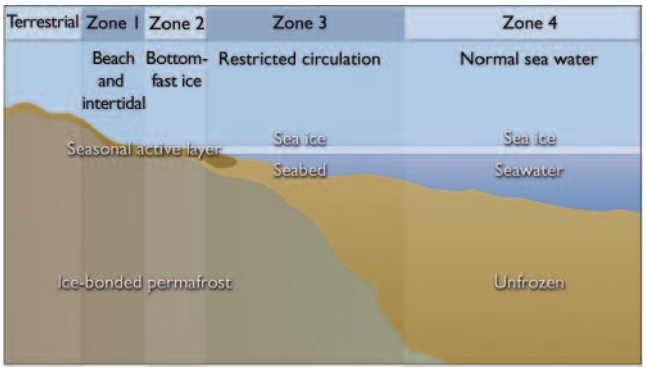

Fig. 6.28. The coastal and offshore permafrost zones (based on Osterkamp, 2001).

Subsea relict permafrost is thought to contain or overlie large volumes of CH_4 in the form of gas hydrates at depths of up to several hundred meters. Degradation of gas hydrates resulting from climate change (section 6.6.2.3) could increase the flux of CH_4 to the atmosphere (Judge and Majorowicz, 1992; Kvenvolden, 1988).

A combination of observations and models has been used to estimate the distribution of subsea permafrost (Fig. 6.27). The distribution is largely inferred from glacial extent during the last glacial maximum, water temperature, and the location of the 100 m depth contour (approximate minimum sea level during the past 100000 years). Narrow zones of coastal permafrost are probably present along most arctic coasts.

Coastal and subsea permafrost can be subdivided into four zones (Fig. 6.28), based primarily on water depth and on the dominant processes that operate in those depth zones (after Osterkamp, 2001). Zone 1 covers the inter- and supra-tidal environments of the beaches and flats. Seaward of the intertidal zone, in Zone 2, the seasonal ice cover freezes to the seabed each year, allowing cold winter temperatures to penetrate the water column and reach the sediments. This occurs in water depths of 1.5 to 2 m. Zone 3 covers areas where water depths are too great for the sea ice to freeze to the seabed; however, under-ice circulation may be restricted, with attendant higher salinities and lower seabed temperatures. In Zone 4, "normal" seawater salinity and temperatures prevail, providing a more or less constant regime. Sea-bottom temperatures on the arctic shelves range from -1.5 to -1.8 °C; salinities range from 30 to 34 (Arctic Climatology Project, 1997, 1998).

6.6.2.2. Recent and ongoing changes

There are no ongoing programs to monitor the state of coastal and subsea permafrost, although some effort is being devoted to monitoring the forcing variables and coastal erosion (Brown J. and Solomon, 1999; Rachold et al., 2002; see also Table 16.8). Therefore, most publications addressing changes in the state of subsea permafrost are model-based and speculative. Zones 1 and 2 are the most dynamic, especially in locations where erosion is rapid (e.g., the Laptev and Beaufort Sea coasts). In these areas, erosion rates of several meters per year cause a rapid transition from terrestrial to nearshore marine conditions. High rates of erosion caused by exposure to waves and storm surges during the open water season lead to deep thermal notch development in cliffs, block failure in the backshore (area reached only by the highest tides), melting of sea-level-straddling massive ice, and possible offshore thermokarst development (e.g., Dallimore et al., 1996; Mackay, 1986; Wolfe et al., 1998). The rate at which destabilization of permafrost in these zones occurs is dependent on the erosion rate, which in turn varies according to storm frequency and severity (Solomon et al., 1994) and the presence or absence of sea ice. The degree to which permafrost destabilization affects erosion remains conjectural. Thaw subsidence in Zones 2 and 3 that accompanies melting of excess ice (ice that is not in thermal equilibrium with the existing soil–ice–air configuration) in the nearshore provides accommodation space for sediments produced by erosion. Thus, there is a potential feedback between high erosion rates and thaw subsidence, but there are few observations to support this hypothesis. An analysis of time series of erosion measurements and environmental forcing (e.g., weather, storms, freeze-thaw cycles) in the Beaufort Sea area did not reveal any trends, but showed pronounced interannual and decadal-scale variability (e.g., Solomon et al., 1994).

Sea-ice thickness plays a major role in the development of subsea permafrost within Zone 2. However, none of the recent analyses of historic data on sea-ice thickness

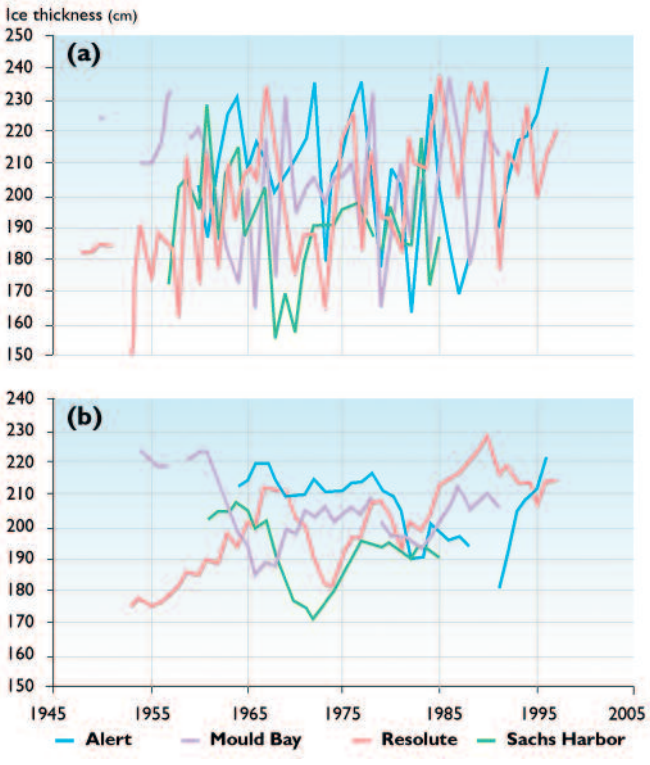

Fig. 6.29. Maximum thickness of landfast ice measured at four coastal locations in the Canadian Arctic, plotted as (a) annual values and (b) five-year moving averages (data from the Canadian Ice Service, 2003).

in the Arctic (e.g., Rothrock et al., 1999; Winsor, 2001, see also section 6.3.2) addresses the state of the sea ice that forms very close to the coast (Manson et al., 2002), since the coastal waters are too shallow for submarines. Time series of ice thickness measurements from several coastal locations extending back to the late 1940s are available from the Canadian Ice Service (Wilson, pers. comm., 2003). Polyakov et al. (2003) describe a similar dataset from Russia. Neither dataset shows any trend over the period of record, which is dominated by large interannual fluctuations. Figure 6.29 illustrates the variability in the annual maximum thickness of landfast ice measured at four coastal locations in the Canadian Arctic. Smoothing the data with a five-year moving average reveals some similarities between the stations.

Air-temperature changes in the Arctic are well documented, and many studies have examined the impact of these changes on the active-layer thickness and temperature of terrestrial permafrost, however, there are no equivalent multi-year studies for coastal permafrost.

Seabed temperature is a critical upper boundary condition for subsea permafrost. Decadally averaged temperatures (1950s–1980s) for various water depths in the Arctic Ocean are available from the National Snow and Ice Data Center in Boulder, Colorado (Arctic Climatology Project, 1997, 1998). These data indicate that there have been decadal-scale changes of a degree or more in the temperatures of shallow water, and smaller changes in deeper water (Fig. 6.30). Interdecadal variability is apparent along the Beaufort Shelf (warmer in the 1960s and 1980s) and the Laptev Sea Shelf (cooler in the 1980s).

6.6.2.3. Projected changes

The stability of coastal and subsea permafrost in a changing climate depends directly on the magnitude of changes in water temperature and salinity, air temperature, sea-ice thickness, and coastal and seabed stability. It is difficult to extract the relevant projections of environmental forcing (subsurface and seabed water temperatures in particular) from any of the scenarios generated by climate models. In general terms:

- The projected increase in air temperature (section 4.4.2) is likely to increase backshore thermokarst development, resulting in more rapid input of material to, and sediment deposition in, the coastal environment. Increased air temperatures will also tend to increase permafrost instability in Zone 1, especially in the supra-tidal environment, and will probably result in increased coastal water temperatures. These factors, cou-

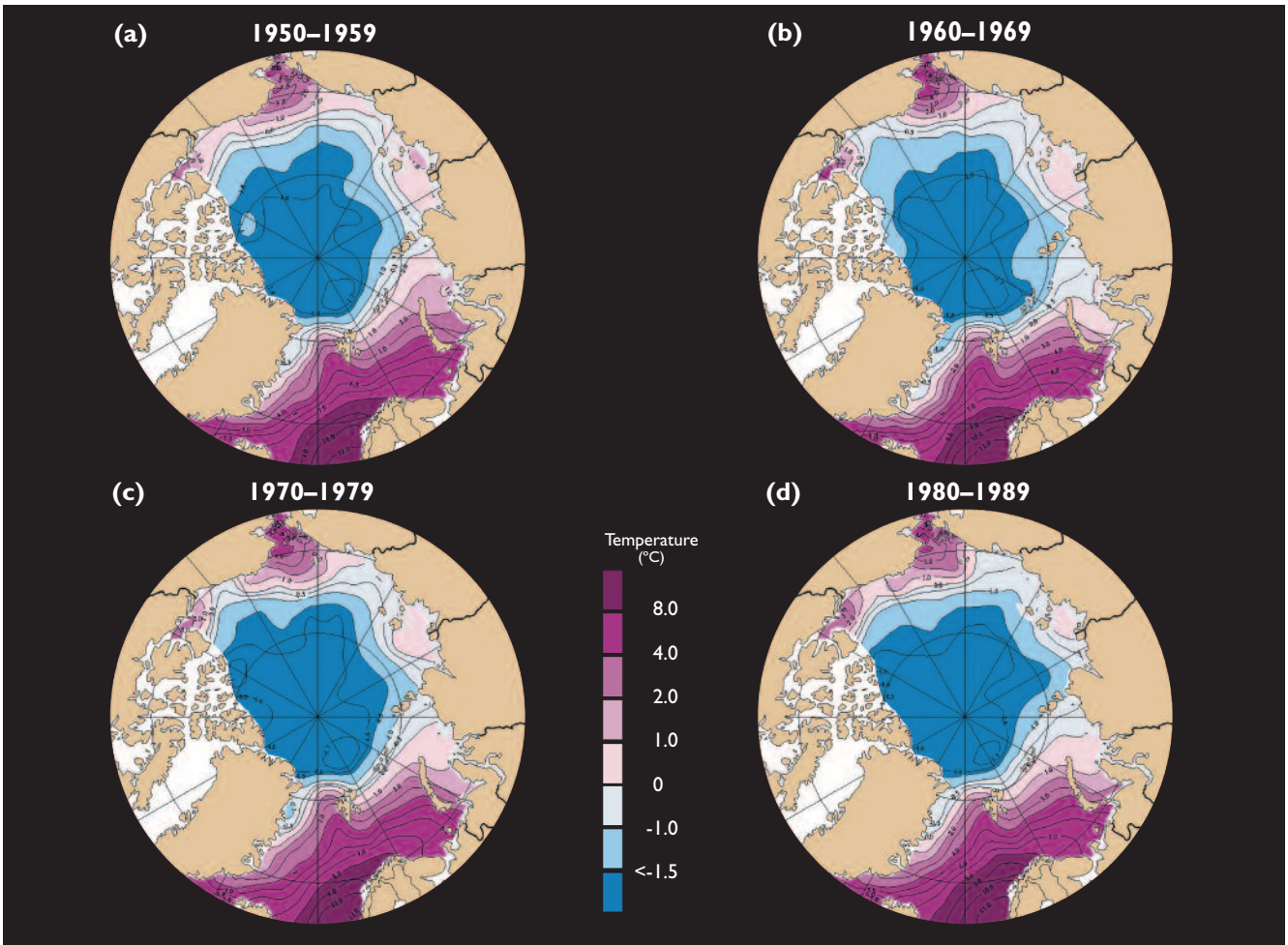

Fig. 6.30. Average decadal summer ocean temperature at 10 m depth from (a) the 1950s to (d) the 1980s (data from the Arctic Climatology Project, 1998).

pled with decreased sea-ice thickness, are likely to cause more rapid warming of permafrost in Zones 1 and 2.
- Projected increases in sea level (section 6.9.3) are likely to shift the location of Zones 1 and 2 to higher elevations, resulting in increased rates of erosion and attendant increases in instability of coastal permafrost.
- Longer open-water seasons, resulting from projected decreases in sea ice cover (section 6.3.3), are likely to expose coastal environments to more storms, resulting in increased rates of backshore erosion. This will lead to higher rates of nearshore deposition in localized areas, with attendant possible permafrost aggradation (e.g., Dyke and Wolfe, 1993). However, rapid backshore erosion is also likely to increase the rate at which terrestrial permafrost is exposed to coastal conditions, leading to warming of terrestrial permafrost in the backshore environment.
- Projected changes in fluvial inflow patterns (section 6.8.3) are likely to change the nearshore and coastal salinity and temperature regimes. Lower flow rates and changes in the timing and duration of floods will affect rates of erosion and deposition, and also the salinity and temperature of the coastal ocean. Higher water temperatures will increase permafrost destabilization; lower flow rates could result in higher coastal salinity, which also would increase rates of permafrost thaw.
- Changes in the thickness and extent of sea ice are likely to affect Zone 3 in that there may be less restriction of circulation as sea-ice conditions become less severe. This would inhibit brine formation in bays, reducing rates of permafrost thawing by an unknown amount. Changing sea-ice regimes will also affect pressure-ridge development, which will change under-ice circulation, but the direction of change is uncertain. It is likely that the effects will be local.
- Changes in sea-bottom water temperature and salinity could possibly occur in Zones 3 and 4, although most AOGCMs do not explicitly project values for these variables. Thawed sediments above the permafrost surface will buffer the effect: a change of 1 °C would take several decades to propagate from the seabed surface to the upper permafrost boundary 10 to 100 m below the seabed surface (Taylor, pers. comm., 2002). Gas hydrates within and beneath the subsea permafrost will also be buffered from the immediate effects of changing seabed conditions and in the near term may be relatively unaffected. Over longer time periods (100 years or more), there is potential for increased instability of subsea gas hydrates in shallow waters of the Arctic. In water deeper than 200 m, other gas hydrates (unrelated to permafrost) that are also susceptible to destabilization by increased bottom-water temperatures may exist close to the seabed surface.

6.6.2.4. Impacts of projected changes

On other parts of the physical system

Decreases in the stability of coastal permafrost are likely to result in greater nearshore thaw subsidence and increased rates of coastal erosion. This will introduce greater sediment loads to the coastal system; higher levels of suspended sediment and changes in depositional patterns may ensue. Increased erosion rates will also result in greater emissions of CO_2 from coastal and nearshore sources, and increased emission rates of CH_4 from terrestrial permafrost. Over the long-term, destabilization of intra-permafrost gas hydrates is likely to enhance climate change.

On ecosystems

Changing deposition patterns and suspended sediment loads along the coast are likely to have impacts on marine ecosystems, including anadromous fish migration, phytoplankton blooms, and benthic communities. Negative or positive impacts are possible. Increased suspended material may increase nutrients, resulting in higher productivity in nutrient-limited systems. Conversely, increased suspended material lowers light levels, resulting in lower productivity. The potential impacts of changes in subsea and coastal permafrost on marine ecosystems are discussed further in Chapter 9.

On people

Decreases in the stability of coastal permafrost will have an impact on coastal infrastructure. Increased erosion rates, caused in part by nearshore thaw subsidence, are likely to affect communities and industrial facilities situated close to the coast. Permafrost thawing and subsidence could affect pipelines in nearshore and coastal environments in excess of their design specifications. Warming and/or thawing permafrost is likely to reduce the foundation strength of wharves and associated pilings. In deeper water (Zones 3 and 4), permafrost warming could affect design considerations for hydrocarbon production facilities, including casing strings and platforms anchored to the seabed. Chapter 16 addresses specific infrastructure issues associated with changes in coastal permafrost.

6.6.2.5. Critical research needs

A circumpolar program to monitor changes in the coastal and offshore cryosphere is required, as is a better understanding of the processes that drive those changes. The Arctic Coastal Dynamics (ACD) project, sponsored by the International Arctic Science Committee and the International Permafrost Association, is promoting the need for such studies. At present, there is no monitoring of coastal and subsea permafrost, and this lack represents a critical gap in the understanding of coastal stability in the Arctic. The absence of monitoring is a result of the difficulty in working in arctic coastal environments,

particularly in Zones 1 and 2. Equipment for measuring temperatures throughout the year must be placed in such a way that cables are not jeopardized by storms and sea ice. The technology exists, but it is more expensive than that used for similar measurements on land.

A comprehensive understanding of coastal permafrost processes, including the interaction between storms and permafrost, is needed. Heat convection is thought to play a major role in coastal permafrost thawing during storms after the thawed overlying material is removed (Kobayashi et al., 1999). However, given the difficulty of making measurements at the shoreline under storm conditions, there are no observations supporting this hypothesis. Laboratory studies could play a role in this regard. Thaw subsidence rates can exceed the rate of eustatic sea-level rise (rise due to changes in the mass of ocean water, see section 6.9.1), and are therefore thought to contribute to coastal erosion, at least at a local scale. However, there are few documented observations of the magnitude of thaw subsidence and/or its role in coastal erosion.

The role of brine exclusion and convection in enhancing coastal and subsea permafrost degradation requires further investigation.

Finally, the gas hydrates in coastal and subsea permafrost require further study in order to evaluate their stability over the range of future climate change scenarios produced by climate models.

6.7. River and lake ice

6.7.1. Background

Ice cover plays a fundamental role in the biological, chemical, and physical processes of arctic freshwater systems (e.g., Adams, 1981; Magnuson et al., 1997; Prowse, 2001; Schindler et al., 1996; Willemse and Tornqvist, 1999; see also section 8.2). In particular, freshwater ice is integral to the hydrological cycle of northern systems. The duration and composition of lake ice, for example, controls the seasonal heat budget of lake systems. This in turn determines the magnitude and timing of evaporation from these systems, ranging from small ponds to large lakes; storage levels in the latter also control the flow of some of the major arctic rivers, such as the Mackenzie. Similarly, river ice has a significant influence on the timing and magnitude of extreme hydrological events, such as low flows (Prowse and Carter, 2002) and floods (Prowse and Beltaos, 2002). Many of these hydrological events are due more to in-channel ice effects than to landscape runoff processes (Gerard, 1990; Prowse, 1994).

Lake ice and river ice also serve as climate indicators, and long-term records of these variables provide useful proxy climate data. For some sites in northern Finland and Siberia, the dates of ice formation and breakup have been recorded since the 16th century (Magnuson et al., 2000). Given the proxy potential of freshwater ice, considerable recent research has focused on the use of remote sensing for documenting ice phenology (e.g., Wynn and Lillesand, 1993) and on the hemispheric process-based modeling of lake-ice patterns for assessing the effects of climate variability and change (e.g., Walsh et al., 1998).

Freeze-over processes differ significantly between lakes and rivers, although the timing of each depends on the magnitude of the open-water heat storage and the autumn rate of cooling. The stratigraphy of lake ice is relatively simple, usually consisting of clear columnar ice, an intermediate layer of translucent granular ice, and a surface layer of snow (e.g., Adams, 1981). In contrast, river ice forms by the dynamic accumulation of various ice forms and is characterized by a more complex vertical and horizontal ice structure (e.g., Prowse, 1995). The thickness and physical characteristics (e.g., optical and mechanical) of the ice cover exert significant control over the thermal and mass balance of the underlying water bodies, and produce important hydrological responses. These in turn affect a number of chemical and biological processes as discussed in section 8.2.

Freeze-up is controlled by a combination of atmospheric heat fluxes. Of all meteorological variables, freeze-up timing correlates best with air temperature in the preceding weeks to months (e.g., Palecki and Barry, 1986; Reycraft and Skinner, 1993). In the case of lakes, area and depth are important determinants of the heat budget and therefore the timing of freeze-up (Stewart and Haugen, 1990). Depth is not as important a factor in determining the timing of lake-ice breakup as it is for freeze-up (Vavrus et al., 1996; Wynn et al., 1996); the timing of lake breakup is determined more by the energy balance characterizing the melt period leading up to the event (e.g., Anderson et al., 1996; Assel and Robertson, 1995). Ice breakup on rivers is a more complex process than that on lakes and, because it is not as strongly related to a single meteorological variable such as air temperature, it is less valuable as a climatic indicator (Barry, 1984). For example, the primary determinant of mechanical strength is insolation-induced decay, which is dependent on solar radiation and ice-cover composition (Prowse and Demuth, 1993). The latter, which can be influenced by snow loading and the generation of surface "snow-ice", also controls the surface albedo and the effectiveness of insolation in reducing ice strength. Ice breakup on northern rivers usually coincides with spring melt of the catchment snow cover and produces the major hydrological event of the year (Church M., 1974; Prowse, 1994).

The most common approach to projecting breakup timing on lakes and rivers employs an air temperature index, such as accumulated degree-days, which reflects the amount of ice deterioration and, in the case of rivers, the magnitude of the snowmelt flood wave (Prowse, 1995). While recognizing that numerous physical and climatological factors influence the rates and

timing of ice formation and decay processes, Magnuson et al. (2000) estimated the change in freeze-up and breakup dates relative to a change in air temperature in the preceding weeks or months to be approximately 5 days/°C based on results from a number of lake- and river-ice case studies. Estimating the severity of breakup requires the use of a wider range of meteorological factors (e.g., Gray and Prowse, 1993).

Ice jams frequently form on rivers, and, because of their high hydraulic resistance, produce flood levels that often far exceed those for equivalent discharge under open-water conditions, usually with a high recurrence interval (Beltaos, 1995; Prowse and Beltaos, 2002). Dredging, blasting, and aerial bombing have been used to try to dislodge ice jams, with varying degrees of success, but these approaches often produce local environmental damage (Burrell, 1995).

One of the most persistent effects of ice on river hydrology is its influence on water levels. Although the additional hydraulic resistance of a stable ice cover tends to elevate channel water levels, the greatest effect occurs when the ice cover is hydraulically rough, as it often is following a dynamically active freeze-up period. In combination with rapid freezing, hydraulic staging of the ice cover can extract significant amounts of water such that a period of low flow prevails. The release of water stored during this period can significantly augment the spring freshet (Prowse and Carter, 2002).

6.7.2. Recent and ongoing changes

Although changes in the thickness and composition of freshwater ice or in the severity of freeze-up and breakup events can have significant implications for numerous physical and ecological processes, available documentation of past changes is largely limited to simple observations of the timing of freeze-up and breakup. Such data are, however, useful indicators of climate change, although long-term records are relatively scarce. Magnuson et al. (2000) assessed freeze-up and breakup trends for Northern Hemisphere lakes and rivers that had records spanning at least 100 years within the period from 1846 to 1995 (only three sites had records beginning prior to 1800). Of the 26 rivers and lakes included in the study, most are located south of 60° N. Over the 150-year period, average freeze-up dates were delayed by 5.8 d/100 yr and average breakup dates advanced by 6.3 d/100 yr, corresponding to an increase in air temperature of about 1.2 °C/100 yr. Magnuson et al. (2000) further observed that the few available longer time series indicate that a trend of reduced ice cover began as early as the 16th century, although rates of change increased after approximately 1850. Figure 6.31 shows the time series of freeze-up and breakup dates for a sample of the rivers and lakes studied. The high-latitude water bodies in Fig. 6.31 (the Mackenzie River in Canada and Kallavesi Lake in Finland) both show general trends toward later freeze-up dates, although decadal-scale variations make trends sensitive to the

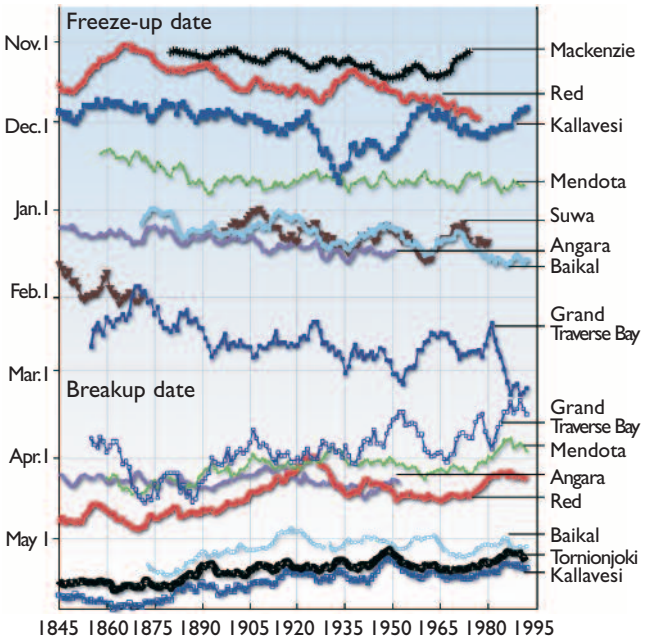

Fig. 6.31. Ten-year running means of freeze-up (top) and breakup (bottom) dates of selected lakes and rivers in the Northern Hemisphere: Mackenzie River (Canada), Red River (Canada), Kallavesi Lake (Finland), Lake Mendota (U.S.), Lake Suwa (Japan), Angara River (eastern Russia), Lake Baikal (eastern Russia), Grand Traverse Bay (Lake Michigan, United States), and Tornionjoki River (Finland) (Magnuson et al., 2000).

beginning and end dates of the calculations. Similar sensitivity is found in the trend toward earlier breakup of Kallavesi Lake, and in the breakup date of the Tanana River at Nenana, Alaska, for which the time series in Fig. 6.32 shows interannual and decadal-scale variations superimposed on the trend toward earlier breakup.

Most of the very long-term records analyzed by Magnuson et al. (2000) are geographically diverse and give little insight into potential regional trends. Moreover, few sites are even located above 60° N. To gain a better understanding of recent and ongoing changes at high latitudes, records shorter than 150 years must be examined. The most comprehensive regional evaluation of freeze-up and breakup dates that

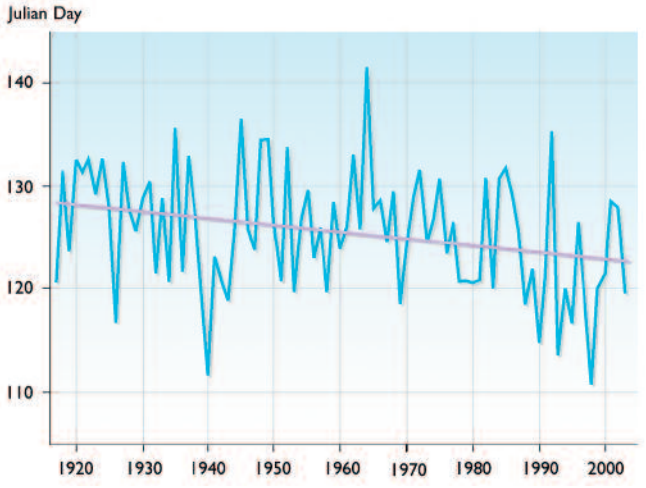

Fig. 6.32. Time series of the breakup date of the Tanana River at Nenana, Alaska (modifed from W. Chapman using data from the National Snow and Ice Data Center, 2003).

includes areas of the Arctic and subarctic was conducted by Ginzburg et al. (1992) and Soldatova (1993), using data from about 1893 to 1985 for homogenous hydrological regions of the Former Soviet Union. Although appreciable interdecadal variability was found, significant long-term spatial patterns and temporal trends in freeze-up and breakup dates were identified for the period. The most significant regional trend was toward later river-ice freeze-up dates in the European part of the Former Soviet Union and western Siberia. A weaker but still significant trend toward earlier freeze-up dates was found for portions of rivers (e.g., the Yenisey and Lena) in central and eastern Siberia (Ginzburg et al., 1992). A similar broad-scale spatial pattern is evident for breakup dates (Soldatova, 1993). Breakup on major rivers in the European part of the Former Soviet Union and western Siberia advanced by an average of 7 to 10 d/100 yr, resulting in a reduction in ice-season duration of up to a month. However, some rivers in central and eastern Siberia exhibited an opposing trend: later breakup dates and hence an increase in ice-season duration. Freeze-up and breakup dates were well correlated (r^2=0.6–0.7) with the mean air temperature in the preceding autumn and spring months, respectively. A gradual advancement in the date of breakup has been documented for lakes in southern Finland (Kuusisto and Elo, 2000) and rivers in northern Sweden/Finland and Latvia (Kuusisto and Elo, 2000; Zachrisson, 1989).

In northwestern North America, studies of the Tanana River (1917–2000; Sagarin and Micheli, 2001) and the Yukon River (1896–1998; Jasek, 1998) indicate that the average date of breakup has advanced by approximately 5 d/100 yr. This trend is characterized by a number of interdecadal cycles. Zhang X. et al. (2001) conducted a Canada-wide assessment of river freeze-up, breakup, and ice duration using records spanning 50 years or less. The major spatial distinction in breakup timing was between eastern and western sites, with the western sites (e.g., the Yukon and other western rivers) showing trends towards earlier breakup dates. Notably, there was also a nation-wide trend to earlier freeze-up dates.

Smith (2000) conducted a study of shorter-term records from nine major arctic and subarctic rivers in Russia. Some trends were opposite to those found for the longer-term and broader regional studies of Ginzburg et al. (1992) and Soldatova (1993), possibly because of the shorter record lengths (54 to 71 years) or differences resulting from site-specific factors. In particular, earlier rather than later freeze-up dates were found for rivers west of and including the Yenisey, whereas later freeze-up dates were observed for rivers in far eastern Siberia. Although Smith (2000) found no statistically significant shifts in breakup timing, there were significant shifts toward an earlier melt onset, producing a trend toward a longer period of pre-breakup melt. According to breakup theory, a longer melt period favors "thermal" breakups – low-energy events that are less likely to produce floods and related disturbances (e.g., Gray and Prowse, 1993). Similar analyses, or studies that focus on breakup characteristics beyond simple timing, have not been conducted elsewhere.

6.7.3. Projected changes

Although many case studies of existing data show relationships between the timing of freeze-up and breakup and the preceding autumn and spring air temperatures, such relationships are not necessarily temporally stable. For example, Livingstone (1999) found that the influence of April air temperatures on Lake Baikal breakup dates has varied considerably over the past 100 years, and accounts for only 12 to 39% of the variance in breakup dates. Furthermore, there is no guarantee that such empirical relationships will hold for future climatic conditions, particularly if they are characterized by significant changes in the composition of the major heat fluxes (e.g., Bonsal and Prowse, 2003).

Considering only the projected changes in air temperature, the general pattern of change in freshwater ice will be a general reduction in ice cover on arctic rivers and lakes. This reduction will be greatest in the regions of greatest warming. The warming varies somewhat from model to model, but is generally larger in the northernmost land areas than in the subpolar land areas. None of the five ACIA-designated models projects a cooling over northern terrestrial regions. However, the reduction in river and lake ice may be modified by changes in precipitation (including snowfall) over the 21st century, and the projected changes in precipitation vary substantially from model to model.

Freeze-up and breakup dates are projected to respond more strongly to warming than to cooling because of albedo–radiation feedbacks (e.g., Vavrus et al., 1996). However, changes in winter precipitation will modify this pattern. Increased snowfall should lead to a delay in breakup owing to additions of white ice and longer-lasting higher albedo. Conversely, decreased snowfall should advance breakup owing to lower spring albedo, although reduced insulation in winter could also lead to enhanced ice growth. Projecting specific regional responses requires detailed physical modeling (employing multi-variable meteorological input) of changes not only in winter snow and ice conditions, but also in the open-water heat budgets that strongly influence freeze-up timing and subsequent ice growth. Projections for river ice are even more complex because the heat budgets of contributing catchment flow must be considered, together with changes in the timing and magnitude of flow that control many of the important river-ice hydrological extremes. Prowse and Beltaos (2002) reviewed a range of the complex interacting hydraulic, mechanical, and thermal changes that could result from shifts in temperature and precipitation. In general, as for lake ice, the duration and composition of river-ice cover would change, as would the potential for extreme conditions during freeze-up and breakup.

6.7.4. Impacts of projected changes

On other parts of the physical system

A number of physical, biological, and chemical changes will result from changes in the timing, composition, and duration of lake- and river-ice cover. Some of the most direct changes will be shifts in the thermal and radiation regimes, which can have indirect effects on freshwater habitat and quality (e.g., water temperature and dissolved oxygen). Hydrological processes (e.g. discharge timing, evaporation) are also likely to be affected. For northern peatlands, ice-induced changes in open-water evaporation and resultant water levels are likely to determine whether they become sources or sinks of CO_2 and CH_4 (section 7.5.3). For regions with extensive lake cover and substantial winter water storage, changes in the timing and magnitude of winter snowfall will produce corresponding changes in the winter pulsing of river discharge. Changes in the timing and severity of freeze-up and breakup will alter the hydrological extremes (e.g., low flows and floods) that dominate the flow regime of northern systems. A change in breakup intensity will also alter channel-forming processes, as well as levels of suspended sediment ultimately carried to the Arctic Ocean.

On ecosystems

Biological and chemical changes are likely to result from changes in the timing and duration of lake- and river-ice cover (section 8.4). A change in breakup intensity will affect the supply of floodwater, organic carbon, and nutrients to riparian zones; the ecosystem health of river deltas is particularly dependent on such fluxes.

On people

Winter roads that use the ice cover of interconnected lakes and rivers service extensive areas of the north, particularly those areas being explored or developed by resource extraction industries. Any changes in the thickness, composition, and/or mechanical strength of such ice will have major transportation and financial implications. The greatest economic impact is likely to stem from a decrease in ice thickness and bearing capacity, which could severely restrict the size and load limit of vehicular traffic. Changing ice regimes will also affect shipping operations, particularly on large Russian rivers where icebreakers are employed to extend the shipping season to northern towns and industries. Considering the high operational costs of ice breaking, any reduction in the duration of the ice season or breakup severity should translate into significant cost savings.

Changes in the ice regime will also require changes in operating strategies for hydroelectric installations, both at the generating facility to reduce impacts from ice (e.g., accumulations of frazil, the slushy ice-water mixture that develops when turbulent water starts to freeze), and for management of downstream flows to minimize negative impacts on river ecology and infrastructure. Major economic savings are likely to accrue to hydroelectric facilities if climate change reduces the length of the ice season. However, if the length of the ice season is reduced, the increased time required for freeze-up to a hydraulically stable ice cover will have at least some negative economic consequences (e.g., the necessary reductions in peak generating capacity during the freeze-up period).

6.7.5. Critical research needs

Critical research needs with regard to river and lake ice include improved understanding of the interacting hydrological and meteorological controls on freeze-up and breakup, reliable projections of changes in these controls over the 21st century, and further refinement of models of lake-ice growth and ablation (e.g., Duguay et al., 2003) and river-ice dynamics (e.g., Petryk, 1995) for use in forecasting future conditions. There is a particular need for more credible model projections of precipitation and surface solar radiative fluxes. Snowfall can influence river and lake ice by changing the composition of the ice cover and, through its effects on insulation and insolation, ice growth and ablation rates. Accumulated winter precipitation also determines the magnitude of the spring runoff, which controls the severity of breakup and associated ice-jam flooding. Surface radiative fluxes are key controls of river and lake ice, affecting both rates of ablation and changes in mechanical strength of the ice cover. However, model projections of future radiative fluxes, which will depend strongly on changes in cloudiness, are highly uncertain.

6.8. Freshwater discharge

6.8.1. Background

Many of the linkages between the arctic system and global climate involve the hydrological cycle. Theoretical arguments and models both suggest that net high-latitude precipitation increases in proportion to increases in mean hemispheric temperature (Manabe and Stouffer, 1993; Rahmstorf and Ganopolsky, 1999). Section 6.2.3 showed that precipitation and precipitation minus evapotranspiration (P-E) are projected to increase in the Arctic as GHG concentrations increase. This is supported by the nearly linear relationship between temperature and ice accumulation found in Greenland ice cores over the past 20 000 years (Van der Veen, 2002). At the same time, increased freshwater export from the Arctic Ocean may reduce North Atlantic Deep Water formation and Atlantic thermohaline circulation (Broecker, 1997). These changes in Atlantic thermohaline circulation may trigger major climatic shifts. Terrestrial discharge, or river runoff, to the Arctic Ocean may therefore have global implications.

To analyze the variability of the Arctic Ocean's freshwater budget, both the Arctic Ocean watershed and the adjacent territories from which the runoff originates (Fig. 6.33) must be considered. The total area of the

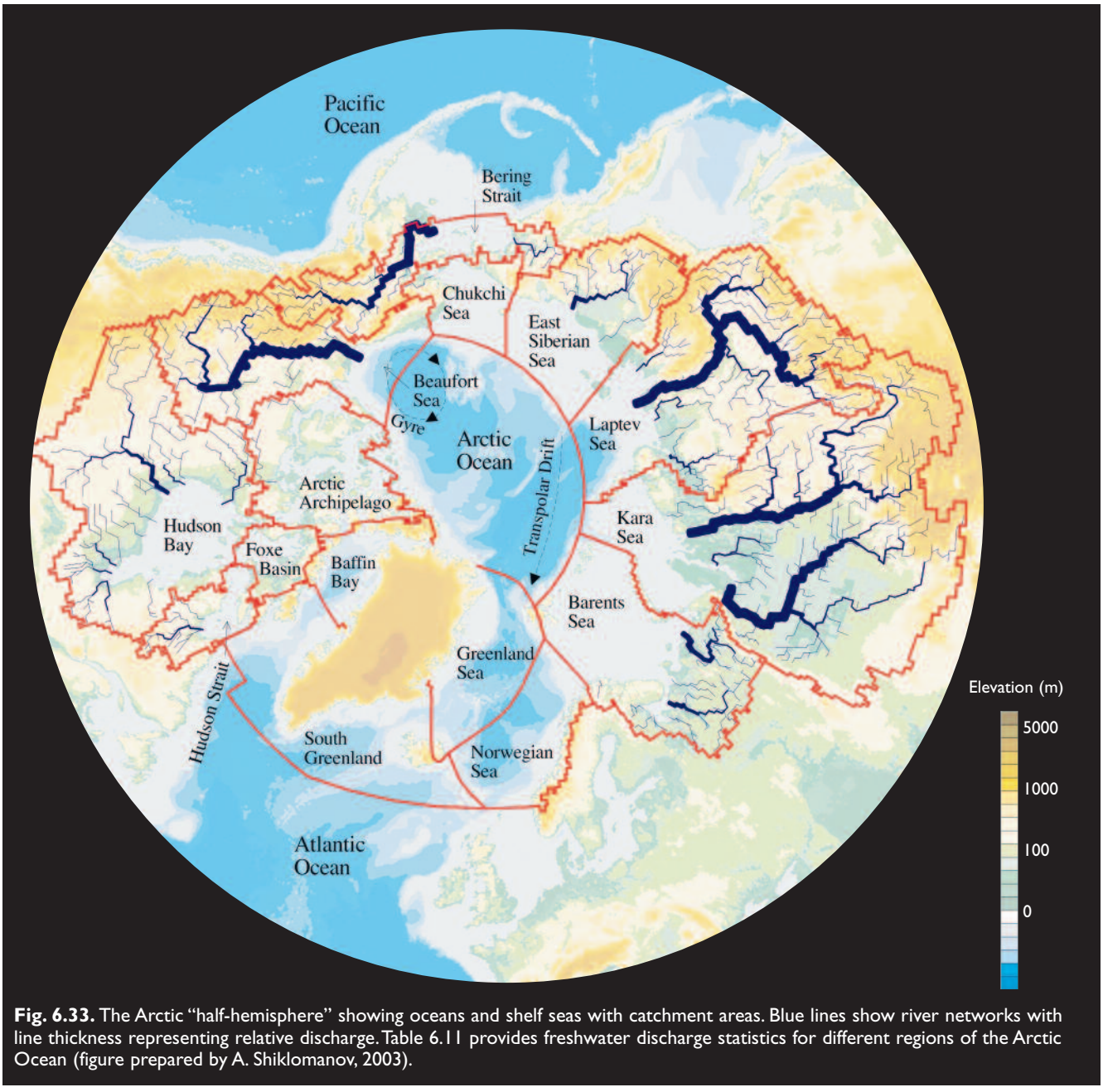

Fig. 6.33. The Arctic "half-hemisphere" showing oceans and shelf seas with catchment areas. Blue lines show river networks with line thickness representing relative discharge. Table 6.11 provides freshwater discharge statistics for different regions of the Arctic Ocean (figure prepared by A. Shiklomanov, 2003).

Arctic Ocean drainage basin, together with the adjacent Hudson Bay and Bering Sea drainage basins, is about 24 million km^2 (Forman et al., 2000; Shiklomanov I. et al., 2000). This huge area includes a wide variety of surface types and climate zones, from semiarid regions in the south to polar deserts in the north.

Table 6.11. Mean annual discharge of freshwater to the Arctic Ocean for the period 1921 to 2000 (Shiklomanov I. et al., 2000, updated by A. Shiklomanov, 2003).

Basin	Discharge (km^3/yr)	Coefficient of variation	Maximum discharge km^3	Maximum discharge year	Minimum discharge km^3	Minimum discharge year
Bering Strait	301	0.09	362	1990	259	1999
Hudson Bay and Strait	946	0.09	1140	1966	733	1989
North America (Arctic Ocean drainage basin only)	1187	0.09	1510	1996	990	1953
North America including Hudson Bay basin	2133	0.07	2475	1996	1800	1998
Europe	697	0.08	884	1938	504	1960
Asia (Arctic Ocean drainage basin only)	2430	0.06	2890	1974	2100	1953
Arctic Ocean drainage basin	4314	0.05	4870	1974	3820	1953
Arctic Ocean drainage basin and Hudson Bay basin	5250	0.04	5950	1974	4700	1953

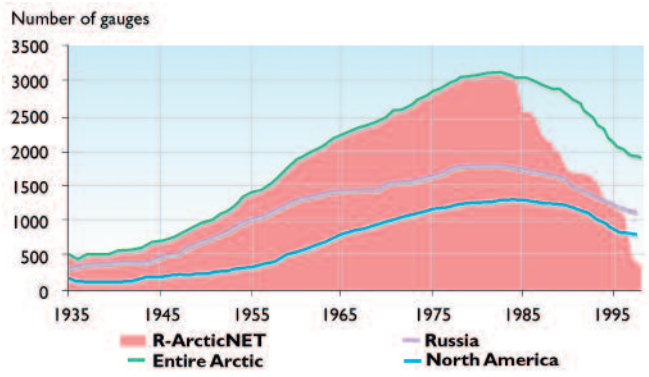

Fig. 6.34. Time series of the number of river discharge gauges in the Arctic Ocean drainage basin, the Russian Arctic, and the North American Arctic. Shaded area represents the number of stations with data that have been included in the R-ArcticNET database of the Arctic-RIMS project (Shiklomanov A. et al., 2002).

The spatial distribution of the hydrological monitoring network in the Arctic is extremely uneven. The greatest numbers of stations are located in Europe, the southern part of western Siberia, and the Hudson Bay drainage basin, while the northern part of the Arctic, including Greenland, the arctic islands, and coastal regions, is essentially unmonitored. Monitoring capacity in both North America and Eurasia peaked in 1985, when the percentage of Arctic Ocean drainage area monitored by gauges was 50.2% in North America, 85.1% in Asia, and 70.7% in Europe (but 0% in Greenland). Since 1985, the number of hydrometric stations has decreased significantly, owing to budget constraints and (in Siberia) population losses. The total number of gauges throughout the Arctic is now 38% lower than in 1985 (Fig. 6.34); in 1999, the discharge monitoring network had the same number of gauges as in 1960 (Shiklomanov A. et al., 2002).

The total freshwater discharge from the land area into the Arctic Ocean is the sum of river discharge into the ocean, glacier and ice sheet discharge, subsurface water flows (mainly from the freeze–thaw cycle in the active layer of permafrost soils), and groundwater flows. Most of the glacier streamflow enters the subpolar seas (e.g., Greenland Sea, Baffin Bay/Davis Strait, Gulf of Alaska) rather than the Arctic Ocean. Subsurface and groundwater flow to the Arctic Ocean is considered to be orders of magnitude lower than river discharge (Grabs et al., 2000), but is very important during winter, when other sources of discharge are substantially reduced. Seasonally frozen ground also affects the interactions between surface runoff, subsurface runoff, and subsurface storage (Bowling et al., 2000).

Estimates of river discharge to the Arctic Ocean are highly dependent on the specification of the contributing area (Prowse and Flegg, 2000). According to a contemporary assessment based on available hydrometric and meteorological information (Shiklomanov I. et al., 2000), the total long-term river discharge from the entire Arctic Ocean drainage basin (including Hudson Bay but not Bering Strait) is 5250 km^3/yr (46% from Asia, 41% from North America and Greenland, and 13% from Europe). Excluding Hudson Bay, direct river discharge to the Arctic Ocean is 4320 km^3/yr (1190, 2430, and 700 km^3/yr from North America, Asia, and Europe respectively). Table 6.11 presents statistics of the annual discharge to the Arctic Ocean from the different drainage areas. The World Climate Research Programme (WCRP, 1996) provided a similar estimate of freshwater flux from land areas to the Arctic Ocean (4269 km^3/yr with 41% attributed to unmeasured discharge). Earlier estimates of total river discharge to the Arctic Ocean were lower: 3300 km^3/yr (Aagaard and Carmack, 1989); 3500 km^3/yr (Ivanov, 1976); and 3740 km^3/yr (Gordeev et al., 1996). These earlier studies underestimated the freshwater discharge to the Arctic Ocean because they did not fully consider the unmonitored discharges from the mainland and/or arctic islands. Shiklomanov I. et al. (2000) discussed methods for estimating runoff from unmonitored areas. The total river discharge to the Arctic Ocean (~4300 km^3/yr) is several times the net input of freshwater from P-E over the Arctic Ocean (assuming an average P-E of 10 to 15 cm/yr (section 6.2) and an area of about 10 million km^2).

The spatial distribution of runoff across the Arctic is highly heterogeneous. When standardized to units of runoff volume per area of a drainage basin, the smallest values (<10 mm/yr) are found in the prairies of Canada and the steppes of West Siberia. The highest values (>1000 mm/yr) are found in Norway, Iceland, and the mountain regions of Siberia (Lammers et al., 2001).

Rivers flowing into the Arctic Ocean are characterized by very low winter runoff, high spring flow rates driven by snowmelt, and rain-induced floods in the summer and autumn. The degree of seasonality depends on climate conditions, land cover, permafrost extent, and level of natural and artificial runoff regulation. Snowmelt contributes up to 80% of the annual runoff in regions with a continental climate and continuous permafrost, such as the northern parts of central and eastern Siberia, and contributes about 50% of the annual runoff in northern Europe and northeastern Canada (AARI, 1985). Most eastern Siberian and northern Canadian rivers with drainage areas smaller than 10^5 km^2 that flow through the continuous permafrost zone have practically no runoff during winter because the supply of groundwater is so low.

6.8.2. Recent and ongoing changes

Shiklomanov I. et al. (2000) calculated time series of river discharge to the Arctic Ocean from the individual drainage areas between 1921 and 1999 based on hydrometeorological observations. Figure 6.35 summarizes the temporal variations by region. Cyclical discharge variations with relatively small positive trends are evident for the Asian and Northern American regions, while river discharge to Hudson Bay decreased by 6% over the period. According to this assessment, annual

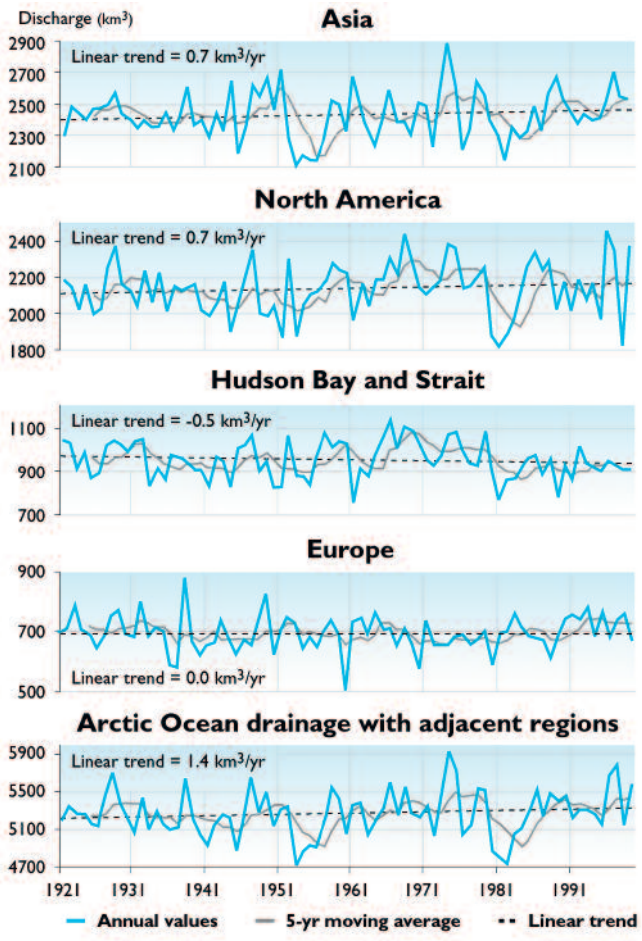

Fig. 6.35. Time series of river discharge to the Arctic Ocean from different parts of the drainage basin between 1921 and 1999 (Shiklomanov I. et al., 2000).

freshwater discharge to the Arctic Ocean increased by 112 km^3 between 1921 and 1999.

In a study that used long-term hydrometric observations for the Eurasian Arctic, Peterson et al. (2002) found that the annual discharge to the Arctic Ocean from the six largest Eurasian rivers increased by 7% between 1936 and 1999. Although the increase is not monotonic (Fig. 6.36), it is statistically significant. The 7% increase in the discharge of these rivers implies that the annual freshwater inflow to the Arctic Ocean is now 128 km^3 greater than it was in the mid-1930s.

Variations in river discharge occur primarily in response to variations in atmospheric forcing, particularly air temperature and precipitation. The ten largest arctic river basins all show an increase in air temperature during the past 30 years (New et al., 2000), as shown in Table 6.12. The greatest runoff increase is observed in the large European rivers (e.g., Severnaya Dvina, Pechora), where significant increases in precipitation have occurred. The largest Siberian river basins (e.g., the Yenisey and Lena), in which permafrost is widespread, show an increase in runoff despite a decreasing trend in precipitation. Factors that may have contributed to this increase include a shorter winter period, faster spring snowmelt (reducing evaporation and infiltration losses), thawing permafrost, and saturated soils resulting from an increase in groundwater storage. However, there are large uncertainties in the precipitation data and the calculated changes in precipitation. The relationship between changes in precipitation and river discharge clearly requires additional investigation.

In addition to its correlation with regional temperature, discharge from the large Siberian rivers is correlated with global mean surface air temperature and with the NAO index (Peterson et al., 2002), as shown in Fig. 6.36. The linkage between the NAO (or its broader manifestation, the AO) and Eurasian temperature and precipitation has been documented by Thompson and Wallace (1998) and Dickson et al. (2000). The strengthened westerlies characteristic of the positive phase of the NAO enhance the transport of moisture and relative warmth across northern Europe and northern Asia (Semiletov et al., 2002). It is apparent from Fig. 6.36 that the NAO (or the AO) should be considered in diagnoses of variations in Eurasian river discharge over interannual to decadal timescales.

Savelieva et al. (2000) related changes in the seasonality of Siberian river discharge in the second half of the 20th century to a climate shift that occurred in the 1970s. A shift in climatic conditions over the Pacific Ocean and Siberia around 1977 has been well-documented (Hare and Mantua, 2000; Minobe, 2000; Overland et al., 1999).

When analyzing seasonal trends in river discharge, the downstream gauges of most of the large rivers cannot be used because of the impoundments within their basins. Even small reservoirs can have a significant impact during times of low flow (winter). For example, Ye B. et al. (2003) showed that a relatively small reservoir in the Lena Basin significantly changed the winter

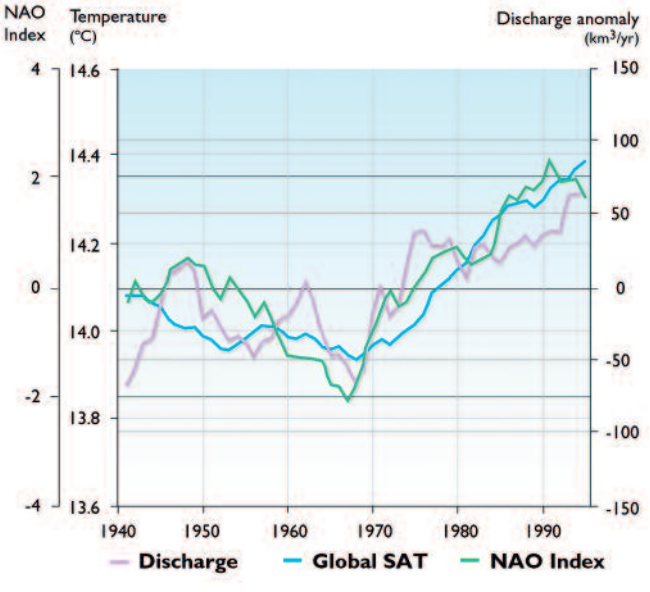

Fig. 6.36. Ten-year running averages of the Eurasian Arctic river discharge anomaly (departure from the 1936–1999 mean), global mean surface air temperature (SAT), and the winter (Dec–Mar) NAO index (Peterson et al., 2002).

discharge regime at downstream locations. Therefore, in a recent attempt to identify seasonal variations and changes in the hydrological regime of the Eurasian Arctic, Georgievsky et al. (2002) analyzed data from 97 rivers with monthly discharge records exceeding 50 years and no significant human influence. The results show that between 1978 and 2000, winter river runoff increased relative to its longer-term mean across most of the region (Fig. 6.37c). Significant increases (10 to 30%) in winter and summer–autumn runoff occurred in rivers located in the part of European Russia that drains into the Arctic Ocean (Fig. 6.37b, c). Even greater changes occurred in Siberia. Winter runoff increased by up to 40 to 60% in the Irtysh Basin and in southeastern Siberia, and by up to 15 to 35% in northern Siberia.

Figure 6.37d shows that the annual runoff in the Eurasian part of the arctic drainage basin has been significantly higher during the last 20 to 25 years, excluding south-central Siberia where annual runoff has been lower than the longer-term average. The most significant increase (>30%) has occurred in European Russia and the western part of the Irtysh Basin. The runoff in the Lena Basin has increased by up to 15 to 25% in the south and by 5 to 15% in the north.

6.8.3. Projected changes

General conclusions about the influence of projected climate change on river discharge to the Arctic Ocean are drawn from a synthesis of studies by various investigators from different countries (e.g., Shiklomanov A., 1994, 1997; Van der Linden et al., 2003). Climate change scenarios used in all of these estimates were generated by various general circulation models (GCMs) forced with doubled atmospheric CO_2 concentrations, with transient increases of CO_2, and/or with other forcing from paleoclimatic reconstructions. The climate scenarios generated by the GCMs have been used to force hydrological models of varying complexity (Shiklomanov I. and Lins, 1991). The projections obtained with this approach go beyond the projections of changes in P-E (section 6.2.3), since they include the effects of changing temperature and changes in the atmospheric circulation (winds) projected by the GCMs. The projections are summarized in Table 6.13.

Miller and Russell (1992) performed one of the first such assessments, using scenarios for doubled atmospheric CO_2 concentrations from the Goddard Institute for Space Studies (GISS) and Canadian GCMs as input to a simple water-budget model. This assessment projected increases of 10 to 45% in the discharges of the large Eurasian and North American rivers (Table 6.13).

Shiklomanov A. (1994) projected the impact of climate change on the annual and seasonal discharges of the rivers in the Yenisey drainage basin using a number of GCM scenarios and paleoclimate reconstructions as input to the detailed hydrological model developed by

Table 6.12. Changes in air temperature, precipitation, and runoff in the largest arctic river basins between 1936 and 1996, computed based on a linear trend (compiled by A. Shiklomanov using data from New et al., 2000).

	Period	Change for the period			Permafrost extent (% of total area)
		Air temperature (°C)	Precipitation (mm/yr)	River runoff[a] (mm/yr)	
Severnaya Dvina	1936–1996	0.3	24	37	0
	1966–1996	1.3	62	44	
Pechora	1936–1996	0.5	60	53	31
	1966–1996	1.7	27	30	
Ob	1936–1996	1.2	3.8	6	19
	1966–1996	2.2	-4	1	
Yenisey	1936–1996	1.2	-11	13	71
	1966–1996	2.5	0	27	
Lena	1936–1996	1.1	-5	22	94
	1966–1996	2.1	-24	10	
Indigirka	1936–1996	0.0	-34	17	100
	1966–1996	1.0	-42	1	
Kolyma	1936–1996	0.0	-29	-5	100
	1966–1996	0.6	-36	15	
Yukon	1957–1996	1.6	19	6	90
	1966–1996	2.2	43	13	
Mackenzie	1966–1996	1.4	-6	-5	55
Back	1966–1996	1.7	6	6	100

[a]Change in river runoff is presented as the net change (mm/yr) in precipitation minus evapotranspiration, which is equivalent to total basin runoff (km^3/yr) divided by the area (km^2) of the drainage basin.

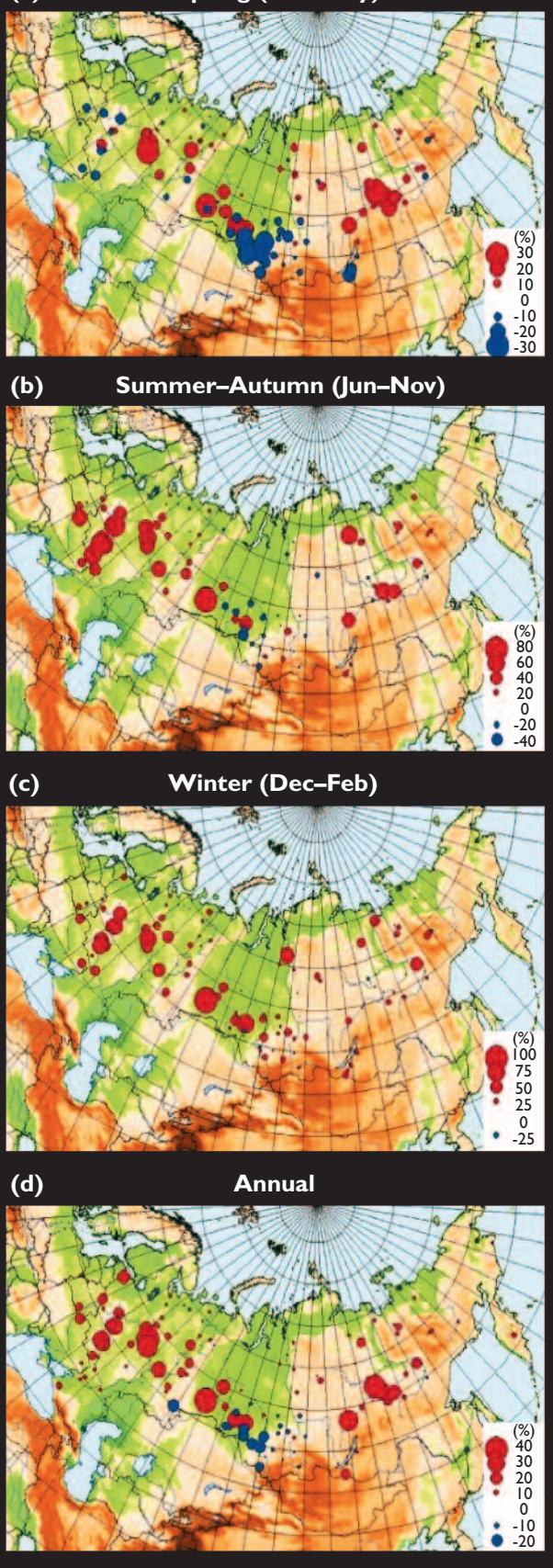

Fig. 6.37. Deviations of the 1978–2000 mean (a) spring, (b) summer–autumn, (c) winter, and (d) annual runoff expressed as a percentage of the long-term mean for each location and season. Red and blue circles denote positive and negative deviations, respectively. The long-term mean is calculated using the entire gauge station history (at least 50 years for all plotted locations). Stations with no deviation in a specific period are not shown. Tan, orange, and brown indicate progressively higher elevations; green indicates low elevations (Georgievsky et al., 2002).

the State Hydrological Institute (Russia) (Table 6.13). According to the more plausible climate scenarios, the mean annual discharge of the Yenisey River is likely to increase by 15 to 20%, and the winter discharge is likely to increase by 50 to 60%. Similar evaluations of river discharge to the Barents Sea drainage basin (Georgievsky et al., 1996) project increases of 14 to 35% and 25 to 46% in the mean annual and winter discharge, respectively (Table 6.13).

Arnell (1999) used six GCM scenarios developed by the Hadley Centre to project changes in runoff from the world's largest rivers between 1961–1990 and 2050. This study projected discharge increases ranging from 3–10% to 30–40% for the largest rivers in the Arctic Ocean drainage basin (Table 6.13). Other assessments (Arora and Boer, 2001; Miller and Russell, 2000; Mokhov et al., 2003) also project significant increases in both the discharge of the largest rivers and in the total river discharge to the Arctic Ocean. Georgievsky et al. (2003) provided projections for the Lena Basin based on a water balance model with a three-layer environment (the active soil layer and two layers of groundwater reservoirs) using input from the HadCM3 model forced with the A2 emissions scenario (section 4.4.1). Annual runoff is projected to increase by 27 mm (12.5%), with higher percentage increases in winter and spring runoff, which would increase the probability of extreme flooding.

The results presented above indicate that, if atmospheric CO_2 concentrations double and the model projections of runoff changes are correct, the total annual discharge to the Arctic Ocean from arctic land areas can be expected to increase by 10 to 20%. The increase in winter discharge is likely to be as high as 50 to 80%. At the same time, 55 to 60% of annual discharge is likely to enter the ocean during the peak runoff season (April–July). It must be emphasized, however, that the B2 emissions scenario (section 4.4.1) used to force the ACIA-designated models does not lead to a doubling of CO_2 concentrations during the 21st century. Relative to the atmospheric CO_2 concentration in 2000 (~370 ppm), the CO_2 concentrations in the B2 emissions scenario increase by about 30% by 2050 and 65% by 2100. (In the A2 emissions scenario, the corresponding increases are about 40% by 2050 and 120% by 2100.)

For this reason, it is not surprising that the 10 to 20% increase in discharge cited above is larger than the ACIA-designated model projections of increases in precipitation and P-E, which are about 10% or slightly less (Fig. 6.2). The projected changes in temperature, precipitation, and river discharge obtained from other forcing scenarios (e.g., Table 6.13) must be tempered accordingly.

6.8.4. Impacts of projected changes

On other parts of physical system

Changes in freshwater runoff are likely to affect upper-ocean salinity, sea-ice production, export of

Table 6.13. Projected change in the discharge of the largest arctic rivers using different climate models and forcing scenarios.

	GCM and forcing scenario	Discharge change (%)		Reference
		Annual discharge	Winter discharge	
Yenisey, Lena, Ob, Kolyma	Canadian[a], GISS[b] 2xCO_2	10–45		Miller and Russell, 1992
Yenisey	SHI[c] 1 °C	9	34	Shiklomanov A., 1994, 1997
	SHI[c] 2 °C	9	61	
	SHI[c] 4 °C	15	325	
	GFDL[d] 2xCO_2	19	70	
	UKMO[e] 2xCO_2	45	80	
Inflow into the Barents Sea	GFDL[d] 2xCO_2; UKMO[e] 2xCO_2	14–35	25–46	Georgievsky et al., 1996
Yenisey	HadCM2[f]; HadCM3[f]; 6 scenarios by 2050	6–14		Arnell, 1999
Lena		12–25		
Ob		3–10		
Kolyma		30–40		
Mackenzie		12–20		
Yukon		20–30		
Arctic total	GISS[b]	12		Miller and Russell, 2000
Eurasian rivers	CO_2: +0.5%/yr to 2100	9		
North American rivers		23		
Lena	HadCM3[f] 2xCO_2	12		Georgievsky et al., 2003
Yenisey	HadCM3[f] 2xCO_2	8		Mokhov and Khon, 2002; Mokhov et al., 2003
Lena		24		
Ob		4		
Yenisey	ECHAM4/OPYC3[g] 2xCO_2	8		Mokhov and Khon, 2002; Mokhov et al., 2003
Lena		22		
Ob		3		
Yenisey	CGC[a] 2xCO_2	18		Arora and Boer, 2001
Lena		19		
Ob		-12		
Mackenzie		20		
Yukon		10		
Usa (Pechora basin)	HadCM2[f] (2080)	-16		Van Der Linden et al., 2003
	HadCM2[f] (2230)	10		

[a]Canadian Centre for Climate Modelling and Analysis; [b]Goddard Institute for Space Studies (United States); [c]State Hydrological Institute (Russia); [d]Geophysical Fluid Dynamics Laboratory (United States); [e]United Kingdom Met Office; [f]Hadley Centre (United Kingdom); [g]Max-Planck Institute for Meteorology (Germany).

freshwater to the North Atlantic subpolar seas, and possibly the thermohaline circulation. In particular, Steele and Boyd (1998) have argued that recent changes in the upper layers of the Arctic Ocean are attributable to altered pathways of Siberian river runoff in the Arctic Ocean.

On ecosystems

Changes in extreme runoff events (floods) are likely to alter biological production and biodiversity in riparian systems (section 8.4). The area of ponds and wetlands, for which water levels are critical, can determine whether vast northern peatlands will become sources or sinks of CO_2 and CH_4 (section 7.5.3). Changes in the fluxes of water and hence nutrients to and from ponds and wetlands will affect aquatic ecology (section 8.4).

On people

Traditional lifestyles are likely to be affected by changes in recharging of ponds and wetlands. Navigability of arctic rivers will be affected if runoff levels change substantially, especially during the warm season. Increases in the frequency and magnitude of extreme discharge events will result in catastrophic floods and are likely to require revisions of current construction requirements (section 16.4). Changes in the thickness and/or duration of freshwater ice cover will affect transportation in northern regions (i.e., ice roads) and will influence expanding development (e.g., oil and gas, diamond, and gold exploration).

6.8.5. Critical research needs

Perhaps the most critical need pertaining to surface flows in the Arctic concerns the network of gauge sta-

tions for monitoring discharge rates. This network has degraded seriously in the past decade, such that present measurements of surface flows in the Arctic are much less complete than in the recent past. Many of the monitoring station closures have occurred in Russia and Canada, and to a lesser extent in Alaska. It is important to reopen some of these stations or otherwise enhance the current monitoring network.

Better estimation of subsurface flows is also required. If permafrost thaws in regions of significant discharge to the Arctic Ocean, a quantitative understanding of subsurface flows will become increasingly essential for closing the arctic hydrological budget. A related need is an improved understanding of the relationship between net atmospheric moisture input (P-E), river discharge, and changes in permafrost. Recent findings by Serreze et al. (2003) and Savelieva et al. (2002) suggested that changes in permafrost may be affecting the linkage between precipitation and river discharge, in terms of the relationships between the water-year means of the two quantities and between the seasonality of the two quantities.

6.9. Sea-level rise and coastal stability

6.9.1. Background

Sea-level rise is one of the most important consequences of climate change and has the potential to cause significant impacts on ecosystems and societies. Changes in sea level will directly affect coastal stability. While section 6.5 discussed glacier wastage as a contributor to sea-level change, the present section addresses sea-level change in a broader context. The consequences for arctic coastal stability serve as the motivation and target of the present discussion of sea level and its variations. Sea level is discussed further in section 2.5.2 and 16.2.4.

Vulnerability to sea-level change varies substantially among arctic coastal regions. Figure 6.38 shows the areas of the Arctic that are presently less than ten meters above mean sea level. Substantial portions of the coasts of Siberia, Alaska, and Canada are low-lying and hence vulnerable to sea-level rise, although the rate of isostatic rebound in eastern Canada is substantial, as discussed below.

"Mean sea level" at the coast is defined as the height of the sea with respect to a local land benchmark, averaged over a long enough period (e.g., a month or a year) that fluctuations caused by waves and tides are largely removed. Changes in mean sea level measured by coastal tide gauges are called "relative sea-level changes", because they can be caused by movement of the land on which the tide gauge is situated or by climate-driven oceanic changes affecting the height of the adjacent sea surface. These two causes of relative sea-level change can have similar rates (several millimeters per year) over decadal or longer timescales. In addition, sea level is affected by changes in the spatial distribution of the water in the ocean resulting from atmosphere–ocean processes, for example, atmospheric (hydrostatic) pressure and storm winds, tides, and changes in the ocean circulation (currents). To infer sea-level changes arising from changes in the atmosphere or the ocean, the movement of the land must be subtracted from the records of tide gauges and geological indicators of past sea level. Because the processes contributing to sea-level change all have significant spatial variability, there will be considerable geographic variability in changes in the rate of relative sea-level rise.

6.9.1.1. Vertical motions of the land surface (isostatic changes)

Widespread land movements are caused by glacio-isostatic adjustment (a slow response to the melting of large ice sheets), and by tectonic land movements that include rapid displacements (earthquakes) and slow movements (associated with mantle convection and sediment transport). Glacio-isostatic adjustment and tectonic movements both vary widely in space. Therefore, sea-level change is not expected to be geographically uniform, and information about its distribution is needed to inform assessments of the impacts on coastal regions.

Glacio-isostatic adjustment is a response of the earth to loading and unloading by glaciers during the last major glaciation and the subsequent deglaciation. Regions that hosted thick accumulations of ice experienced subsidence followed by rebound when the ice retreated. Other parts of the earth experienced both subsidence and uplift or subsidence alone. Because the response of the earth's crust and mantle is slow, recovery from this loading and unloading is still occurring (Peltier, 2001, 2004). Glacio-isostatic adjustment varies considerably around the Arctic, from uplift in the Canadian Archipelago, Greenland, and Norway to subsidence along the Beaufort Sea and Siberian coasts. Tectonic motion is caused by movements of the crustal plates that result in rapid changes (earthquakes) or slow, gentle uplift or subsidence. Local loading of the crust by sediment (e.g., in deltas) can also cause subsidence.

6.9.1.2. Climate-driven oceanic changes affecting the height of the sea surface

In the absence of vertical motions of the land surface, there are two main components of sea-level rise:

- "steric rise", which refers to processes that cause an increase in ocean volume without a change in mass, primarily through changes in temperature (thermal expansion) and salinity (freshening); and
- "eustatic rise", which refers (at least in the oceanographic community) to changes resulting from an increase in the mass of water. Increased runoff from terrestrial regions, including glaciers and ice sheets, contributes directly to eustatic rise.

Changes in the amount of water stored on land will alter the mass of the ocean. (Sea level will be unaffected by

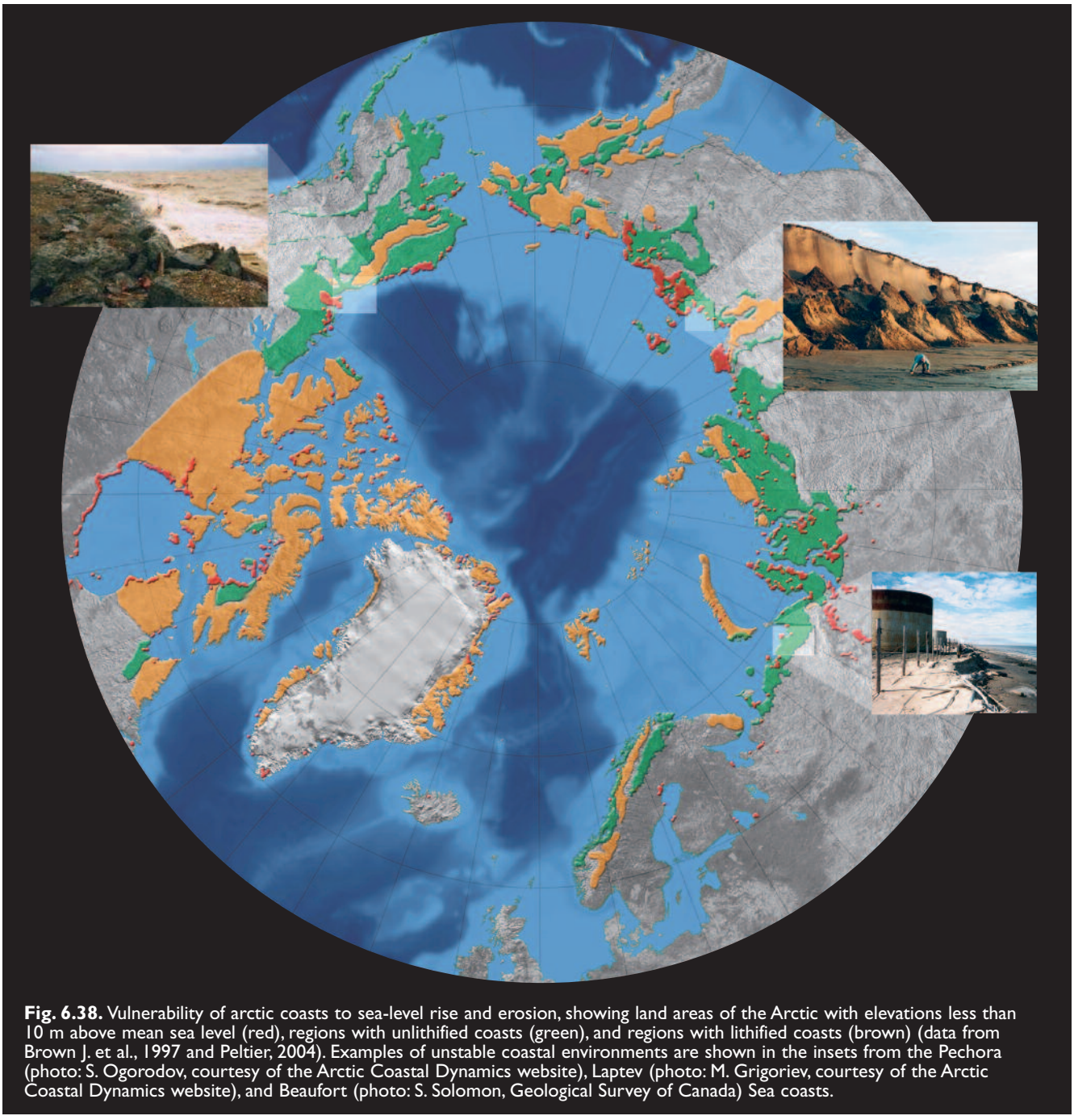

Fig. 6.38. Vulnerability of arctic coasts to sea-level rise and erosion, showing land areas of the Arctic with elevations less than 10 m above mean sea level (red), regions with unlithified coasts (green), and regions with lithified coasts (brown) (data from Brown J. et al., 1997 and Peltier, 2004). Examples of unstable coastal environments are shown in the insets from the Pechora (photo: S. Ogorodov, courtesy of the Arctic Coastal Dynamics website), Laptev (photo: M. Grigoriev, courtesy of the Arctic Coastal Dynamics website), and Beaufort (photo: S. Solomon, Geological Survey of Canada) Sea coasts.

the melting of sea ice, which displaces the volume of ocean water equivalent to its mass.) Climate change is projected to reduce the amount of water frozen in glaciers and ice caps owing to increased melting and evaporation (section 6.5.3). Greater melting of, and evaporation from, the Greenland and Antarctic ice sheets are also projected, but might be offset by increased precipitation, especially over Antarctica. Recent laser altimetry work by the National Aeronautics and Space Administration (NASA) shows that increased precipitation over Greenland does not presently balance the increased melting at lower elevations (Zwally et al., 2002). Increased discharge of ice from the ice sheets into the ocean is also possible. The ice sheets respond to climate change over timescales of up to millennia, so they could still be gaining or losing mass in response to climate variations that occurred as far back as the last glacial period, and they will continue to change for thousands of years after climate stabilizes. In addition to changes in glaciers and ice sheets, groundwater extraction and impounding of water in reservoirs can affect sea level.

6.9.1.3. Variations in sea level arising from atmosphere–ocean processes (including sea ice)

A variety of atmosphere–ocean processes contribute to spatial and temporal variations in sea level. The frequency, direction, magnitude, and duration of winds are the important variables which, when combined with water depth and coastal morphology, determine wave and storm-surge forcing at the coast. Storm surges form in response to lowered atmospheric pressure in cyclonic weather systems and accumulation of water in shallow coastal areas due to wind stress. Storm surges can cause

increases in water level many times greater than the normal tidal range. Associated waves can directly impact coastal bluffs, resulting in rapid coastal retreat.

Changes in meteorological forcing over time can be identified using data from the terrestrial and ice-island weather observation networks that have been active in the circumpolar coastal and ocean region since the 1940s. Of the parameters observed at a weather station, winds represent the single most important forcing agent for the coastal regime, driving waves and surges and affecting sea-ice formation and presence. It is important to consider the distributions of wind speeds rather than the averages, because the greatest impacts are typically associated with high-magnitude winds. A strong wind event can also break up existing sea ice, further exposing the coast to wave activity.

Wind speeds in excess of 10 m/s are considered strong enough to have an impact on the coastal regime (Solomon et al., 1994) when occurring during the open water period (broadly defined as July through October, although there is regional variability). Serreze et al. (2000) summarized a number of studies that have identified a decreasing trend in sea-level pressure over the Arctic Ocean. This has been linked to an increasing trend in both the frequency (trend significant in all seasons) and intensity (trend significant in summer) of cyclonic activity (McCabe et al., 2001; Serreze et al., 2000), although these trends are not apparent at all sites (e.g., Barrow, Alaska; Lynch et al., 2004). At many sites in the circumpolar coastal station network, there was also a decrease between 1950 and 2000 in the observed time between cyclonic events during the open-water season (Atkinson, pers. comm., 2003).

Wind forcing of oceanographic processes in the Arctic is moderated by the presence of sea ice throughout much of the year. Severe winter storms, which have such a devastating effect on temperate coasts, have little impact on arctic shores because sea ice protects the Arctic Ocean coastline from waves for eight months or more of the year. The impacts of changes in the duration of the open-water season depend on not only the magnitude, duration, and direction of winds, but also on the extent and concentration of sea ice. Sea ice affects wave generation and, to a lesser extent, the magnitude of storm surges. The duration of the open-water season varies considerably both spatially and temporally. Some parts of the Canadian Archipelago are never ice-free, while sea ice is rare in the vicinity of northern Norway (under the influence of the Gulf Stream). In some locations, interannual variations in the duration and extent of the open water range from a few weeks and several kilometers of fetch to eight to ten weeks and hundreds of kilometers of fetch, as in the Beaufort Sea in late summer and early autumn. Changes in the duration of the open-water season will be critical to the future impacts of coastal storms in the Arctic. There are various examples of Inuit peoples having difficulty coping with thinning ice, retreating ice-floe edges, and increasing storm frequency during the last decade (Kerr, 2002). These experiences indicate that, while sea-level rise is one of the most well known possible consequences of climate change, the fate of sea ice may be equally or more important to natural and human coastal systems.

Sea-ice pressure-ridge keels and icebergs scour the seabed, resulting in a characteristic roughened or ploughed seabed morphology that may affect resuspension rates and could change the degree of consolidation of the seabed surface. This process may be responsible for enhanced coastal retreat along parts of the Canadian Beaufort Sea coast.

Compounding the problem of sea-level change are concerns about arctic coastal stability, which directly affects human settlements and development. The stability of any coast is a function of the interaction between meteorological and oceanographic forcing and the physical properties of coastal materials. Short-term (hours to days) meteorological and oceanographic events are superimposed on the medium-term elevation of the sea surface, which changes seasonally and interannually due to natural climate variability, and over the longer term due to the combination of vertical motion of the land and the volume and distribution of the global ocean.

High-latitude coastal environments differ from their temperate counterparts in several important ways. The interaction between the atmosphere and the ocean that produces waves and storm surges is mediated by the presence and concentration of sea ice, while coastal materials are either strengthened or destabilized by the presence of permafrost, the abundance of ground ice, and associated temperature regimes (Are, 1988; Kobayashi et al., 1999).

Arctic coasts are as variable as coasts in temperate regions. The most unstable coasts are those that are composed of unlithified sediments (Fig. 6.38). These sediments were deposited during the past glacial and interglacial periods, are affected by permafrost erosion, and contain variable, sometimes significant, amounts of ground ice. Unlithified sediments are concentrated along much of the Russian coast and along the Beaufort Sea coast. Bedrock coasts are located in the Canadian Archipelago, and along Greenland, Norway, and extreme western Russia. The bedrock coasts generally coincide with those areas that experienced extensive glaciation during the Holocene. Even along bedrock and fjord-dominated coasts, beaches and deltas do occur, and those are usually where human settlements and infrastructure are concentrated (section 16.3).

6.9.2. Recent and ongoing changes

According to the IPCC (2001), sea level has risen more than 120 m over the past 20 000 years as a result of mass loss from melting ice sheets. The IPCC also reports that, based on geological data, global mean sea level may have

increased at an average rate of about 0.5 mm/yr over the last 6000 years and at an average rate of 0.1 to 0.2 mm/yr over the last 3000 years. In addition, vertical land movements are still occurring today.

The IPCC (2001) consensus value for the current rate of sea-level rise is 1 to 2 mm/yr. Recent results from global tide gauge analyses (length <70 years) show that the present global mean rate of sea-level rise is closer to 2 mm/yr (Douglas, 2001; Peltier, 2001 as reported in Cabanes et al., 2001). Complex short-term variations are superimposed on this rise, complicating the evaluation of trends (Fig. 6.39).

While both steric rise and eustatic rise are thought to be responsible for the current increase in sea level (Douglas et al., 2001), Cabanes et al. (2001) recently used a combination of ocean temperature measurements and satellite observations of sea level to argue that nearly all the present sea-level rise can be accounted for by steric processes alone. Others (e.g., Meier and Wahr, 2002; Munk, 2002) have countered that, due to melting glaciers, the eustatic contribution is significant. Munk (2003) and others report observed recent freshening of ocean water, which also suggests an increase in freshwater discharge from the land. These arguments, combined with new data from satellite-borne altimeters and gravity-measuring instruments and new calculations of glacio-isostatic adjustments, make this a complex subject for which there is no firm consensus, but rather an evolving spectrum of views.

The mass of the ocean, and thus sea level, changes as water is exchanged with glaciers and ice caps. Observational and modeling studies of glaciers and ice caps (section 6.5) indicate a contribution to sea-level rise of 0.2 to 0.4 mm/yr averaged over the 20th century. Modeling studies suggest that climate changes during the 20th century have led to contributions of -0.2 to 0.0 mm/yr from Antarctica (the result of increasing precipitation) and 0.0 to 0.1 mm/yr from Greenland (from changes in both precipitation and runoff).

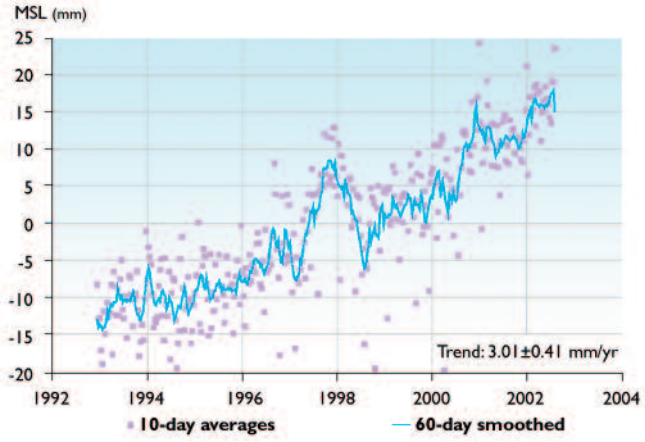

Fig. 6.39. Temporal variations in global mean sea level (MSL) computed from TOPEX/POSEIDON measurements between December 1992 and July 2002 (Leuliette et al., 2004; http://sealevel.colorado.edu).

Rates of change in the Arctic similar to the global values have been documented. Sea-level curves for the Beaufort Sea shelf suggest a rapid rise (~7 to 8 mm/yr) between 10000–8000 and 3000 years BP, and a slower average rise (~1.1 to 2.5 mm/yr) from 3000 years BP to the present (Campeau et al., 2000; Hill et al., 1993). These rates refer to relative sea-level rise and therefore include the isostatic contribution. Multi-decadal tide gauge data from Russian Arctic stations show relative sea-level rise of 0.3 to 3.2 mm/yr (Fig. 6.40; Proshutinsky et al., 2001). Data from additional stations in Alaska (Zervas, 2001) show mostly falling sea levels in the Pacific region (probably related to tectonic activity) and a single station in the Canadian Arctic showing rising sea level (Douglas et al., 2001). Analyses reported by Proshutinsky (pers. comm., 2003) indicate that in the Russian sector of the Arctic Ocean, sea level increased by an average of 1.85 mm/yr over the past 50 years (after correction for glacio-isostatic adjustments). Most of the increase is attributed to a combination of steric effects (0.64 mm/yr), decreasing sea-level pressure (0.56 mm/yr), and increasing cyclonic curvature of the mean wind field (0.19 mm/yr). For comparison, the IPCC (2001) reports observational estimates of the steric effect of about 1 mm/yr over recent decades, similar to values of 0.7 to 1.1 mm/yr simulated by AOGCMs over a comparable period. Averaged over the 20th century, AOGCM simulations suggest thermal expansion rates of 0.3 to 0.7 mm/yr.

Sea-ice conditions, especially greater amounts of open water, also contribute to increasing coastal instability. Figure 6.40 contrasts the present-day September sea-ice extent with that projected by the ACIA models for the 2071–2090 time slice. The significant projected increase in open-water extent is likely to create more energetic wave and swell conditions at the coast resulting in greater coastal instability.

The ACD project (section 6.6.2.5) was initiated in 1999 to compile circumpolar coastal change data, to develop a comprehensive set of monitoring sites, and to synthesize information about historical coastal environmental forcing. Based in part on information from the ACD project, it is clear that large regions of the arctic coast are undergoing rapid change. For example, Rachold et al. (2002) reported that the average rate of retreat of the Laptev Sea coast is 2.5 m/yr, a rate that contributes more sediment and organic carbon to the sea than does the Lena River. Retreat also predominates along the coast of the Beaufort Sea and large portions of the Russian coast. However, most arctic coastal stability monitoring records are too short and infrequent to identify trends in rates of retreat. The records show considerable annual and decadal variation in recent rates of retreat, which are attributed to variability in the frequency and severity of coastal storms and variations in open-water extent.

6.9.3. Projected changes

IPCC (2001) projections of the components contributing to sea-level change between 1990 and 2100 are as

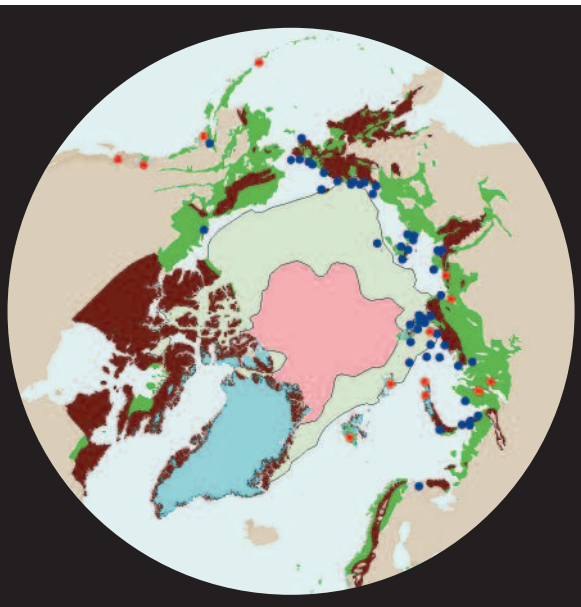

Fig. 6.40. Factors affecting coastal stability in the Arctic. Blue dots show stations where relative sea level (RSL) is rising; red dots show stations where RSL is falling. The light green area in the Arctic Ocean represents present-day September sea-ice extent (concentrations exceeding 15% in at least half the Septembers from 1980 to 1999). The pink area is the corresponding ACIA model-projected sea-ice extent (ice present in September in more than 50% of the years from 2071–2090; five-model average). Regions with unlithified coasts are shown in dark green, while regions with lithified coasts are shown in dark brown (data from Proshutinsky et al., 2001; Proshutinsky, pers. comm., 2003; Zervas, 2001; and the Hadley Centre's HadISST dataset).

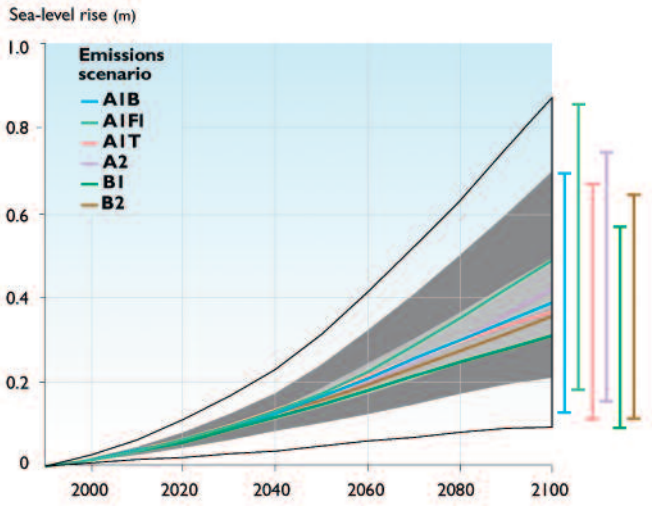

Fig. 6.41. Projected global sea-level rise between 1990 and 2100 using 35 different emissions scenarios. Thermal expansion and land ice changes were calculated using a simple climate model calibrated separately for each of seven AOGCMs. Contributions from changes in permafrost, the effect of sediment deposition, and the long-term adjustment of the ice sheets to past climate change were added. Each of the six colored lines is the average of all the model projections for one of six illustrative emissions scenarios; vertical bars at the right show the range of these projections. The region of light shading shows the range of the seven-model average projection for all 35 scenarios. The dark shading shows the entire range of projections by the seven models for the 35 scenarios. The outermost lines delineate the range of projections from all models and scenarios with the additional uncertainties due to changes in land ice, permafrost, and sediment deposition included (IPCC, 2001).

follows: thermal expansion of 0.11 to 0.43 m, accelerating throughout the 21st century; a glacier contribution of 0.01 to 0.23 m; a Greenland contribution of -0.02 to 0.09 m; and an Antarctic contribution of -0.17 to 0.02 m. The glacier and Greenland contributions are consistent with the estimate of 0.04 m derived from the ACIA-designated models forced with the B2 emissions scenario (section 6.5). Including thawing of permafrost, sediment deposition, and the ongoing contributions from ice sheets as a result of climate change since the Last Glacial Maximum, projected global average sea-level rise between 1990 and 2100 ranges from 0.09 to 0.88 m over the 35 emissions scenarios used by the IPCC (Fig. 6.41).

The wide range in the projections shown in Fig. 6.41 reflects systematic uncertainties in modeling. The central value of 0.48 m represents more than a doubling of the mean rate of global sea-level rise over the 20th century. Based on the summation of the components contributing to sea-level rise, the IPCC projects that global sea level will rise by 0.11 to 0.77 m between 1990 and 2100 (Church J. et al., 1991; IPCC, 2001). However, the large variation among the models is an outstanding feature of the IPCC projections of sea-level rise. Moreover, sea-level rise will depend strongly on the actual GHG emissions (for which any scenario beyond the 21st century is highly uncertain) and the behavior of glaciers and ice sheets, particularly the Greenland and the West Antarctic Ice Sheets. The range in the projections given above makes no allowance for instability of the West Antarctic Ice Sheet, although it is now widely agreed that major loss of grounded ice and accelerated sea-level rise due to West Antarctic Ice Sheet instability are very unlikely during the 21st century.

One of the important results of these model studies is that projected sea-level rise is not globally uniform. In particular, the greatest sea-level increases are projected for the Arctic, based on output from seven of nine models (Gregory, pers. comm., 2003). Figure 6.42 shows the IPCC (2001) model-projected sea-level changes after transformation to the same polar projection, providing a better depiction of spatial variability in the Arctic.

The IPCC (2001) stated that confidence in the regional distribution of sea-level change projected by AOGCMs is low because there is little similarity between model projections for various regions. One of the reasons for these regional differences may be the across-model variations in projected freshening of the Arctic Ocean owing to increased runoff or precipitation over the ocean (Bryan, 1996; Miller and Russell, 2000). Using the NASA–GISS atmosphere–ocean model, Miller and Russell (2000) project that arctic sea level will rise by 0.73 m between 2000 and 2100, of which 0.42 m is due to thermal expansion and about 0.31 m is from increased freshwater input, which also reduces the salinity. The mean global sea-level rise projected by the NASA–GISS model is 0.45 m during the same period.

Land movements, both isostatic and tectonic, will continue throughout the 21st century at rates that are unaffected by climate change. It is possible that by 2100, many regions currently experiencing decreases in relative sea level will instead have a rising relative sea level. Extreme high-water levels will occur with increasing frequency as a result of projected mean sea-level rise. Their frequency is likely to be further increased if storms become more frequent or severe as a result of climate change.

Projected decreases in sea-ice extent (section 6.3.3; see also section 16.2.5) will result in longer open-water seasons and an increased probability that severe storm events will occur without the protection of winter ice cover.

6.9.4. Impacts of projected changes

On other parts of the physical system

Increases in sea level are likely to increase coastal erosion rates in low-elevation areas and affect sediment transport in coastal regions. The salinity of bays, estuaries, and low-lying coastal areas is likely to increase as sea level rises. Spatial variations in sea-level changes may alter ocean currents and sediment transport. An increase in the duration of the open-water season will increase the frequency of wave-induced mixing, sediment transport, and storm surges during shoulder seasons, especially the autumn.

On ecosystems

Extensive coastal lowlands and immense deltas host ecosystems that will be affected by increases in sea level. Wetlands are likely to move farther inland, and coastal flood events will increase. Salinity will increase in coastal marine ecosystems that are now freshened by terrestrial discharge. If storm surges and coastal flood events increase in frequency and/or intensity, bird and fishery habitats in the affected areas are likely to be adversely affected. Decreased sea-ice coverage, which increases the probability that arctic storms will occur over open water, may change the timing and extent of mixing regimes and water–sediment interaction in coastal waters, with potential effects on benthic and coastal ecosystems.

On people

In the Arctic, many communities and much of the infrastructure are located on the coast and are therefore vulnerable to projected changes. Coastal erosion will have impacts on infrastructure and other human activities in the vicinity of coastlines (section 16.4.3). The frequency

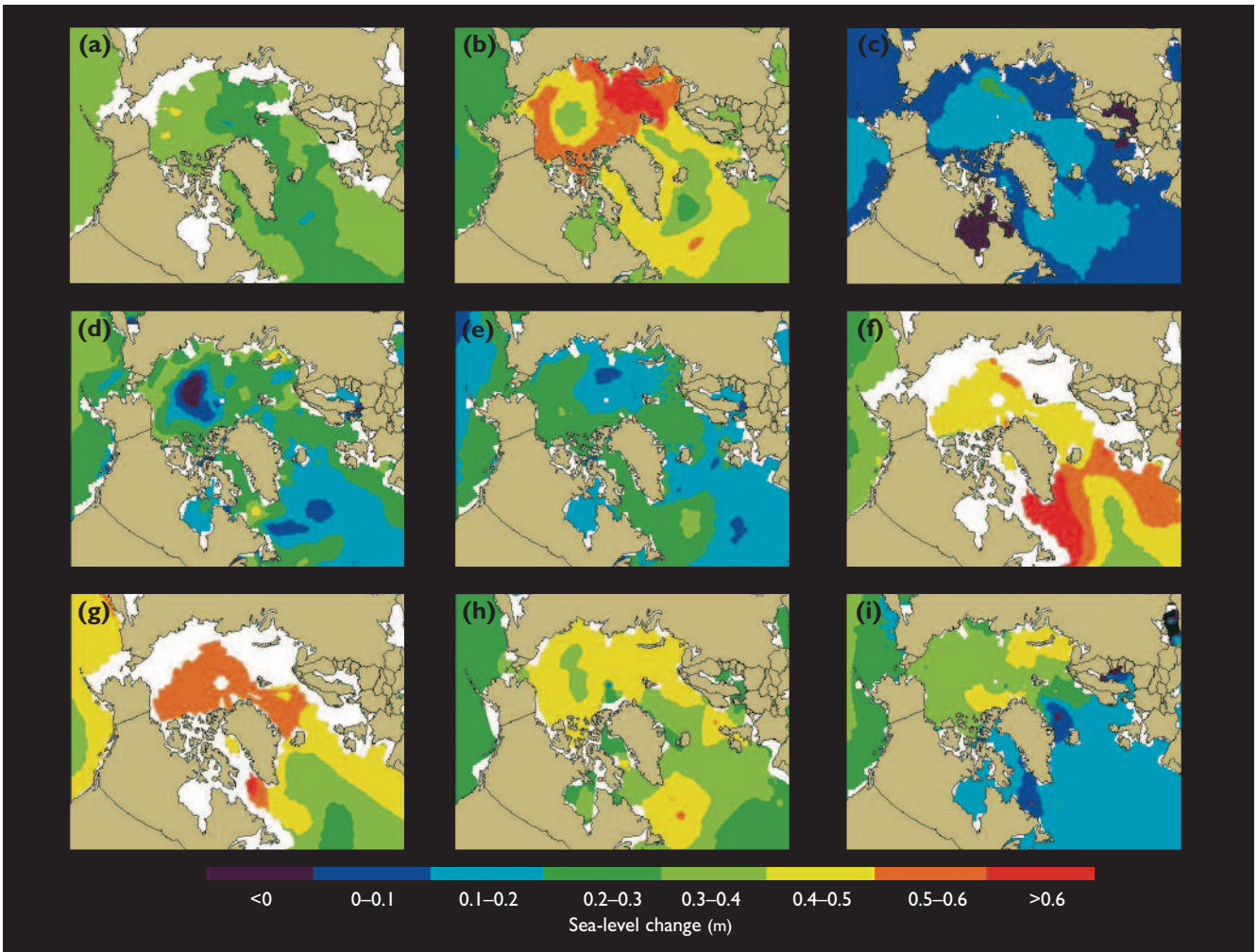

Fig. 6.42. Projected sea-level rise between 2000 and 2100 based on output from nine global climate models: (a) CSIRO Mk2 GS; (b) GFDL-R3_c; (c) MRI2 GS; (d) HadCM3 GSIO; (e) HadCM2 GS; (f) CMC2 GS; (g) SMC1 GS; (h) GFDL r15 b; and (i) ECHAM4/OPYC3 G (figure courtesy of J. Gregory, 2003; see IPCC (2001) for description of models and scenarios used).

and severity of coastal flood events are likely to increase, and the severity may be compounded by the loss of sea ice along the coast during the autumn and spring seasons during which, under present climate conditions, coastal waters are usually ice-covered.

6.9.5. Critical research needs

The IPCC (2001) estimated that eustatic sea-level rise over the past 100 years was 0.10 to 0.20 m, which is higher than the estimated total sea-level rise over the same period. This discrepancy in estimates of historical change points to the imperfect state of current knowledge of sea-level variations. Similarly, the relative importance of eustatic and steric contributions to recent sea-level rise is a subject of current disagreement, as noted in section 6.9.2. Attribution is a key issue in understanding and projecting sea-level change, and must be regarded as a key research need.

Uncertainties in the projected sea-level changes are very large, although improved observations and modeling have reduced some uncertainties since publication of the Second Assessment Report (IPCC, 1996). The present wide range of projections is partially a consequence of uncertainties in the scenarios of future GHG forcing, as well as uncertainties in the response of different global climate models to this forcing. It is also a consequence of how different models simulate (or do not simulate) the response of glaciers, ice sheets, and the oceans to climate change. In order to more realistically capture glacier and ice sheet responses, models will need to resolve the topographic features that surround most glaciers (and the topography of the larger ice sheets). Topographic resolution is essential for simulation of the precipitation and melt regimes, including the location of the equilibrium line, of significant glaciers. Other research needs for projecting the response of glaciers and ice sheets are discussed in section 6.5.5. The discharge of glacial meltwater to the ocean creates spatial gradients in sea level and upper-ocean salinity, both of which will trigger oceanic responses. These responses are not well understood and are poorly simulated, yet are crucial to projecting regional variations in sea-level rise.

The contribution of Antarctica to future changes in sea level remains a major uncertainty. Whether or not an increase in precipitation will offset the effects of enhanced melt in a warmer climate is a first-order question that needs to be addressed. Changes in the West Antarctic Ice Sheet have the potential to contribute significantly to future changes in global sea level.

For model simulations to be useful in assessments of coastal stability, enhanced resolution of coastlines is required in order to simulate realistically the sharp near-coastal gradients that are likely to characterize GHG-induced changes in temperature and precipitation. Credible simulations of changes in storminess and surface winds will also require improved model resolution and parameterizations of surface fluxes in high latitudes.

Finally, assessments of coastal vulnerability in the Arctic suffer from the limitations of the observational network for monitoring coastal surface winds and coastal stability. Data from the existing station network are of limited utility for driving numerical wave and surge models, which require offshore wind fields. The availability of surface wind data from the Arctic Ocean is poorer still. Evaluations of current trends in storm events and the associated coastal vulnerabilities will require additional sources of reliable surface wind data from coastal and offshore areas in the Arctic. Observations of coastal responses to wind and sea-level forcing are also essential in order to quantify the relationships between environmental processes and coastal impacts.

Acknowledgements

The authors thank William Chapman of the University of Illinois for providing information on the model-derived scenarios.

Personal communications and unpublished data

Anisimov, O., 2003. State Hydrological Institute, St. Petersburg, Russia.
Arctic Coastal Dynamics program, www.awi-potsdam.de/www-pot/geo/acd.html.
Atkinson, D., 2003. National Research Council of Canada.
Bitz, C., 2003. University of Washington.
Canadian Ice Service, http://ice-glaces.ec.gc.ca/App/WsvPageDsp.cfm?ID=210&LnId=6&Lang=eng.
Chapman, W., 2003. University of Illinois.
Dyurgerov, M., 2003. Cooperative Institute for Research in Environmental Sciences, University of Colorado.
Glazovsky, A.F., 2003. Russian Academy of Sciences.
Gregory, J., 2003. University College of Reading, United Kingdom.
Hadley Centre for Climate Prediction and Research, United Kingdom, http://badc.nerc.ac.uk/data/hadisst/.
Jakobsson, T., 2003. Icelandic Meteorological Office.
Koerner, R.M., 2003. Geological Survey of Canada.
National Snow and Ice Data Center, Boulder, Colorado.
Oerlemans, J., 2003. Utrecht University, the Netherlands.
Parkinson, C., 2003. NASA Goddard Space Flight Center.
Proshutinsky, A., 2003. Woods Hole Oceanographic Institution, Massachusetts.
Robinson, D., 2003. Snow Data Resource Center, Rutgers University Climate Laboratory, Piscataway, New Jersey.
Romanovsky, V., 2003, 2004. Geophysical Institute, University of Alaska, Fairbanks.
Shiklomanov, A., 2003. University of New Hampshire.
Steffen, K., 2003. Cooperative Institute for Research in Environmental Sciences, University of Colorado.
Taylor, A.E., 2002. Geological Survey of Canada.
Wilson, K.J., 2003. Canadian Ice Service.

References

Aagaard, K. and E.C. Carmack, 1989. The role of sea ice and other freshwater in the Arctic circulation. Journal of Geophysical Research, 94:14485–14498.
AARI, 1985. Arctic Atlas. Arctic and Antarctic Research Institute, Moscow, 204pp. (In Russian)
Adams, W.P., 1981. Snow and ice on lakes. In: D.M. Gray and D.H. Male (eds.). Handbook of Snow, pp. 437–474. Pergamon Press.
Agnew, T.A., B. Alt, R. De Abreu and S. Jeffers, 2003. The loss of decades old sea ice plugs in the Canadian Arctic islands. Sixth Conference on Polar Meteorology and Oceanography, American Meteorological Society, paper 1.5.
Allard, M., B. Wang and J.A. Pilon, 1995. Recent cooling along the southern shore of Hudson Strait, Quebec, Canada, documented from permafrost temperature measurements. Arctic and Alpine Research, 27:157–166.

Ambach, W., 1979. Zur Wärmehaushalt des Grönlandischen Inlandeises: Vergleichende Studie im Akkumulationsgebiet- und Ablationsgebiet. Polarforschung, 49:44–54.

Anderson, W.L., D.M. Robertson and J.J. Magnuson, 1996. Evidence of recent warming and El Niño-related variations in ice breakup of Wisconsin lakes. Limnology and Oceanography, 41:815–821.

Anisimov, O.A. and M.A. Belolutskaia, 2002. Assessment of the impacts of climate change and degradation of permafrost on infrastructure in the northern Russia. Meteorology and Hydrology, 9:15–22. (In Russian)

Anisimov, O.A. and M.A. Belolutskaia, in press a. Impacts of changing climate on permafrost: predictive modeling approach and evaluation of uncertainties. In: Yu. Izrael (ed.). Problems of Ecological Monitoring and Ecosystems Modeling. Moscow. (In Russian)

Anisimov, O.A. and M.A. Belolutskaia, in press b. Modeling climate-permafrost interaction: effects of vegetation. Meteorology and Hydrology. (In Russian)

Anisimov, O.A. and B. Fitzharris, 2001. Polar Regions (Arctic and Antarctic). In: J. McCarthy, O. Canziani, N.A. Leary, D.J. Dokken and K.S. White (eds.). Climate Change 2001: Impacts, Adaptation, and Vulnerability, pp. 801–841. Contribution of Working Group II to the Third Assessment Report of the Intergovernmental Panel on Climate Change. Cambridge University Press.

Anisimov, O.A. and F.E. Nelson, 1997. Permafrost zonation and climate change: Results from transient general circulation models. Climatic Change, 35:241–258.

Anisimov, O.A. and V.Yu. Poliakov, 2003. GIS assessment of climate-change impacts in permafrost regions. Proceedings of the Eighth International Permafrost Conference, vol. 1, pp. 9–14.

Anisimov, O.A., N.J. Shiklomanov and F.E. Nelson, 1997. Effects of global warming on permafrost and active layer thickness: results from transient general circulation models. Global and Planetary Change, 15:61–77.

Anisimov, O.A., A.A. Velichko, P.F. Demchenko, E.V. Eliseev, I.I. Mokhov and V.P. Nechaev, 2002. Impacts of climate change on permafrost in the past, present, and future. Proceedings of Russian Academy of Science, Physics of Atmosphere and Ocean, 38(7): 23–51.

Anisimov, O.A., M.A. Beloloutskaia and V.A. Lobanov, 2003. Observed climatic and environmental changes in the high latitudes of the Northern Hemisphere. Meteorology and Hydrology, 2:18–30. (In Russian)

Anon, 1999. Final Report. Land Arctic Physical Process (LAPP). Contract No. ENV4-CT95-0093. 1 April 1996 to 31 March 1999. 134pp.

Arctic Climatology Project, 1997. Environmental Working Group Joint U.S.-Russian Atlas of the Arctic Ocean - Winter Period. L. Timokhov and F. Tanis (eds.). Environmental Research Institute of Michigan in association with the National Snow and Ice Data Center, Ann Arbor, Michigan. CD-ROM.

Arctic Climatology Project, 1998. Environmental Working Group Joint U.S.-Russian Atlas of the Arctic Ocean - Summer Period. L. Timokhov and F. Tanis (eds.). Environmental Research Institute of Michigan in association with the National Snow and Ice Data Center, Ann Arbor, Michigan. CD-ROM.

Are, F.A., 1988. Thermal abrasion of sea coasts (Parts I and II). Polar Geography and Geology, 12:1–157.

Arendt, A.A., K.E. Echelmeyer, W.D. Harrison, C.A. Lingle and V.B. Valentine, 2002. Rapid wastage of Alaska glaciers and their contribution to rising sea level. Science, 297:382–386.

Armstrong, R. and M. Brodzik, 2001. Validation of passive microwave snow algorithms. In: M. Owe, K. Brubaker, J. Ritchie and A. Rango (eds.). Remote Sensing and Hydrology 2000. International Association of Hydrological Sciences, Publ. No. 267, pp. 87–92.

Arnell, N.W., 1999. Climate change and global water resources. Global Environmental Change, 9:31–49.

Arora, V.K. and G.J. Boer, 2001. Effects of simulated climate change on the hydrology of major river basins. Journal of Geophysical Research, 106(D4):3335–3348.

Assel, R.A. and D.M. Robertson, 1995. Changes in winter air temperatures near Lake Michigan, 1851–1993, as determined from regional lake-ice records. Limnology and Oceanography, 40:165–176.

Barry, R.G., 1984. Possible CO_2-induced warming effects on the cryosphere. In: N.-A. Morner and W. Karlin (eds.). Climatic Changes on a Yearly to Millennial Basis, pp. 571–604. D. Reidel.

Beltaos, S. (ed.), 1995. River Ice Jams. Water Resources Publications, Colorado, 372pp.

Björnsson, H., F. Pálsson and S. Gudmundsson, 2001. Jökulsárlón at Breidamerkursandur, Vatnajökull, Iceland: 20th century changes and future outlook. Jökull, 50:1–18.

Björnsson, H., F. Pálsson and H.H. Haraldsson, 2002. Mass balance of Vatnajökull (1991–2001) and Langjökull (1996–2001), Iceland. Jökull, 51:75–78.

Bogdanova, E.G., B.M. Ilyin and I.V. Dragomilova, 2002. Application of an improved bias correction model to precipitation measured at Russian North Pole drifting stations. Journal of Hydrometeorology, 3:700–713.

Bonsal, B.R. and T.D. Prowse, 2003. Trends and variability in spring and autumn 0 °C-isotherm dates over Canada. Climatic Change, 57: 342–358.

Bowling, L.C., D.P. Lettenmaer and B.N. Matheussen, 2000. Hydroclimatology of the Arctic Drainage Basin. In: E.L. Lewis, E.P. Jones, P. Lemke, T.D. Prowse and P. Wadhams (eds.). The Freshwater Budget of the Arctic Ocean, pp. 47–90. NATO Meeting/NATO ASI Series, Kluwer Academic Publishers.

Broecker, W.S., 1997. Thermohaline circulation, the Achilles heel of our climate system: will man-made CO_2 upset the current balance? Science, 278:1582–1588.

Brown, J. and S.M. Solomon, 1999. Arctic Coastal Dynamics. Report of an International Workshop. Geological Survey of Canada, Open File 3929.

Brown, J., O.J. Ferrians, J.A. Heginbottom and E.S. Melnikov, 1997. Circum-Arctic Map of Permafrost and Ground-ice Conditions. U.S.G.S. Circum-Pacific Map series, Map CP-45. U.S. Geological Survey.

Brown, J., O.J. Ferrians Jr., J.A. Heginbottom and E.S. Melnikov, 1998. Circum-Arctic Map of Permafrost and Ground-Ice Conditions. National Snow and Ice Data Center/World Data Center for Glaciology, Boulder, Colorado. Digital Media.

Brown, J., K.M. Hinkel and F.E. Nelson, 2000. The Circumpolar Active Layer Monitoring (CALM) program: Research designs and initial results. Polar Geography, 24:163–258.

Brown, R.D., 2000. Northern Hemisphere snow cover variability and change, 1915–1997. Journal of Climate, 13:2339–2355.

Brown, R.D. and R.O. Braaten, 1998. Spatial and temporal variability of Canadian monthly snow depths. Atmosphere-Ocean, 36:37–45.

Bruland, O. and E. Cooper, 2001. Snow distribution and vegetation. In: P. Kuhry (ed.). Proceedings of Arctic Feedbacks to Global Change. Rovaniemen Paintuskeskus Oy, Rovaniemi, Finland, pp. 110.

Bryan, K., 1996. The steric component of sea level rise associated with enhanced greenhouse warming: a model study. Climate Dynamics, 12:545–555.

Burgess, M.M., S.L. Smith, J. Brown, V. Romanovsky and K. Hinkel, 2000. Global Terrestrial Network for Permafrost (GTNet-P): Permafrost monitoring contributing to global climate observations. Geological Survey of Canada, Current Research 2000-E14, 8pp.

Burrell, B.C., 1995. Mitigation. In: S. Beltaos (ed.). River Ice Jams, pp. 205–239. Water Resources Publications, Colorado.

Cabanes, C., A. Cazenave and C. Le Provost, 2001. Sea level rise during past 40 years determined from satellite and *in situ* observations. Science, 294:840–842.

Callaghan, T.V. and S. Jonasson, 1995. Implications for changes in Arctic plant biodiversity from environmental manipulation experiments. In: F.S. Chapin III and C.H. Korner (eds.). Arctic and Alpine Biodiversity: Patterns, Causes and Ecosystem Consequences, pp. 151–164. Springer-Verlag.

Campeau, S., A. Hequette and R. Pienitz, 2000. Late Holocene diatom biostratigraphy and sea-level changes in the southeastern Beaufort Sea. Canadian Journal of Earth Sciences, 37:63–80.

Cavalieri, D.J., 2002. A link between Fram Strait sea ice export and atmospheric planetary wave phase. Geophysical Research Letters, 20(12):10.1029/2002GL014684.

Cavalieri, D.J., C.L. Parkinson and K.Y. Vinnikov, 2003. 30-year satellite record reveals contrasting Arctic and Antarctic decadal sea ice variability. Geophysical Research Letters, 30(18), 1970, doi:10.1029/2003GL018031.

Chang, A.T.C., J.L. Foster and D.K. Hall, 1987. Nimbus-7 derived global snow cover parameters. Annals of Glaciology, 9:39–44.

Chudinova, S.M., S.S. Bykhovets, V.A. Sorokovikov, D.A. Gilichinsky, T-J. Zhang and R.G. Barry, 2003. Could the current warming endanger the status of frozen ground regions of Eurasia? In: W. Haeberli and D. Brandova (eds.). Permafrost. Extended Abstracts reporting current research and new investigation, pp. 21–22. Eighth International Conference on Permafrost, University of Zurich.

Church, J.A., J.S. Godfrey, D.R. Jackell and T.J. McDougall, 1991. A model of sea level rise caused by ocean thermal expansion. Journal of Climate, 4:438–456.

Church, J.A., J.M. Gregory, P. Huybrechts, M. Kuhn, L. Lambeck, T. Nhuan, M.Y. Qin and P.L. Woodworth, 2001. Changes in sea level. In: J.T. Houghton, Y. Ding, D.J. Griggs, M. Nogeur, P.J. Van der Linden, X.Dai, K. Maskell, C.A. Johnson (eds). Climate Change 2001. The Scientific Basis, pp. 641–693. Intergovernmental Panel on Climate Change, Cambridge University Press.

Church, M., 1974. Hydrology and permafrost with reference to northern North America. In: Permafrost Hydrology, Proceedings of Workshop Seminar 1974, pp. 7–20. Canadian National Committee for the International Hydrological Decade, Ottawa.

Cohen, S.J. (ed.), 1997. Mackenzie Basin Impact Study (MBIS): Final Report. Environment Canada.

Colony, R., V.F. Radionov and F.J. Tanis, 1998. Measurements of precipitation and snow pack at Russian North Pole drifting stations. Polar Record, 34:3–14.

Comiso, J.C., 2002. A rapidly declining perennial sea ice cover in the Arctic. Geophysical Research Letters, 29(20):1956, doi:10.1029/2002GL015650.

Couture, R., S. Smith, S.D. Robinson, M.M. Burgess and S. Solomon, 2003. On the hazards to infrastructure in the Canadian North associated with thawing of permafrost. Proceedings of Geohazards 2003, Third Canadian Conference on Geotechnique and Natural Hazards, pp. 97–104. Canadian Geotechnical Society.

Dallimore, S.R., S.A. Wolfe and S.M. Solomon, 1996. Influence of ground ice and permafrost on coastal evolution, Richards Island, Beaufort Sea, N.W.T. Canadian Journal of Earth Sciences, 33: 664–675.

Dankers, R. and S.M. De Jong, 2004. Monitoring snow-cover dynamics in northern Fennoscandia with SPOT Vegetation Images. International Journal of Remote Sensing, 25(15):2933–2949.

Demuth, M.N., A. Pietroniro, T. Ouarda and J. Yetter, 2002. The Impact of Climate Change on the Glaciers of the Canadian Rocky Mountain Eastern Slopes and Implications for Water Resource Adaptation in the Canadian Prairies. Geological Survey of Canada Open File 4322.

Dickson, R.R., T.J. Osborn, J.W. Hurrell, J. Meincke, J. Blindheim, B. Adlandsvik, T. Vinje, G. Alekseev and W. Maslowski, 2000. The Arctic Ocean response to the North Atlantic Oscillation. Journal of Climate, 13:2671–2696.

Douglas, B.C., 2001. Sea level changes in the era of the recording. In: B. Douglas, M. Kearney and S. Leatherman (eds.). Sea Level Rise: History and Consequences, pp. 37–64. Academic Press.

Douglas, B.C., M. Kearney and S. Leatherman (eds.), 2001. Sea Level Rise: History and Consequences. Academic Press, 232pp.

Dowdeswell, J.A. and J.O. Hagen, 2004. Arctic ice masses. Chapter 15. In: J.L. Bamber and A.J. Payne (eds.). Mass Balance of the Cryosphere. Cambridge University Press, 712pp.

Dowdeswell, J.A., J.O. Hagen, H. Bjornsson, A.F. Glazovsky, W.D. Harrison, P. Holmlund, J. Jania, R.M. Koerner, B. Lefauconnier, C.S.L. Ommanney and R.H. Thomas, 1997. The mass balance of circum-Arctic glaciers and recent climate change. Quaternary Research, 48:1–14.

Duguay, C.R., G.M. Flato, M.O. Jeffries, P. Menard, K. Morris and W.R. Rouse, 2003. Ice-cover variability on shallow lakes at high latitudes: model simulations and observations. Hydrological Processes, 17:3465–3483.

Dyke, L.D. and S. Wolfe, 1993. Ground temperatures and recent coastal change at the north end of Richards Island, Mackenzie Delta, Northwest Territories. In: Current Research, Part E, Geological Survey of Canada Paper 93-1E, pp. 83–91.

Dyurgerov, M.B. and M.F. Meier, 1997. Year-to-year fluctuations of global mass balance of small glaciers and their contribution to sea-level change. Arctic and Alpine Research, 29:392–401.

Fallot, J.-M., R.G. Barry and D. Hoogstrate, 1997. Variations of mean cold season temperature, precipitation and snow depths during the last 100 years in the Former Soviet Union (FSU). Hydrological Sciences Journal, 42:301–327.

Fedorov, A.N., 1996. Effects of recent climate change on permafrost landscapes in central Sakha. Polar Geography, 20:99–108.

Flato, G.M., 2004. Sea-ice and its response to CO_2 forcing as simulated by global climate models. Climate Dynamics, 23:229–241.

Forland, E.J. and I. Hanssen-Bauer, 2000. Increased precipitation in the Norwegian Arctic: True or false? Climatic Change, 46:485–509.

Forman, S.L., W. Maslowski, J.T. Andrews, D. Lubinski, M. Steele, J. Zhang, R.B. Lammers and B.J. Peterson, 2000. Researchers explore arctic freshwater's role in ocean circulation. Eos, Transactions, American Geophysical Union, 81(16):169–174.

Frei, A., J.A. Miller and D.A. Robinson, 2003. Improved simulations of snow extent in the second phase of the Atmospheric Model Intercomparison Project (AMIP-2). Journal of Geophysical Research, 108(D12):4369, doi:10.1029/2002JD003030.

Fukuda, M., 1994. Methane flux from thawing Siberian permafrost (ice complexes) results from field observations. Eos, Transactions, American Geophysical Union, 75:86.

Garagulya, L.S., 1990. Application of Mathematical Methods and Computers in Investigations of Geocryological Processes. Moscow State University Press, Moscow, 124pp.

Georgievsky, V.Yu., A.V. Ezhov, A.L. Shalygin, I.A. Shiklomanov and A.I. Shiklomanov, 1996. Evaluation of possible climate change impact on hydrological regime and water resources of the former USSR rivers. Meteorology and Hydrology, 11:89–99. (In Russian)

Georgievsky, V.Yu., I.A. Shiklomanov and A.L. Shalygin, 2002. Long-term Variations in the Runoff over the Russian Territory. Report of the State Hydrological Institute, St. Petersburg, Russia, 85pp.

Georgievsky, V.Yu., I.A. Shiklomanov and A.L. Shalygin, 2003. Possible Changes of Water Resources and Water Regimes in the Lena Basin Due to Global Climate Warming. Report of the State Hydrological Institute, St. Petersburg, Russia.

Gerard, R., 1990. Hydrology of floating ice. In: T.D. Prowse and C.S.O. Ommanney (eds.). Northern Hydrology: Canadian Perspectives, pp. 103–134. NHRI Science Report No. 1. National Hydrology Research Institute, Environment Canada.

Ginzburg, B.M., K.N. Polyakova and I.I. Soldatova, 1992. Secular changes in dates of ice formation on rivers and their relationship with climate change. Soviet Meteorology and Hydrology, 12:57–64.

Glazovsky, A.F., 1996. Russian Arctic. In: J. Jania and J.O. Hagen (eds.). Mass Balance of Arctic Glaciers, pp. 44–53. International Arctic Science Committee Report No. 5.

Goodison, B.E. and A.E. Walker, 1995. Canadian development and use of snow cover information from passive microwave satellite data. In: B.T. Choudhury, Y.H. Kerr, E.G. Njoku and P. Pampaloni (eds.). Passive Microwave Remote Sensing of Land-Atmosphere Interactions, pp. 245–261. VSP BV Zeitt, Netherlands.

Goodison, B.E. and D.Q. Yang, 1996. In-situ measurements of solid precipitation in high latitudes: the need for correction. Proceedings of the workshop on the ACSYS Solid Precipitation Climatology Project, WCRP-93, WMO/TD No.739 3–17pp.

Goodison, B.E., P.Y.T. Louie and D. Yang, 1998. WMO Solid Precipitation Measurement Intercomparison, Final Report. WMO TD-No. 872. World Meteorological Organization, 212pp.

Gordeev, V.V., J.M. Martin, I.S. Sidorov and M.V. Sidorova, 1996. A reassessment of the Eurasian river input of water, sediment, major elements, and nutrients to the Arctic Ocean. American Journal of Science, 296:664–691.

Grabs, W.E., F. Portmann and T. de Couet, 2000. Discharge observation networks in Arctic regions: Computations of the river runoff into the Arctic Ocean, its seasonality and variability. In: E.L. Lewis, E.P. Jones, P. Lemke, T.D. Prowse and P. Wadhams (eds.). The Freshwater Budget of the Arctic Ocean, NATO Science Series, pp. 249–268. Kluwer Academic Publishers.

Gray, D.M. and T.D. Prowse, 1993. Snow and floating ice. In: D. Maidment (ed.). Handbook of Hydrology, pp. 7.1–7.58. McGraw-Hill.

Groisman, P.Y. and D.R. Easterling, 1994. Variability and trends of total precipitation and snowfall over the United States and Canada. Journal of Climate, 7:184–205.

Hagen, J.O. and O. Liestøl, 1990. Long term glacier mass balance investigations in Svalbard 1950–1988. Annals of Glaciology, 14:102–106.

Hall, D.K., G.A. Riggs, V.V. Salomonson, N.E. DiGirolamo and K.J. Bayr, 2002. MODIS snow-cover products. Remote Sensing of Environment, 83:181–194.

Hare, S.R. and N.J. Mantua, 2000. Empirical evidence for North Pacific regime shifts in 1977 and 1989. Progress in Oceanography, 47(2–4):103–147.

Harris, C. and W. Haeberli, 2003. Warming Permafrost in the Mountains of Europe. World Meteorological Organization Bulletin, 52(3), 6pp.

Hill, P.R., A. Héquette and M.H. Ruz, 1993. Holocene sea level history of the Canadian Beaufort Shelf. Canadian Journal of Earth Sciences, 30:103–108.

Hilmer, M. and T. Jung, 2000. Evidence for a recent change in the link between the North Atlantic Oscillation and Arctic sea ice export. Geophysical Research Letters, 27:989–992.

Holloway, G. and T. Sou, 2002. Has Arctic sea ice rapidly thinned? Journal of Climate, 15:1691–1701.

Hubberten, H.-W. and N.N. Romanovskii, 2003. The main features of permafrost in the Laptev Sea, Russia – a review. In: M. Phillips (ed.). ICOP 2003: Permafrost. Proceedings of the Eighth International Permafrost Conference, Zurich. pp. 431–436. A.A. Balkema.

IPCC, 1996. Climate Change 1995: The Science of Climate Change. J.T. Houghton, L.G. Meira Filho, B.A. Callender, N. Harris, A. Kattenberg and K. Maskell (eds.). Intergovernmental Panel on Climate Change, Cambridge University Press, 572pp.

IPCC, 2001. Climate Change 2001: The Scientific Basis. Contribution of Working Group I to the Third Assessment Report of the Intergovernmental Panel on Climate Change. J.T. Houghton, Y. Ding, D.J. Griggs, M. Noguer, P.J. van der Linden, X. Dai, K. Maskell and C.A. Johnson (eds.). Cambridge University Press, 881pp.

Isaksen, K., P. Holmlund, J.L. Sollid and C. Harris, 2001. Three deep alpine-permafrost boreholes in Svalbard and Scandinavia. Permafrost and Periglacial Processes, 12:13–25.

Ivanov, V.V., 1976. Fresh water balance of the Arctic Ocean. Proceedings of the Arctic and Antarctic Research Institute, 323:138–147.

Jania, J., and J.O. Hagen (eds.), 1996. Mass Balance of Arctic Glaciers. International Arctic Science Committee Report No. 5, 62pp.

Jania, J. and M. Kaczmarska, 1997. Hans Glacier – a tidewater glacier in southern Spitsbergen: summary of some results. In: C.J. Van der Veen (ed.). Calving Glaciers: Report of a workshop, February 28–March 2, 1997, pp. 95–104. Byrd Polar Research Center, Report No. 15. Ohio State University.

Jasek, M.J., 1998. 1998 break-up and flood on the Yukon River at Dawson – Did El Niño and climate play a role? In: Proceedings of the Fourteenth International Ice Symposium, Potsdam, New York Vol. 2, pp. 761–768.

Johannessen, O.M., E.V. Shalina and M.W. Miles, 1999. Satellite evidence for an Arctic sea ice cover in transformation. Science, 286:1937–1939.

Jóhannesson, T. and O. Sigurðsson, 1998. Interpretation of glacier variations in Iceland 1930–1995. Jökull, 45:27–33.

Judge, A.S. and J.A. Majorowicz, 1992. Geothermal conditions for gas hydrate stability in the Beaufort-Mackenzie area: the global change aspect. Palaeogeography, Palaeoclimatology, Palaeoecology (Global and Planetary Change Section), 98:251–263.

Karl, T., 1998. Regional trends and variations of temperature and precipitation. In: R.T. Watson, M.C. Zinyowera, R.H. Moss and D.J. Dokken (eds.). The Regional Impacts of Climate Change: An Assessment of Vulnerability, pp. 412–425. Intergovernmental Panel on Climate Change, Cambridge University Press.

Kattsov, V.M. and J.E. Walsh, 2000. Twentieth-century trends of Arctic precipitation from observational data and a climate model simulation. Journal of Climate, 13:1362–1370.

Kerr, R., 2002. A warmer Arctic means change for all. Science, 297:1490–1492.

Kobayashi, N., J.C. Vidrine, R.B. Nairn and S.M. Solomon, 1999. Erosion of frozen cliffs due to storm surge on the Beaufort Sea Coast. Journal of Coastal Research, 15:332–344.

Koch, L., 1945. The east Greenland ice. Meddelelser om Grønland, 130(3):1–374.

Koerner, R.M., 1996. Canadian Arctic. In: J. Jania and J.O. Hagen (eds.). Mass Balance of Arctic Glaciers. International Arctic Science Committee, Rep. No. 5.

Koerner, R.M., 2002. Glaciers of the High Arctic Islands. In: R.S. Williams and J.G. Ferrigno (eds.). Satellite Image Atlas of Glaciers of the World: Glaciers of North America, pp. J111–J146. U.S. Geological Survey Professional Paper 1386–J.

Koerner, R.M. and L. Lundgaard, 1995. Glaciers and global warming. Geographie physique et Quaternaire, 49:429–434.

Koryakin, V.S., 1997. Glaciers of Novaya Zemlya. Zemlya i Vselennaya (Earth and Universe), 1:17–24. (In Russian)

Krabill, W., W. Abdalati, E. Frederick, S. Manizade, C. Martin, J. Sonntag, R. Swift, R. Thomas, W. Wright and J. Yungel, 1999. Greenland Ice Sheet: High-elevation balance and peripheral thinning. Science, 289:428–430.

Krupnik, I. and D. Jolly (eds.), 2002. The Earth is Faster Now: Indigenous Observations of Arctic Environmental Change. Arctic Research Consortium of the United States, Fairbanks, Alaska, 384pp.

Kudryavtsev, V.A., 1974. Fundamentals of Frost Forecasting to Geological Engineering Investigations. Nauka, Moscow, 222pp.

Kuusisto, E. and A.-R. Elo, 2000. Lake and river ice variables as climate indicators in Northern Europe. Internationale Vereinigung fur Theoretische und Angewandte Limnologie: Verhandlungen, 27:2761–2764.

Kvenvolden, K.A., 1988. Methane hydrates and global climate. Global Biogeochemical Cycles, 2:221–229.

Kwok, R., 2000. Recent changes in Arctic Ocean sea ice motion associated with the North Atlantic Oscillation. Geophysical Research Letters, 27:775–778.

Kwok, R. and D.A. Rothrock, 1999. Variability of Fram Strait ice flux and North Atlantic Oscillation. Journal of Geophysical Research, 104:5177–5189.

Lachenbruch, A.H. and B.V. Marshall, 1986. Changing climate: geothermal evidence from permafrost in the Alaskan Arctic. Science, 234:689–696.

Lammers, R.B., A.I. Shiklomanov, C.J. Vorosmarty, B.M. Fekete and B.J. Peterson, 2001. Assessment of contemporary arctic river runoff based on observation discharge records. Journal of Geophysical Research, 106(D4):3321–3334.

Lefauconnier, B., J.O. Hagen and J.P. Rudant, 1994. Flow speed and calving rate of Kongsbreen Glacier, 79° N, Spitsbergen, Svalbard, using SPOT images. Polar Research, 13(1):59–65.

Lefauconnier, B., J.O. Hagen, J.B. Ørbeck, K. Melvold and E. Isaksson, 1999. Glacier balance trends in the Kongsfjorden area, western Spitsbergen, Svalbard, in relation to the climate. Polar Research, 18(2):307–313.

Leuliette, E.W., R.S. Nerem and G.T. Mitchum, 2004. Calibration of TOPEX/Poseidon and Jason altimeter data to construct a continuous record of mean sea level change. Marine Geodesy, 27(1–2):79–94.

Ling, F. and T. Zhang, 2003. Impact of the timing and duration of seasonal snow cover on the active layer and permafrost in the Alaskan Arctic. Permafrost and Periglacial Processes, 14:141–150.

Livingstone, D.M., 1999. Ice break-up on southern Lake Baikal and its relationship to local and regional air temperatures in Siberia and to the North Atlantic Oscillation. Limnology and Oceanography, 44:1486–1497.

Lynch, A.H., J.A. Curry, R.D. Brunner and J.A. Maslanik, 2004. Towards an integrated assessment of the impacts of extreme wind events on Barrow, Alaska. Bulletin of the American Meteorological Society, 85:209–221.

Mackay, J.R., 1972. Offshore permafrost and ground ice, Southern Beaufort Sea, Canada. Canadian Journal of Earth Sciences, 9:1550–1561.

Mackay, J.R., 1986. Fifty years (1935 to 1985) of coastal retreat west of Tuktoyaktuk, District of Mackenzie. Geological Survey of Canada, Paper 86-1A:727–735.

Magnuson, J.J., K.E. Webster, R.A. Assel, C.J. Bowser, P.J. Dillon, J.G. Eaton, H.E. Evans, E.J. Fee, R.I. Hall, L.R. Mortsch, D.W. Schindler and F.H. Quinn, 1997. Potential effects of climate changes on aquatic systems: Laurentian Great Lakes and Precambrian Shield Region. In: C.E. Cushing (ed.). Freshwater Ecosystems and Climate Change in North America, pp. 7–53. John Wiley and Sons.

Magnuson, J.J., D.M. Robertson, R.H. Wynne, B.J. Benson, D.M. Livingstone, T. Arai, R.A. Assel, R.D. Barry, V. Card, E. Kuusisto, N.G. Granin, T.D. Prowse, K.M. Stewart and V.S. Vuglinski, 2000. Ice cover phenologies of lakes and rivers in the Northern Hemisphere and climate warming. Science, 289(5485):1743–1746.

Malevsky-Malevich, S.P., E.K. Molkentin, E.D. Nadyozhina, T.V. Pavlova and O.B. Shklyarevich, 2003. Possible changes of active layer depth in the permafrost areas of Russia in the 21st century. Russian Meteorology and Hydrology, (12):80–88.

Manabe, S. and R.J. Stouffer, 1993. Century-scale effects of increased atmospheric CO_2 on the ocean-atmosphere system. Nature, 364(6434):215–218.

Manson, G.K., S.M. Solomon, J.J. van der Sanden, D.L. Forbes, I.K. Peterson, S.J. Prinsenberg, D. Frobel, T.L. Lynds and T.L. Webster, 2002. Discrimination of nearshore, shoreface and estuarine ice on the north shore of Prince Edward Island, Canada, using Radarsat-1 and airborne polarimetric c-band SAR. In: Proceedings of the Seventh International Conference on Remote Sensing for Marine and Coastal Environments. Miami, Florida. 20–22 May 2002. Document 0043, 7pp.

Mauritzen, C. and S. Hakkinen, 1997. Sensitivity of thermohaline circulation to sea ice forcing in an arctic-North Atlantic model. Journal of Geophysical Research, 102:3257–3260.

McCabe, G.J., M.P. Clark and M.C. Serreze, 2001. Trends in northern hemisphere surface cyclone frequency and intensity. Journal of Climate, 14:2763–2768.

Meier, M.F. and M.B. Dyurgerov, 2002. How Alaska affects the world. Science, 297:350–351.

Meier, M.F. and J.M. Wahr, 2002. Sea level is rising: Do we know why? Proceedings of the National Academy of Sciences, 99(10): 6524–6526.

Meshcherskaya, A.V., I.G. Belyankina and M.P. Golod, 1995. Monitoring tolshching cnozhnogo pokprova v osnovioi zerno proizvodyaschei zone Byvshego SSSR za period instrumental'nykh nablyugenii, Izvestiya Akad. Nauk SSR, Sser. Geograf., 101–110.

Miller, J.R. and G.L. Russell, 1992. The impact of global warming on river runoff. Journal of Geophysical Research, 97(D3):2757–2764.

Miller, J.R. and G.L. Russell, 2000. Projected impact of climate change on the freshwater and salt budgets of the Arctic Ocean by a global climate model. Geophysical Research Letters, 27:1183–1186.
Minobe, S., 2000. Spatio-temporal structure of the pentadecadal variability over the North Pacific. Progress in Oceanography, 47(2–4):381–407.
Mokhov, I.I. and V.Ch. Khon, 2002. Hydrological regime in basins of Siberian rivers: Model estimates of changes in the 21st century. Meteorology and Hydrology, 8:77–92. (In Russian)
Mokhov, I.I., V.A. Semenov and V.Ch. Khon, 2003. Estimates of possible regional hydrologic regime changes in the 21st century based on Global Climate Models. Izvestiya, Atmospheric and Oceanic Physics, 39(2):130–144.
Möller, D., 1996. Die Höhen und Höhenänderungen des Inlandeises. Die Weiterfürung der geodätischen Arbeiten der Internationalen Glaziologischen Grönland-Expedition (EGIG) durch das Institut für Vermessungskunde der TU Braunschweig 1987–1993. Deutsche Geodätische Kommission bei der Bayrischen Akademie der Wissenschaften, Reihe B, Angewandte Geodäsie, Heft Nr. 303. Verlag der Bayrischen Akademie der Wissenschaften: 49–58.
Munk, W., 2002. Twentieth century sea level: An enigma. Proceedings of the National Academy of Sciences, 99:6550–6555.
Munk, W., 2003. Ocean freshening, sea level rising. Science, 300: 2041–2043.
Nelson, F.E., 2003. Geocryology: (Un)frozen in time. Science, 299:1673–1675.
Nelson, F.E., O.A. Anisimov and N.I. Shiklomanov, 2001. Subsidence risk from thawing permafrost. Nature, 410:889–890.
New, M., M. Hulme and P. Jones, 2000. Representing twentieth-century space-time climate variability. Part II: Development of 1901–96 monthly grids of terrestrial surface climate. Journal of Climate, 13:2217–2238.
NRCC, 1988. Glossary of Permafrost and Related Ground-ice Terms. Permafrost Subcommittee, National Research Council of Canada, Technical Memorandum 142, 156pp.
Oberman, N.G. and G.G. Mazhitova, 2001. Permafrost dynamics in the north-east of European Russia at the end of the 20th century. Norwegian Journal of Geography, 55:241–244.
Óerlemans, J. and B.K. Reichert, 2000. Relating glacier mass balance to meteorological data using a Seasonal Sensitivity Characteristic (SSC). Journal of Glaciology, 46:1–6.
Ogilvie, A.E.J. and T. Jonsson, 2001. 'Little Ice Age' research: A perspective from Iceland. Climatic Change, 48:9–52.
Ohmura, A., 1997. New temperature distribution maps for Greenland. Zeitschrift fur Gletscherkunde und Glazialgeologie, 23:1–45.
Ohmura, A., M. Wild and L. Bengtsson, 1996. A possible change in mass balance of Greenland and Antarctic ice sheets. Journal of Climate, 9:2124–2137.
Oki, T., K. Musiake, H. Matsuyama and K. Masuda, 1995. Global atmospheric water balance and runoff from large river basins. Hydrological Processes, 9:655–678.
Osterkamp, T.E., 2001. Sub-sea permafrost. In: Encyclopedia of Ocean Sciences, pp. 2902–2912. Academic Press.
Osterkamp, T.E., 2003. A thermal history of permafrost in Alaska. Proceedings of Eighth International Conference on Permafrost, Zurich, pp. 863–868.
Osterkamp, T.E. and W.D. Harrison, 1977. Sub-sea permafrost regime at Prudhoe Bay, Alaska, U.S.A. Journal of Glaciology, 19:627–637.
Osterkamp, T.E. and V.E. Romanovsky, 1999. Evidence for warming and thawing of discontinuous permafrost in Alaska. Permafrost and Periglacial Processes, 10(1):17–37.
Osterkamp, T.E., L. Viereck, Y. Shur, M.T. Jorgenson, C. Racine, A. Doyle and R.D. Boone, 2000. Observations of thermokarst and its impact on boreal forests in Alaska, U.S.A. Arctic, Antarctic and Alpine Research, 32:303–315.
Overland, J.E., J.M. Adams and M.A. Bond, 1999. Decadal variability of the Aleutian Low and its relation to high latitude circulation. Journal of Climate, 12:1542–1548.
Paeth, H., A. Hense and R. Hagenbrock, 2002. Comments on 'Twentieth-century trends of Arctic precipitation from observational data and a climate model simulation.' Journal of Climate, 15: 800–803.
Palecki, M.A. and R.G. Barry, 1986. Freeze-up and break-up of lakes as an index of temperature changes during the transition seasons: a case study for Finland. Journal of Climate and Applied Meteorology, 25:893–902.
Parkinson, C.L., 2000. Recent trend reversals in Arctic sea ice extents: Possible connections to the North Atlantic Oscillation. Polar Geography, 24:1–12.
Parkinson, C.L., D.J. Cavalieri, P. Gloersen, H.J. Zwally and J.C. Comiso, 1999. Arctic sea ice extents, areas and trends. Journal of Geophysical Research, 104:20837–20856.
Paterson, W.S.B. and N. Reeh, 2001. Thinning of the ice sheet in northwest Greenland over the past forty years. Nature, 414:60–62.
Pavlov, A.V., 1994. Current changes of climate and permafrost in the Arctic and Sub-Arctic of Russia. Permafrost and Periglacial Processes, 5:101–110.
Pavlov, A.V. and N.G. Moskalenko, 2002. The thermal regime of soils in the north of western Siberia. Permafrost and Periglacial Processes, 13:43–51.
Peltier, W.R., 2001. Global glacial isostatic adjustment and modern instrumental records of relative sea level history. In: B. Douglas, M. Kearney and S. Leatherman (eds.). Sea Level Rise: History and Consequences. International Geophysics Series, 75:65–95.
Peltier, W.R., 2004. Global glacial isostasy and the surface of the ice-age Earth: the ICE-5G(VM2) model and GRACE. Annual Review of Earth and Planetary Sciences, 32:111–149.
Persson, P.O.G., C.W. Fairall, E.L. Andreas, P.S. Guest and D.K. Perovich, 2002. Measurements near the atmospheric surface flux group tower at SHEBA: Near surface conditions and surface energy budget. Journal of Geophysical Research, 107(C10), doi: 10.1029/2002JC000705.
Peterson, B.J., R.M. Holmes, J.W. McClelland, C.J. Vorosmarty, R.B. Lammers, A.I. Shiklomanov, I.A. Shiklomanov and S. Rahmstorf, 2002. Increasing river discharge to the Arctic Ocean. Science, 298:2171–2173.
Petryk, S., 1995. Numerical modeling. In: S. Beltaos (ed.). River Ice Jams, pp. 147–172. Water Resources Publications, Colorado.
Péwé, T.L., 1983. Alpine permafrost in the contiguous United States: A review. Arctic and Alpine Research, 15:145–156.
Pfeffer, W.T., J. Cohn, M.F. Meier and R.M. Krimmel, 2000. Alaskan glacier beats a rapid retreat. Eos, Transactions, American Geophysical Union, 81:48.
Polyakov, I., G. Alexeev, R. Bekryaev, U.S. Bhatt, R. Colony, M. Johnson, V. Karklin, D. Walsh and A. Yulin, 2003. Long-term variability of ice in the arctic marginal seas. Journal of Climate, 16:2078–2085.
Pomeroy, J.W. and L. Li, 2000. Prairie and Arctic areal snow cover mass balance using a blowing snow model. Journal of Geophysical Research, 105(D21):26610–26634.
Proshutinsky, A. and M. Johnson, 1997. Two circulation regimes of the wind-driven Arctic Ocean. Journal of Geophysical Research, 102:12493–12514.
Proshutinsky, A., V. Pavlov and R.H. Bourke, 2001. Sea level rise in the Arctic Ocean. Geophysical Research Letters, 28:2237–2240.
Prowse, T.D., 1994. The environmental significance of ice to cold-regions streamflow. Freshwater Biology, 32(2):241–260.
Prowse, T.D., 1995. River ice processes. In: S. Beltaos (ed.). River Ice Jams, pp. 29–70. Water Resources Publications, USA.
Prowse, T.D., 2001. River-ice ecology: Part A) Hydrologic, geomorphic and water-quality aspects. Journal of Cold Regions Engineering, 15(1):1–16.
Prowse, T.D. and S. Beltaos, 2002. Climatic control of river-ice hydrology: a review. Hydrological Processes, 16(4):805–822.
Prowse, T.D. and T. Carter, 2002. Significance of ice-induced hydraulic storage to spring runoff: a case study of the Mackenzie River. Hydrological Processes 16(4):779–788.
Prowse, T.D. and M.N. Demuth, 1993. Strength variability of major river-ice types. Nordic Hydrology, 24(3):169–182.
Prowse, T.D. and P.O. Flegg, 2000. The magnitude of river flow to the Arctic Ocean: dependence on contributing area. Hydrological Processes, 14(16–17):3185–3188.
Rachold, V., J. Brown and S.M. Solomon, 2002. Arctic Coastal Dynamics. Report of an International Workshop, Potsdam (Germany) 26–30 November 2001. Report on Polar Research 413, 27 extended abstracts, 103 pp.
Radionov, V.F., N.N. Bryazgin and E.I. Alexandrov, 1997. The Snow Cover of the Arctic Basin. Tech. Rep. APL-UW TR 9701. Applied Physics Laboratory, University of Washington, Seattle, 95pp.
Rahmstorf, S. and A. Ganopolski, 1999. Long-term global warming scenarios computed with an efficient coupled climate model. Climatic Change, 43:353–367.
Ramsay, B.H., 1998. The interactive multisensor snow and ice mapping system. Hydrological Processes, 12:1537–1546.
Reichert, B.K., L. Bengtsson and J. Oerlemans, 2001. Midlatitude forcing mechanisms for glacier mass balance investigated using general circulation models. Journal of Climate, 14:3767–3784.
Reycraft, J. and W. Skinner, 1993. Canadian lake ice conditions: An indicator of climate variability. Climatic Perspectives, 15:9–15.
Rignot, E. and R.H. Thomas, 2002. Mass balance of the polar ice sheets. Science, 297:1502–1506.
Rigor, I.G., J.M. Wallace and R.L. Colony, 2002. Response of sea ice to the Arctic Oscillation. Journal of Climate, 15:2648–2663.

Riseborough, D.W., 1990. Soil latent heat as a filter of the climate signal in permafrost. In: Proceedings of the Fifth Canadian Permafrost Conference, Université Laval, Quebec, Collection Nordicana No. 54, pp. 199–205.

Robinson, D.A., 1993. Hemispheric snow cover from satellites. Annals of Glaciology, 17:367–371.

Robinson, D.A., M.C. Serreze, R.G. Barry, G. Scharfen and G. Kukla, 1992. Large-scale patterns of snow melt and parameterized surface albedo in the Arctic Basin. Journal of Climate, 5:1109–1119.

Romanovsky, V.E. and T.E. Osterkamp, 1995. Interannual variations of the thermal regime of the active layer and near-surface permafrost in northern Alaska. Permafrost and Periglacial Processes, 6:313–335.

Romanovsky, V.E., M. Burgess, S. Smith, K. Yoshikawa and J. Brown, 2002. Permafrost temperature records: Indicators of climate change. Eos, Transactions, American Geophysical Union, 83:589–594.

Rothrock, D.A., Y. Yu and G.A. Maykut, 1999. Thinning of the Arctic sea-ice cover. Geophysical Research Letters, 26:3469–3472.

Rouse, W.R., E.M. Blyth, R.W. Crawford, J.R. Gyakum, J.R. Janowicz, B. Kochtubajda, H.G. Leighton, P. Marsh, L. Martz, A. Pietroniro, H. Ritchie, W.M. Schertzer, E.D. Soulis, R.E. Stewart, G.S. Strong and M.K. Woo, 2003. Energy and water cycles in a high-latitude north-flowing river system. Bulletin of the American Meteorological Society, 84:73–87.

Sagarin, R. and F. Micheli, 2001. Climate change in nontraditional data sets. Science, 294:811.

Savelieva, N.I., I.P. Semiletov, L.N. Vasilevskaya and S.P. Pugach, 2000. A climate shift in seasonal values of meteorological and hydrological parameters for Northeastern Asia. Progress in Oceanography, 47:279–297.

Savelieva, N.I., I.P. Semiletov, L.N. Vasilevskaya and S.P. Pugach, 2002. Climatic variability of the Siberian rivers seasonal discharge. In: I.P. Semiletov (ed.). Hydrometeorological and Biogeochemistry Research in the Arctic. Trudy Arctic Regional Center, 2:9–22. (In Russian)

Sazonova, T.S. and V.E. Romanovsky, 2003. A model for regional-scale estimation of temporal and spatial variability of active-layer thickness and mean annual ground temperatures. Permafrost and Periglacial Processes, 14(2):125–139.

Sazonova, T.S., V.E. Romanovsky, J.E. Walsh and D.O. Sergueev, 2004. Permafrost dynamics in the 20th and 21st centuries along the East Siberian transect. Journal of Geophysical Research, 109, doi:10.1029/2003JD003680.

Schindler, D.W., S.E. Bayley, B.R. Parker, K.G. Beaty, D.R. Cruikshank, E.J. Fee, E.U. Schindler and M.P. Stainton, 1996. The effects of climate warming on the properties of boreal lakes and streams at the Experimental Lakes Area, northwestern Ontario. Limnology and Oceanography, 41:1004–1017.

Sellman, P.V. and D.M. Hopkins, 1984. Subsea permafrost distribution on the Alaskan Shelf. In: Final Proceedings of the Fourth International Permafrost Conference, 17–22 July 1983, pp. 75–82. National Academy Press, Washington, D.C.

Semiletov, I.P., N.I. Savelieva and G.E. Weller, 2002. Cause and effect linkages between atmosphere, the Siberian rivers and conditions in the Russian shelf seas. In: I.P. Semiletov (ed.). Changes in the Atmosphere-Land-Sea System in the American Arctic. Proceedings of the Arctic Regional Center, Vladivostok, 3:63–97.

Serreze, M.C., J.E. Walsh, F.S. Chapin III, T. Osterkamp, M. Dyurgerov, V. Romanovsky, W.C. Oechel, J. Morison, T. Zhang and R.G. Barry, 2000. Observational evidence of recent changes in the northern high-latitude environment. Climatic Change, 46:159–207.

Serreze, M.C., D.H. Bromwich, M.P. Clark, A.J. Etringer, T. Zhang and R. Lammers, 2003. Large-scale hydro-climatology of the terrestrial Arctic drainage system. Journal of Geophysical Research, 108(D2). doi:10.1029/2001JD000919.

Sharkhuu, N., 2003. Recent changes in permafrost of Mongolia. Proceedings of the Eighth International Conference on Permafrost, pp. 1029–1034.

Shiklomanov, A.I., 1994. Influence of anthropogenic changes in global climate on the Yenisey River Runoff. Meteorology and Hydrology, 2:84–93. (In Russian)

Shiklomanov, A.I., 1997. On the effect of anthropogenic change in the global climate on river runoff in the Yenisei basin. In: Runoff Computations for Water Projects. Proceedings of the St. Petersburg Symposium 30 Oct.–03 Nov. 1995, pp. 113–119. IHP-V UNESCO Technical Document in Hydrology N9.

Shiklomanov, A.I., R.B. Lammers and C.J. Vorosmarty, 2002. Widespread decline in hydrological monitoring threatens pan-Arctic research. Eos, Transactions, American Geophysical Union, 83(2):13,16,17.

Shiklomanov, I.A. and H. Lins, 1991. Effect of climate change on hydrology and water management. Meteorology and Hydrology, 4:51–65. (In Russian)

Shiklomanov, I.A., A.I. Shiklomanov, R.B. Lammers, B.J. Peterson and C.J. Vorosmarty, 2000. The dynamics of river water inflow to the Arctic Ocean. In: E.L. Lewis, E.P. Jones, P. Lemke, T.D. Prowse and P. Wadhams (eds.). The Freshwater Budget of the Arctic Ocean, pp. 281–296. Kluwer Academic Publishers.

Sigurðsson, O., 1998. Glacier variations in Iceland 1930–1995 – From the database of the Iceland Glaciological Society. Jökull, 45:3–25.

Sigurðsson, O., 2002. Jöklabreytingar 1930–1960,1960–1990 og 1999–2000. (Glacier variations 1930–1960, 1960–1990 and 1999–2000.) Jökull, 51:79–86.

Sigurðsson, O., 2005. Variations of termini of glaciers in Iceland in recent centuries and their connection with climate. In: C. Caseldine, A. Russell, J. Hardardóttir and O. Knudsen (eds.). Iceland - Modern Processes and Past Environments, pp. 180–192. Elsevier.

Smith, L.C., 2000. Trends in Russian Arctic river-ice formation and breakup, 1917–1994. Physical Geography, 21:46–56.

Smith, S.L. and M.M. Burgess, 1999. Mapping the sensitivity of Canadian permafrost to climate warming. In: M. Tranter, R. Armstrong, E. Brun, G. Jones, M. Sharp and M. Williams (eds.). Interactions Between the Cryosphere, Climate and Greenhouse Gases, pp. 71–80. IAHS Publication No. 256.

Smith, S.L., M.M. Burgess and F.M. Nixon, 2001. Response of active-layer and permafrost temperatures to warming during 1998 in the Mackenzie Delta, Northwest Territories and at Canadian Forces Station Alert and Baker Lake, Nunavut. Geological Survey of Canada Current Research 2001-E5, 8pp.

Smith, S.L., M.M. Burgess and A.E. Taylor, 2003. High Arctic permafrost observatory at Alert, Nunavut – analysis of a 23-year data set. Proceedings of the Eighth International Conference on Permafrost, 1073–1078.

Sokratov, S.A. and R.G. Barry, 2002. Intraseasonal variations in the thermoinsulation effect of snow cover on soil temperatures and energy balance. Journal of Geophysical Research, 107(D9–10), ACL 13 1–7.

Soldatova, I.I., 1993. Secular variations in river break-up dates and their relationship with climate variation. Russian Meteorology and Hydrology, 9:70–76.

Solomon, S.M., D.L. Forbes and B. Kierstead, 1994. Coastal Impacts of Climate Change: Beaufort Sea Erosion Study. Geological Survey of Canada, Open File 2890, 85pp.

Staub, B. and C. Rosenzweig, 1987. Global Gridded Data Sets of Soil Type, Soil Texture, Surface Slope and Other Properties. National Center for Atmospheric Research, Boulder, Colorado. (In digital format available on Global Ecosystem's Database CD, version 1, 1991)

Steele, M. and T. Boyd, 1998. Retreat of the cold halocline layer in the Arctic Ocean. Journal of Geophysical Research, 103:10419–10435.

Stewart, K.M. and R.K. Haugen, 1990. Influence of lake morphometry on ice dates. Internationale Vereinigung fur Theoretische und Angewandte Limnologie: Verhandlungen, 24:122–127.

Stieglitz, M., S.J. Dery, V.E. Romanovsky and T.E. Osterkamp, 2003. The role of snow cover in the warming of arctic permafrost. Geophysical Research Letters, 30(13), doi:10.1029/2003GL017337.

Thompson, D.W. and J.M. Wallace, 1998. The Arctic Oscillation signature in the wintertime geopotential height and temperature fields. Geophysical Research Letters, 25:1297–1230.

Thoroddsen, T., 1917. Arferdi a Islandi i thusund ar, Hid islenzka fraedafelag, Copenhagen.

Tucker, W.B. III, J.W. Weatherly, D.T. Eppler, L.D. Farmer and D.L. Bentley, 2001. Evidence for rapid thinning of sea ice in the western Arctic Ocean at the end of the 1980s. Geophysical Research Letters, 28:2851–2854.

Van de Wal, R.S.W. and M. Wild, 2001. Modelling the response of glaciers to climate change by applying volume-area scaling in combination with a high-resolution GCM. Climate Dynamics, 18:359–366.

Van de Wal, R.S.W., M. Wild and J. de Wolde, 2001. Short-term volume changes of the Greenland ice sheet in response to doubled CO_2 conditions. Tellus, 53B:94–102.

Van der Linden, S., T. Virtanen, N. Oberman and P. Kuhry, 2003. Sensitivity analysis of discharge in the arctic Usa basin, East-European Russia. Climatic Change, 57:139–161.

Van der Veen, C.J., 1996. Tidewater calving. Journal of Glaciology, 41:375–385.

Van der Veen, C.J. (ed.), 1997. Calving Glaciers: Report of a workshop, February 28 – March 2, 1996. BPRC Report No. 15. Byrd Polar Research Center, Ohio State University, 194pp.

Van der Veen, C.J., 2002. Polar ice sheets and global sea level: how well can we predict the future? Global and Planetary Change, 32:165–194.

Vavrus, S.J., R.H. Wynne and J.A. Foley, 1996. Measuring the sensitivity of southern Wisconsin lake ice to climate variations and lake depth using a numerical model. Limnology and Oceanography, 41:822–831.

Vigdorchik, M.E., 1980. Arctic Pleistocene History and the Development of Submarine Permafrost. Westview Press, Colorado, 286pp.
Vinje, T., 2001. Anomalies and trends of sea ice extent and atmospheric circulation in the Nordic Seas during the period 1864–1998. Journal of Climate, 14:255–267.
Vinnikov, K.Y., A. Robock, R.J. Stouffer, J.E. Walsh, C.L. Parkinson, D.J. Cavalieri, J.F.B. Mitchell, D. Garrett and V.F. Zakharov, 1999. Global warming and Northern Hemisphere sea ice extent. Science, 286:1934–1937.
Wadhams, P. and N.R. Davis, 2000. Further evidence of ice thinning in the Arctic Ocean. Geophysical Research Letters, 27:3973–3975.
Walsh, S.E., S.J. Vavrus, J.A. Foley, A. Fisher, R.H. Wynne and J.D. Lenters, 1998. Global patterns of lake ice phenology and climate: model simulations and observations. Journal of Geophysical Research, 103:28825–28837.
Washburn, A.L., 1956. Classification of patterned ground and review of suggested origins. Geological Society of America Bulletin, 67:823–865.
WCRP, 1996. Proceedings of the workshop on the Implementation of the Arctic Precipitation Data Archive (APDA) at the Global Precipitation Climate Centre (GPCC), Offenbach, Germany. World Climate Research Programme. Report No. WCRP-98, 44pp.
Weidick, A., 1968. Observation on some Holocene glacier fluctuations in West Greenland. Meddelelser om Grønland, 165(6) 202pp.
Weidick, A., C.E. Bøggild and O.B. Olesen, 1992. Glacier Inventory and Atlas of West Greenland. Report 158. Grønlands Geologiske Undersøgelse, 194pp.
Willemse, N.W. and T.E. Tornqvist, 1999. Holocene century-scale temperature variability from West Greenland lake records. Geology, 27(7):580–584.
Williams, P.J. and M.W. Smith, 1989. The Frozen Earth: Fundamentals of Geocryology. Cambridge University Press, 306pp.
Williams, R.S. Jr., 1986. Glaciers and glacial landforms. Chapter 9. In: N.M. Short and R.W. Blair Jr. (eds.). Geomorphology from Space. A Global Overview of Regional Landforms. NASA Special Publication SP-486, pp. 521–596.
Williams, R.S. Jr. and J.G. Ferrigno (eds.), 2002. Satellite Image Atlas of Glaciers of the World: Glaciers of North America. U.S. Geological Survey, Washington, D.C., 405pp.
Winsor, P., 2001. Arctic sea ice thickness remained constant during the 1990s. Geophysical Research Letters, 28(6):1039–1041.
Winther, J.-G., 1993. Short- and long-term variability of snow albedo. Nordic Hydrology, 24:199–212.
Wolfe, S.A, S.R. Dallimore and S.M. Solomon, 1998. Coastal permafrost investigations along a rapidly eroding shoreline, Tuktoyaktuk, N.W.T. In: A.G. Lewkowicz and M. Allard (eds.). Proceedings of the Seventh International Conference on Permafrost, pp. 1125–1131.
Wright, J.F., M.W. Smith and A.E. Taylor, 2000. Potential changes in permafrost distribution in the Fort Simpson and Norman Wells Area. In: L.D. Dyke and G.R. Brooks (eds.). The Physical Environment of the Mackenzie Valley, Northwest Territories: A Base Line for the Assessment of Environmental Change, pp. 197–207. Geological Survey of Canada Bulletin 547.
Wynn, R.H. and T.M. Lillesand, 1993. Satellite observation of lake ice as a climatic indicator: initial results from state-wide monitoring in Wisconsin. Photogrammetric Engineering and Remote Sensing, 59:1023–1031.
Wynn, R.H., J.J. Magnuson, M.K. Clayton, T.M. Lillesand and D.C. Rodman, 1996. Determinants of temporal coherence in the satellite-derived 1987–1994 ice breakup dates of lakes on the Laurentian Shield. Limnology and Oceanography, 41:831–838.
Yang, D., 1999. An improved precipitation climatology for the Arctic Ocean. Geophysical Research Letters, 26:1625–1628.
Ye, B., D. Yang and D. Kane, 2003. Changes in Lena River streamflow hydrology: Human impacts versus natural variations. Water Resources Research, 39(7), doi:10.1029/2003WR001991.
Ye, H., 2001. Increases in snow season length due to earlier first snow and later last snow dates over north central and northwest Asia during 1937–94. Geophysical Research Letters, 28:551–554.
Ye, H., H. Cho and P.E. Gustafson, 1998. The changes in Russian winter snow accumulation during 1936–1983 and its spatial patterns. Journal of Climate, 11:856–863.
Zachrisson, G., 1989. Climate variation and ice conditions in the River Torneälven. In: Proceedings of the Conference on Climate and Water, Helsinki. Publications of the Academy of Finland, Vol. 1:353–364.
Zeeberg, J.J. and S.L. Forman, 2001. Changes in glacier extent on north Novaya Zemlya in the twentieth century. The Holocene, 11(2):161–175.
Zervas, C. 2001. Sea Level Variations of the United States 1854–1999. NOAA Technical Report NOS CO-OPS 36. National Oceanic and Atmospheric Administration, Silver Spring, Maryland, 65pp+appendices.
Zhang, T., J.A. Heginbottom, R.G. Barry and J. Brown, 2000. Further statistics on the distribution of permafrost and ground ice in the Northern Hemisphere. Polar Geography, 24(2):125–131.
Zhang, X., K.D. Harvey, W.D. Hogg and T.R. Yuzyk, 2001. Trends in Canadian streamflow. Water Resources Research, 37:987–998.
Zhuang, Q., V.E. Romanovsky and A.D. McGuire, 2001. Incorporation of a permafrost model into a large-scale ecosystem model: Evaluation of temporal and spatial scaling issues in simulating soil thermal dynamics. Journal of Geophysical Research, 106(24):33649–33670.
Zwally, H.J., W. Abdalati, T. Herring, K. Larson, J. Saba and K. Steffen, 2002. Surface melt-induced acceleration of Greenland ice-sheet flow. Science, 297:218–222